Olfactory processing in honeybee Kenyon cells and the involvement of the GABAergic system

Dissertation zur Erlangung des akademischen Grades des Doktors der Naturwissenschaften (Dr. rer. nat.)

eingereicht am Fachbereich Biologie, Chemie, Pharmazie
der Freien Universität Berlin

vorgelegt von

Anja Froese

aus Neuruppin

August 2009

Diese Arbeit wurde im Zeitraum von 2006 bis 2009 im Institut für Biologie, Neurobiologie in der Arbeitsgruppe von Prof. Menzel und hauptsächlich unter der Leitung von Prof. Menzel angefertigt.
Bei den Experimenten zur Etablierung der Elektroporation hat Dr. Gerard Leboulle die Planung und Durchführung der Versuche mit betreut.

1. Gutachter: Prof. Dr. Randolf Menzel
2. Gutachter: Prof. Dr. Martin Nawrot

Disputation am ___02.10.2009__

Table of Contents

Abbreviations

AL	antennal lobe
AP	action potential
BMI	bicuculline methiodide
CLSM	confocal laser scanning microscope
GABA	gamma-aminobutyric acid
ISI	inter stimulus interval
KC	Kenyon cell
lACT	lateral antenno-cerebralis tract
LFP	local field potential
LN	local interneurons
mACT	median antenno-cerebralis tract
MB	mushroom body
OB	olfactory bulb
PBS	phosphate buffered saline
PCA	principle component analysis
PCT	proto-cerebral-tract
PFA	paraform aldehyde
PTX	picrotoxin
ROI	region of interest
RT	room temperature
SEM	standard error of the mean
SFA	spike frequency adaptation

Zusammenfassung

In der vorliegenden Arbeit wurden Duft - Repräsentation und - Prozessierung in den intrinsischen Neuronen des Pilzkörpers der Honigbiene, *Apis mellifera,* untersucht. Dazu wurden die zu untersuchenden Zellen zunächst retrograd gefärbt um dann eine opto-physiologische Methode, das Calcium Imaging, anzuwenden.
Gegenstand dieser Arbeit waren die sogenannten clawed Kenyon Zellen, welche in der Lippe des Pilzkörpers olfaktorischen Eingang bekommen. Die Lippe ist ein Teil des Calyx‘, welcher der sensorische Eingangsbereich des Pilzkörpers ist. Die Kenyon Zellen sind Interneurone zweiter Ordnung im olfaktorischen Verarbeitungsweg. Sie kommen, verglichen mit den ihnen vorgeschalteten Projektionsneuronen und den ihnen nachgeschalteten Ausgangsneuronen, in sehr großer Zahl vor. Dies lässt auf eine Umorganisation des Kodierungsprinzips von einer Zellebene auf die nächste schließen. Dieses Prinzip ist das Untersuchungsobjekt dieser Arbeit.

Bereits bekannt ist, dass die Kodierung in Kenyon Zellen in kombinatorischer Weise geschieht. Jede Zellen reagiert nur auf ausgewählte Düfte und die Antwort besteht aus nur wenigen Aktionspotentialen.
Es wurde während dieser Arbeit untersucht, ob einzelne Kenyon Zellen auch selektiv auf bestimmte Duftkonzentrationen antworten. Untersuchungen zur Konzentration-abhängigkeit von Duftantworten im Pilzkörper ergaben, (1) dass individuelle Zellen nicht spezifisch für enge Konzentrationsspannen sind, (2) Die gemittelte Antwortstärke positiv mit der Duftkonzentration korreliert, und (3) die Stärke von duftvermittelte Antworten am Ende des Stimulus, sogenannten OFF-Antworten, konzentrationsabhängig ist.
Mittels der Applikation von GABA-Rezeptor-Antagonisten konnte (4) gezeigt werden, dass die Duftantworten auf hochkonzentriere Düfte durch eine GABAerge Inhibition an ionotrophen und metabotrophen Rezeptoren beeinflusst wird. Dies wird als ein Regulierungsmechanismus angesehen.

Desweiteren wurden zeitliche Eigenschaften der Aktivität von Kenyon Zellen betrachtet. Dies ergab, dass die zeitliche Ausdehnung der Aktivität nicht von der Länge des Stimulus‘ abhängt. Ferner ist die zeitlich sparsame Antwort nicht von der Ausschüttung des Transmitters GABA abhängig, wie bisher angenommen, sondern es handelt sich dabei um

einen zell-intrinsischen Mechanismus, der dazu führt, das die duftvermittelte Aktivität schnell zurückgeht.
Weiterhin wurden physiologische Unterschiede zwischen den beiden Calyces eines Pilzkörpers aufgezeigt, und zwar in Bezug auf die Antwortstärke und ihre Beeinflussung durch GABA.

Es kann geschlussfolgert werden, dass die Duft – Prozessierung ein hoch komplexer Vorgang ist und diverse GABAerge Netzwerke die Duftrepräsentation in den Pilzkörpern mitgestalten. Die Entschlüsselung der Prinzipien der Duftkodierung erfordert weitere Bemühungen unter Einbeziehung neuer Techniken und Forschungsansätze. Erste Schritte zu einem neuen Ansatz für die selektivere Färbung von Zellen mittels *in vivo* Elektroporation wurden vorgestellt.

Summary

In this thesis I investigated the representation and processing of odor information in mushroom body intrinsic cells of the honeybee *Apis mellifera*. For this purpose I applied a calcium imaging technique after retrogradly staining the cells.
Subject of this work were in particular the clawed Kenyon cells (KC) receiving olfactory input in the lip neuropil of the mushroom body calyces. They are the second order interneurons in the olfactory pathway and exist in extremely high number compared to the MB afferent neurons - the projection neurons, and the efferent output neurons. This suggests a reorganization of the coding principles which is the subject of study in my thesis.

Coding in KCs is without much doubt done in a combinatorial way; individual cells were shown to respond in a sparse manner upon olfactory stimuli, i.e. each cell responds only to selected odors and its responses consist of only a few spikes.
I analyzed whether KCs are also selective for particular odor concentrations. Investigating the concentration dependency of odor responses in the MB I could (1) show that individual Kenyon cells are not selective for narrow ranges of concentration and (2) the response magnitude over the monitored region is positively correlated to the odor concentration; (3) odor evoked responses at odor offset also show concentration dependency.
Application of GABA receptor antagonists revealed (4) that odor responses to high odor concentrations are mediated by GABAergic inhibition via ionotrophic and metabotrophic GABA receptors. This can be understood as a gain control mechanism.

I also addressed the temporal characteristics of KC firing and found that responses are invariant for different stimulus lengths. Further, I found that temporal sparseness is not caused by GABA transmission, as it was proposed previously, but by a neuron intrinsic mechanism that leads to a fast decay of any odor evoked calcium response.
In addition I show physiological differences between median and lateral calyces in respect to the response strength and their impairment by GABA.

Taken together, I conclude that odor processing is complex and involves several GABAergic networks which interact in the odor representation in the mushroom body. Deciphering the principles of odor processing in the mushroom body still needs further efforts using advanced technologies and new scientific strategies. I introduce first steps towards a new approach for staining cells more selectively via *in vivo* electroporation.

1. Introduction

Sensing odors is an important ability of all animal species providing signals of the surrounding environment. Smelling is a chemical sense, which developed early in evolution. Studying olfaction became a big field of neuroscientific research. Today, we understand much about how odors are perceived and conveyed to the brain by olfactory sensory neurons and how information is processed in the first olfactory neuropil. Still little is known how this information is presented in higher order brain centers, how it is processed during learning and memory formation, and how it affects behavior.

Studying Olfaction in insects

Smelling stands for the chemosensory perception of chemical substances which are, in the case of terrestrial animals, airborne, volatile molecules; in the case of aquatic animals the substances are present in the water.

The similarities in the organization of the olfactory pathway between species are striking; even between arthropods and vertebrates there is a high degree of homology (Ache and Young, 2005;Davis, 2004;Hildebrand and Shepherd, 1997). The common anatomical organizations as well as the same functional principles are conserved.

By means of odors, animals collect information about food sources and food quality, avoid danger like predators or fire, find potential mates, recognize social relations, do homing, undergo symbiotic associations, and mark their territories. Smell can even trigger memories. The sensed substances can be either classical odorants or pheromones; in nature they are rarely single components but complex mixtures. In fact, the olfactory world is extremely wide. There is a vast number of different odorants which can occur in all kinds of mixtures and their concentration can span several orders of magnitude, but they still can be recognized as the same odor.

Why do we study olfaction in insects? The olfactory pathway is used as a model for neuronal processing of information collected from a complex outer world as well as for neuronal plasticity related to different forms of olfactory learning.

The principles of processing odor information are still poorly understood. Since these principles seem to be very alike in insects and in vertebrates, insects are important models

for studying olfaction. They possess a relatively simple brain which is easily accessible and includes a smaller number of neurons - less than 1 million in the honeybee worker (Witthöft, 1967).

The honeybee *Apis mellifera* is for a long time used as a model for learning and memory formation, for navigation and cognition, as well as for olfactory sensing and information processing. The honeybee's nervous systems is also a model for studying neuronal and synaptic plasticity in the contexts of learning and of experience-dependent or -independent development (Velarde et al., 2009;Krofczik et al., 2008;Farris et al., 2001).
The honeybee is a suitable model system in neurobiology because bees are relatively easy to breed, they have high genetic homogeneity between nest mates, and they have a rich behavioral repertoire which is accessible for studies, e.g. with respect to navigation and inside-the-hive interactions. Not least, the genome of *Apis mellifera* has been sequenced (Weinstock, 2006). Because honeybees are eusocial insects, they must have found a sophisticated way to communicate within the hive, an ability which is usually seen in connection with a relatively highly developed nervous system.

The Olfactory pathway

Antennal lobe

Olfactory receptor neurons are the link between the environment and the animals' neuronal olfactory pathway. They are primary neurons expressing olfactory receptors, usually only one receptor type per neuron. These receptors are spatially organized in a stereotype manner: in vertebrates they are located in the olfactory epithelium in the nasal cavity; in insects they are found mainly on the antennae (de Bruyne et al., 2001). In bees, antennal sensory neurons express their receptors inside of poreplate sensillae (Brockmann and Brückner, 1995). Olfactory receptors are G-protein coupled receptors coded by the biggest gene family in the mammalian genome (Buck and Axel, 1991). In the mouse about 1300 different receptors exist and in humans still about 350 different olfactory receptors are encoded; the genome of the adult fruitfly *Drosophila melanogaster* contains 57 receptor genes (Vosshall et al., 2000).

Odor molecules interact with their respective receptor via olfactory binding proteins. All receptors are very specific, but still many of them can be activated by different molecules, but to a different extend. In addition, most odor molecules can activate several receptors which enables odor coding in a combinatorial way (de Bruyne et al., 2001).

The target of olfactory receptor neurons is an extremely conserved blueprint: sensory neurons project to the first olfactory relay station, which is the olfactory bulb (OB) in vertebrates or the equivalent structure in insects and other arthropods: the antennal lobe (AL). Here, all the spatially distributed sensory neurons of the periphery expressing the same receptor converge on one (or few) round structure called glomerulus (mice: Mombaerts et al., 1996; *Drosophila*: Vosshall et al., 2000). Within the AL glomeruli, the receptor neurons, about 60.000 in the honeybee, converge onto 800 projection neurons (PN), the efferent neurons of the AL (Bicker et al., 1993). Homolog to the insects' PNs are the mitral cells in vertebrates.

AL and OB are bilateral symmetrical structures and stereotypically organized within species (Galizia et al., 1998; for AL architecture see: Stocker et al., 1990). Although the AL architecture of different invertebrate species is very similar, there are differences for instance in the number of glomeruli. In the honeybee there are about 160 of them. In contrast, there are only about 50 in the adult fruitfly but about 450 in the carpenter ant (Zube et al., 2008). In the olfactory bulb of a mouse one can find about 1800 glomeruli (Mombaerts et al., 1996).

The glomeruli are interconnected by several networks of local inhibitory, but also excitatory, interneurons. Those networks differ with respect to their transmitter, their morphology and in their target: some have their targets at the presynapse, others at the postsynaptic site of the synapse between sensory neurons and PN within the glomeruli. Some local interneurons (LN) connect only few neighboring glomeruli, other show a global distribution (Wilson and Laurent, 2005). The LN outnumber all other AL neurons. They count about 4.000 in the honeybee (Witthöft, 1967). Here are two different inhibitory GABAergic networks (Sachse and Galizia, 2002) and one inhibitory histamineergic network (Sachse et al., 2006) described. In *Drosophila*, also an excitatory, cholinergic network was discovered (Shang et al., 2007;Olsen et al., 2007). It is likely that an excitatory network is present in the honeybee as well.

From each glomerulus about 5 PNs emerge and target higher brain regions. In the honeybee, the uniglomerular PNs leave the AL via two tracts: the lateral antenna cerebralis tract (lACT) and the median antenna cerebralis tract (mACT) (Bicker et al., 1993). Both innervate the input regions of the mushroom bodies (MB) and the lateral protocerebral lobe. The input regions of the MB are termed calyces due to their cup like shape. A third tract, the mlACT, only innervates the lateral protocerebral lobe and consists of multiglomerular PNs (Abel et al., 2001). Mitral cells in mammals target the olfactory cortex.

Mushroom bodies and their intrinsic neurons

PN of the olfactory pathway diverge to a much higher number of MB intrinsic cells - the Kenyon cells (KC) (Kenyon, 1896;Strausfeld et al., 2000;Farris et al., 2004) whereas each PN innervates several KCs and each KC gets input from several PN. Kenyon cells are the principle neurons of the MB. In the worker honeybee, there are about 170,000 on each hemisphere (Witthöft, 1967); in the fruitfly *Drosophila melanogaster* there are about 2,500 KCs (Aso et al., 2009).

The mushroom bodies (MB) are outstanding paired structures in the brain of insects and other arthropods which were first described by Dujardin (Dujardin, 1850). They are of high scientific interest since they are such prominent structures and seen as the main processing and integration center for olfactory input (Strausfeld et al., 1998) as well as the seat of memory traces and as being involved in learning and memory formation (review: Menzel, 1983;Heisenberg, 2003;Heisenberg, 1989).

MBs are the second order neuropil in the olfactory pathway and thus functionally comparable with the olfactory cortex in vertebrates. This main input region is located at the dorsal side of the MBs. During evolution some insect species developed mushroom bodies with two calyces (Strausfeld et al., 1998). Also the honeybee has two calyces at each MB: a median and a lateral calyx. The calyces of honeybees are very prominent structures, organized in substructures: the lip, the collar, and the basal ring (Mobbs, 1982). The development of such enhanced input regions is usually brought in connection with increased requirements in social insects.

All KC have their somata and their dendrites inside or attached to the calyces and send their thin axons in bundles of parallel neurons towards the ventral parts of the MB - the

lobes. Most KCs have bifurcating axons projecting to two lobes; one lobe is oriented medial and one vertical.

KCs receive different kinds of sensory input in the calyces: olfactory input via the AL, visual input via the optic lobes, as well as mechanosensory input. Different sensory information are transferred to the different substructures of the calyx: The lip, which is the most dorsal substructure, receives input from the antennal lobe, the collar receives visual input, the basal ring receives input from different modalities and is further subdivided into two layers, one receiving input from the antennal lobe the other one receiving visual input. (Gronenberg and López-Riquelme, 2004;Schröter and Menzel, 2003;Rybak and Menzel, 1993;Mobbs, 1982).

The lip region of the MB calyx, as the dendritic input site of olfactory KCs will be the focus of this work.

KCs are grouped in two main groups: KC type I and KC type II. The somata of KCs type I are located inside the calyx, somata of KCs type II at its outer brim. Each of this group can be further subdivided into many more groups according to dendritic morphology, location within the MB, expression of different peptides, time of development, and functional role (Fukushima and Kanzaki, 2009;Aso et al., 2009;Farris et al., 2004;Strausfeld et al., 2000;Rybak and Menzel, 1993;Rybak and Menzel, 1993;Mobbs, 1982;Tanaka et al., 2008).

KCs of type II, also termed clawed Kenyon cells or KC type 5, have morphologically typical dendrites in the calyx neuropil of the MB (Strausfeld, 2002;Rybak and Menzel, 1993;Mobbs, 1982). Some KCs type II innervate all regions of the calyx (Farris et al., 2004) and are therefore expected to get sensory input from different modalities whereas some seem to be restricted only to the lip or collar (Rybak and Menzel, 1993;Mobbs, 1982).

Each honeybee MB contains about 50,000 clawed KCs (Witthöft, 1967). Except from their claw like dendrites they are defined by the location of their somata outside the calyx. Clawed KCs are the first ones cleaving from MB neuroblasts which are located in the middle of each developing calyx (Farris et al., 2001). Due to the high number of KCs, the early-born KC somata get gradually pushed outwards to the periphery by the succeeding cells and this way their somata have their final location outside the calyx neuropil.

The KCs class I, having their somata inside the calyx, can be distinguished in two main groups on the basis of their diameter: smaller cells are located in the center of the calyx, larger cells fill the remaining space of the calyx (Mobbs, 1982).
It is well described that the majority of KCs responds to odor stimuli. Mainly KCs of type II are involved in olfactory processing and are therefore subject of this work, but also a population of KC type I processes olfactory information.

Other structures of the MB are the peduncle and the lobes: KCs project from the calyx into the peduncle and bifurcate into the lobes. In the honeybee usually α- (vertical) and β- (medial) lobe are distinguished. It is unclear, whether an appropriate γ lobe exists as it is described for the fruitfly *Drosophila*. KCs innervating the *Drosophila* γ lobe do not bifurcate (Farris et al., 2004;Strausfeld, 2002). Also in honeybees some clawed KCs were described as being unbranched and projecting only towards the vertical lobe / α-lobe forming a discrete γ-lobe (Farris et al., 2004;Strausfeld, 2002). Other studies also described clawed KCs as bifurcating into both lobes (Mobbs, 1982;Rybak and Menzel, 1993). Anyhow, the ventral third of the honeybee α-lobe is a somewhat discriminative structure, irrespective whether it is homologous to the *Drosophila* γ-lobe or not. This structure is composed of the axons of olfactory class II KCs.
The dorsal part of the α-lobe is innervated by KCs class I. Here, the substructures of the calyces with their specific input modalities are also apparent: strata can be differentiated which correspond to the calycal substructures lip, collar, and basal ring (Rybak and Menzel, 1993).

The lobes of the MB are considered as the main output site of KC, but also here KCs might receive inputs from MB extrinsic neurons (Ito et al., 1998; Tanaka et al., 2008; Johard et al., 2008). Also in the peduncle KCs form spines and blebs, they supposably synapse onto other KCs or onto extrinsic neurons (Mobbs, 1982).

Mushroom body extrinsic neurons

Within the lobes, KCs target on different types of MB extrinsic neurons which were intensively studied mainly in the context of learning and plasticity (Okada et al., 2007;Okada and Menzel, 2006;Strube-Bloss, 2008;Hähnel, 2009;Menzel and Manz,

2005;Grünewald, 1999b). In D*rosophila* 17 types of MB extrinsic neurons were described recently (Tanaka et al., 2008).

Since MB are required for learning and memory formation (Komischke et al., 2005;Menzel, 1983;Heisenberg, 2003), it was a crucial finding that another important neuron, the VUMmx1 (Hammer, 1993) is innervating the MB calyces. This octopaminergic neuron represents the reward pathway in the honeybee brain.

One group of extrinsic neurons is referred to as the PCT- (proto-cerebral-tract) neurons or A3 neurons (Rybak and Menzel, 1993). The PCT-tract counts about 110 fibers (Bicker, 1999). They are of special interest forming a feedback loop to the MB calyces where olfactory KCs get their main excitatory input from PNs emerging from the antennal lobe. Within the lip of the MB calyx, PCT neurons innervate the microglomeruli, structures in which PNs form synaptic boutons and synapse on KC dendrites (Yamagata, 2008;Krofczik et al., 2009;Ganeshina and Menzel, 2001;Ganeshina et al., 2006;Groh and Rössler, 2008). PCT neurons were described as being mostly GABAergic (Grünewald, 1999b).

A backfill staining of MB neurons in a honeybee brain is shown in Figure 1-1 A as it was usually performed for the experiments described in this work. It displays some of the neurons which were described here.

A B

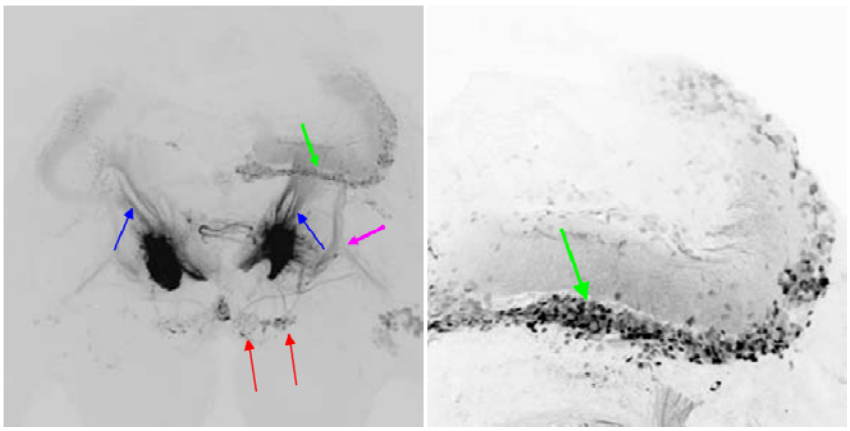

Figure 1-1 : backfill of mushroom body Kenyon cells in the honeybee
A: Overview scan from CLSM showing staining in both mushroom bodies, in the right hemisphere (left in the picture) mainly KCs innervating the lateral calyx are stained, in the left hemisphere (right in the picture) the median calyx is stained.
Blue arrows: bundles of KC axons in the peduncle projecting from the calyces to the lobes.
Magenta arrow: stained PCT tract, the somata of PCT neurons are depicted right in the picture.
Red arrows: somata cluster of MB extrinsic neurons of A1/A2 cluster
B: Zoomed views of the left median calyx, somata of class II KCs are stained (green arrow)

The green arrows indicate somata at the outer brim of a median calyx, the blue arrows point to KC axons running through the peduncle, the magenta and red arrows point to MB extrinsic neurons: PCT-neurons (magenta) and extrinsic neurons of the so called A1/A2 cluster (red).
Figure 1-1 B shows an enlargement of the scan. Here, the lip neuropil is clearly visible; somata of clawed KCs at the outer brim of the lip are prominently stained.

In search of the olfactory code

Several morphological and physiological studies have been undertaken at the AL and the OB to understand the principles of odor coding. Using optophysiological methods it was founds that the glomeruli, which are termed as the functional units of the AL, form distinct areas of activity. Each odor evokes activity in a specific subset of glomeruli by means of the activation via the respective sensory neurons and the connecting interneurons. Spatial, stereotype patterns of odor-evoked glomerular activity coding for different odor qualities have been found in insects (Joerges et al., 1997), rodents (Rubin and Katz, 1999), and zebrafish (Friedrich and Korsching, 1997).
The spatial pattern, as it was found in the honeybee AL, even allowed determination of physiological distances between odors with more or less similar molecular structures (Ditzen, 2005;Sachse et al., 1999). These distances are correlated with perceptual differences: perceptual generalization between odors depends on functional group and carbon chain length (Guerrieri et al., 2005). Also mitral/tufted cells in mice were found to encode specific odorant attributes implying that each mitral/tufted cell is narrowly tuned to a particular stimulus characteristic (Davison and Katz, 2007).

Odors are not only coded in spatial patterns but also in temporal patterns of activity (honeybee: Galizia et al., 2000; mammals: Spors and Grinvald, 2002). Temporal responses differe across glomeruli and are stimulus dependent (Carlsson et al., 2005).
Evidence that odors are coded by much finer scaled temporal cues was found in the locust. Here, the coding of odor qualities lies in the synchronicity of PN firing and the phase locking to the local field potential (LFP) (rewiewed in: Laurent, 2002;Stopfer et al., 2003).

The PN, emerging from the honeybee AL in two tracts, differ in their responses to odors. For mACT neurons a broad odor tuning was found, whereas lACT neurons show a rather narrow odor-tuning (Yamagata, 2008).

The coding and learning of different odor qualities has been studied intensively on the neuronal level as well as on the behavioral level. Another aspect of odor perception and coding is how odor intensity is treated in the olfactory system, this aspect will be investigated in this work.

In behavioral assays it was shown that insects can learn to distinguish not only different odors but also different concentrations of the same odor (Yarali et al., 2009;Pelz et al., 1997). On the neuronal level it was discovered that PNs respond in a dose dependent manner in the way that the firing rate and therefore the response strength increases, whereas in some individual glomeruli the strength of inhibition increases (honeybee: Sachse and Galizia, 2003; locust: Stopfer et al., 2003;*Drosophila*: Silbering et al., 2008; also in zebrafish OB: Friedrich and Korsching, 1997). In contrast, in the carpenter ant *Campanotus floridanus* the response duration rather than the strength is proposed to be a reliable measure for coding intensity (Zube et al., 2008).

Recently, also for the PN output sites, the boutons in the MB calyx, a dose dependency was demonstrated (Yamagata, 2008); here boutons of both tracts, l- and mACT, show a rather complex concentration dependency with excitation as well as inhibition; yet over all, the concentration dependency is clearly positive in mACT neurons but odor specific in lACT neurons.

In locusts, increasing odor concentration lead to changes in firing pattern very much like those changes caused by different odors. In some PNs the firing rate increased with concentration, in others, firing rate were highest at lowest concentration, the summed output of the AL varied little over concentrations (Stopfer et al., 2003); coding lies in tighter synchronization of PNs which is related to increased efficacy of inhibition by local interneuron.

Olfactory coding in Kenyon cells

Besides the first olfactory neuropil also KCs have been studied in different insects using electrophysiological and optophysiological methods. In contrast to PN, they are

remarkable silent at rest; individual KCs are known to respond sparse in several ways (Demmer and Kloppenburg, 2009;Ito et al., 2008;Broome et al., 2006;Szyszka et al., 2005;Wüstenberg et al., 2004;Stopfer et al., 2003;Perez-Orive et al., 2002): 1) They are odor specific. The term lifetime sparseness refers to cells responding to only few odors. 2) Only few cells respond to a particular odor, here the term population sparseness is used. This corresponds also to spatial sparseness, which was described in the honeybee and was concluded from data accounting responses in somata. 3) KCs respond temporally sparse which means only single or few spikes are generated in response to stimulation. Spiking occurs almost entirely to an odor onset and sometimes offset with very few spikes occurring in between.
I aimed to unveil some aspects of the mechanisms of temporal sparseness in KCs.

In the calyx a rather small number of PNs targets a 100 fold higher number of KC. How the read out occurs here, is still unknown.
The high degree of stereotypy in morphology and odor responsiveness of the receptor neurons, the glomeruli, and the PNs raises the question, if such patterning is further conveyed. Stereotype response patterns were describes for the *Drosophila* calyx (Wang et al., 2004) but other authors failed to find stereotypy in KCs (Murthy et al., 2008) and call the calyx the first non-stereotype element in the olfactory pathway.

GABA in the insect brain

The stereotype odor evoked spatial and temporal patterning in the first stages of the olfactory pathway is shaped by lateral inhibition via LNs in the AL. The most important inhibitory neurotransmitter is GABA (γ aminobutyric acid). GABAergic networks were found in the AL which is a very well studied model for inhibitory networks since it is an confined neuropil and includes different networks of GABAergic LNs. Such networks were for instance found in the honeybee (Sachse and Galizia, 2002), in *Drosophila* (Wilson and Laurent, 2005), in the cockroach (Husch et al., 2009), in moth (Berg et al., 2009), and in locusts (MacLeod et al., 1998).
GABA binds to ionotropic ($GABA_A$) and metabotropic ($GABA_B$) receptors. The $GABA_A$ receptor is a chloride channel and binding of GABA inhibits neurotransmission by hyperpolarizing the postsynaptic membrane and thus reduceing excitability (for reviews,

see MacDermott et al., 1999). Metabotrophic $GABA_B$ receptors are described to couple to intracellular signaling pathways (Olianas and Onali, 1999; Mezler et al., 2001). Although GABA receptors in insects might not be identical to vertebrate receptors I will term them as $GABA_A$ and $GABA_B$ receptors within this work.

In the olfactory pathway of the honeybee, GABA has not only been found within the AL, but also in the PNs of the mlACT tract (Schäfer and Bicker, 1986), a tract consisting of mulitglomerular PNs and projecting from the AL to the lateral horn. Further, GABA was detected within the MB calyces (Grünewald, 1999b;Ganeshina and Menzel, 2001), where MB extrinsic neurons, the PCT neurons, provide GABAergic feedback to the microglomeruli in the lip neuropil.

Findings in the locust showed that GABA is involved in the synchronization of PNs assemblies which is needed for odor coding (Laurent et al., 1996). Based on that it was tested in honeybees, using a behavioral learning paradigm, how GABA is involved in odor perception. It was found that application of a GABA blocker (picrotoxin) to the AL impairs the differentiation of molecularly similar odorants, but not that of dissimilar odorants (Stopfer et al., 1997).

For the experiments described in this work, a pharmacological approach was used to study the influence of GABA onto KCs by applying different GABA receptor antagonists to the brain. Those drugs were originally generated for the use in mammals, but were found to be effective in insects as well. Picrotoxin (PTX) and bicuculline (BMI) are $GABA_A$ receptor antagonists having different molecular targets (Christensen et al., 1998), CGP54626 blocks $GABA_B$ receptors (Rotte et al., 2009;Root et al., 2008;Olsen and Wilson, 2008;Wilson and Laurent, 2005).

The calcium imaging technique

The technique applied in this work is *in vivo* calcium imaging, an established optophysiological method. It was intensively applied on the honeybee AL (Joerges et al., 1997;Faber and Menzel, 2001) as well as on the MB calyx (Szyszka et al., 2008).

For calcium imaging, fluorescent dyes are used which change their emission features according to different amounts of calcium ions surrounding them. This fluorescence can be investigated and recorded by all kinds of techniques ranging from normal fluorescence wide field microscopes equipped with a CCD camera to multi-photon microscopes with photomultipliers.

To record the activity of many neurons simultaneously, calcium imaging has become a widespread technique. It reflects changes in the intracellular Ca^{2+} concentration. The measured calcium changes can be correlated with neuronal activity. It has been shown that calcium activity correlates with data obtained from electrophysiological recordings: In the locust antennal lobe firing rates could be reconstructed from dendritic calcium signals with a 80-90% accuracy by combining intracellular electrophysiology and multi-photon calcium imaging *in vivo* under use of the calcium indicator Oregon Green BAPTA-1 (Moreaux and Laurent, 2007). At this, calcium signals may not be coupled exclusively to action potential but can also be evoked by sub threshold depolarization.

In honeybees, intracellularly stained PN, filled with the calcium sensitive dye fura-2, were eletrophysiologically recorded and optically imaged (Galizia and Kimmerle, 2004). A high correlation between data from both methods was found.

For the mitral/tufted cells in rats it was shown by combing intracellular recordings and two-photon calcium imaging that both methods unveil changes in membrane potential even below the threshold for AP firing (Charpak et al., 2001).

Calcium imaging allows investigating neuronal activity in a relatively large part of the brain.

Aim of this work

The goal of this thesis is to understand more about the principles of odor coding realized in the honeybee mushroom body.

Therefore, I first address the question how Kenyon cells, the mushroom body intrinsic cells, process information of odor stimuli ranging over several magnitudes of odor concentration. I ask, if perception is tuned by the neurotransmitter GABA, which is the main inhibitory transmitter in the insect brain.

I also deal with the issue of temporal coding of olfactory information since there is much evidence that spatial and temporal characteristics of the olfactory code are intrinsically

tied. Also in respect to temporal coding the influence of GABA is investigated since GABA might be involved in temporal sparsening of Kenyon cell activity.

Further, I ask if a spatial response map is conveyed to the lip neuropil of the calyx, the olfactory input region of the mushroom body, as it is know from the upstream neuropil, the antennal lobe in insects or its mammalian counterpart, the olfactory bulb.

I also address the influence of GABA on off-responses which often can be measured in Kenyon cells, as well as the representation of odor mixtures in the mushroom body.

In order to investigate these questions, I have optically recorded odor representations in the mushroom body input region and pharmacologically manipulated the network with different GABA receptor antagonists.

Finally, I introduce a new approach for inserting fluorescent dyes into living cells via electroporation. This technique could help to push the boundaries of our calcium imaging technique.

2. Materials and Methods

2.1 Imaging experiments

Bee preparation and dye loading

Experimental procedure were decribes in detail in Hähnel et al. (Haehnel et al., 2009). In brief: Foraging honeybees *Apis mellifera* were either caught from the entrance of an outdoor hive or, during winter months, from an indoors flight room. After immobilizing the bees on ice, they were fixed in a plexiglas chamber at the eyes and the thorax using dental wax and fed with two drops of a 30% sucrose solution about 30 min later.

For dye loading, the antennae were fixated to the head with n-eicosan (Sigma Aldrich, Germany) and a small window between the median ocellus and the base of the antennae was cut into the head capsule. Having a frontal view on the brain, glands and airbags were carefully moved to the side in order to expose the brain surface above the α-lobes. The tip of a glass electrode (Kwik-Fil™, WPI, Sarasota, USA) was coated with a paste-like 10:1 mixture of the calcium sensitive dye FURA-2 dextran (10,000MW, Molecular Probes, Eugene, USA) and the lysine fixable dye tetramethylrhodamine-dextran (10,000 MW, Molecular Probes, Eugene, USA) dissolved in distilled water. The dye loaded electrode was injected either into the ventral median part of the α-lobe, aiming to stain clawed KCs projection to the median calyx or into the ventral lateral part, to stain the same type of KCs but those projecting to the lateral calyx.

In order to stain PN dendrites in the antennal lobe, the dye loaded electrode was injected into the deutocerebrum lateral to the dorsal part of the α-lobe, aiming to inject into PNs of the lACT.

When the brain appeared dry, a few drops of Ringer solution (130mM NaCl, 6mM KCl, 4mM $MgCl_2$, 5mM $CaCl_2$, 160 mM sucrose, 25mM glucose, 10mM HEPES, pH 6.7, 500 mOsmol; all chemicals from Sigma Aldrich) were applied. After dye injection, the head capsule was closed again with the original piece of cuticle, and bees were stored in a humid dark chamber at about 18-20°C for at least 3 hours or overnight. In the latter case bees were fed to satiation in the evening.

Before experiment, the head was fixated to the chamber more tightly using hard wax, the cuticle piece was removed, the window was enlarged, and tracheae were detached. In earlier experiments, legs and wings were removed to avoid movement of the bee and the brain, respectively. In later experiments the whole thorax and abdomen were pressed to the chamber using a piece of rubber foam attached to the chamber by some adhesive tape. In this latter preparation legs and wings were not cut.

A second hole was cut into the head to allow for overstretching of the esophagus to further prevent movement (adapted from Mauelshagen, 1993).

If no pharmacological experiments were accomplished, the space in the head capsule above the brain was filled with a drop of two component silicone (Kwik-Sil™, WPI, Sarasota, USA). All gaps between the head and the recording chamber were sealed with wax and silicone.

If sealing of the brain needed to be avoided for later drug application, the chamber and all gaps between head and chamber were sealed with wax and vaseline and ringer solution was dropped onto the brain.

Experiments began about 15 min after preparation.

Figure 2-1 illustrates a coarse reconstruction of stained KCs from two bees which were stained in the way described here. In Figure 2-1 A, the MB lobe from the right brain hemisphere is displayed. Stained KCs mainly project into the lateral calyx. Some axons projecting towards the median calyx are also clearly distinguishable, however, in the median calyx there is no staining within the lip region visible. At the lateral calyx one can see staining of somata and dendrites. In Figure 2-1 B the MB of the left brain hemisphere was reconstructed including staining of KCs projecting into the median calyx. The staining within the lip covers most of its volume. Due to the injection site located in the α-lobe, which is one output region of the MB, there is a lot of fixated dye in this region and clear structures like a bundle of axon branches are not visible in the α-lobe. What can clearly be spotted are thick bundles of axons running through the peduncles and connecting the input site in the lip with the output sites in the α-and β-lobe.

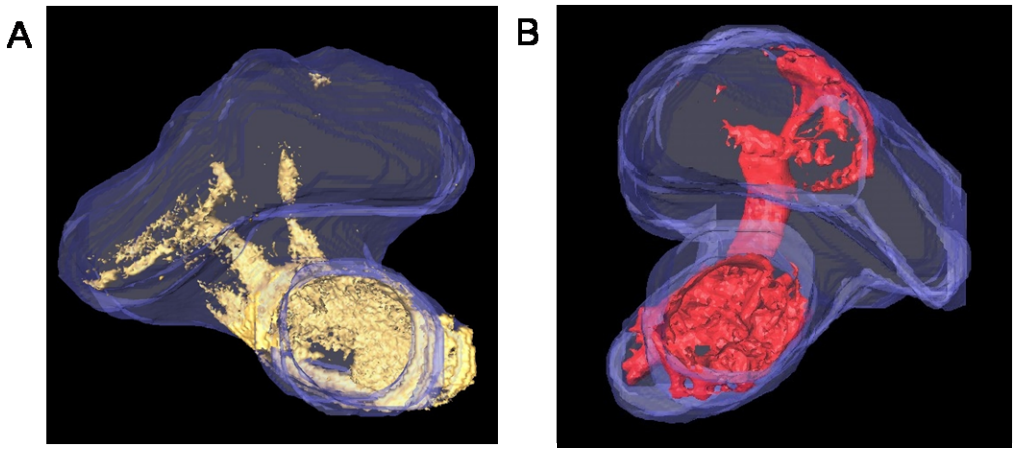

Figure 2-1 : Reconstruction of MB intrinsic neurons from mass staining, dye was injected into the ventral part of the α-lobe
Reconstruction of the outlines of the MB neuropil in blue
A: MB of the right hemisphere; in yellow: stained structures (rhodamine dye) scanned with CLSM after fixation; stained are KC axons in the lobes and in the peduncle as well as dendrites and somata of class II KCs in the lateral calyx.
B: MB of the left hemisphere; in red: stained structures (rhodamine dye) scanned with CLSM after fixation; stained are KC axons in the lobes and in the peduncle as well as dendritic structures in the median calyx.

Odor preparation

In most experiments an assortment of 13 pure odors was used (Sigma Aldrich, Germany), either the whole set or only a selection. These odors were:

1-hexanol (6ol), 2-hexanol (2-6ol), hexanal (6al), hexanone (6on),

1-heptanol (7ol), 2-heptanol (2-7ol), heptanol (7al), heptanone (7on),

1-octanol (8ol), 2-octanol (2-8ol), octanal (8al), octanone (8on), and linalool (lin).

Except for the highest odor concentration in the concentration series, odors were diluted in paraffine oil (FLUKA, Buchs, Switzerland) to the respective concentration. If not indicated otherwise, an odor concentration of 10^{-2} (1%) was used.

During experiments dealing with odor mixtures, the following odors (Sigma Aldrich, Germany) were used (according to Krofczik et al., 2009):

nonanol (9ol), 1-hexanol (6ol), 2-heptanone (2-7on), and their tertiary mixture called mix A,

pentanal (5al), nonanal (9al), 1,8 cineole, and their tertiary mixture called mix B.

These odors were diluted 1:10 in mineral oil (Sigma Aldrich, Germany).

All odor concentration are declared in percent by volume (v/v).

For odor application, 16 µl of liquid were put on a piece of filter paper which was placed in a Pasteur pipette. A 1000 µl pipette tip was placed at the end of the glass pipette which in turn was connected via teflon tubes to the olfactometer.

Pharmacology

A 100mM stock solution of picrotoxin (PTX, Sigma Aldrich, Germany) in DMSO (Sigma Aldrich, Germany) was prepared and stored at -20°C. Before experiment, the stock solution was further diluted in ringer to a final concentration of 10^{-4}M, 10^{-5}M or 10^{-6}M.

For bicuculline (bicuculline methiodide, BMI, Sigma Aldrich, Germany) a 10mM stock solution in distilled water was prepared and further diluted in ringer to a final concentration of 10^{-5}M.

CGP54626 (CGP, Tocris Bioscience, USA) was available as a 100mM stock solution in DMSO which was further diluted with ringer to concentrations of $2x10^{-5}$M, 10^{-4}M or $5x10^{-4}$M.

150 µl of diluted drug solution were bath applied to the brain after pre-treatment measurements. Therefore, some ringer solution was sucked off and substituted by drug solution. About 10 min later, measurements started. A wash out of the drug was not possible since experiments were run on intact animals and the solution perfused the whole animal's body. In fact, the attempt to wash out the drug often led to an increased drug effect which is most likely due to an even better penetration of the tissue with drug molecules. More washing would have been needed but the preparation used here allows only temporally limited manipulation. Waldrop et al. (Waldrop et al., 1987) described as well that it took more than 20 minutes to wash out picrotoxin form *Manduca* antennal lobe.

Control experiments with DMSO were performed with a concentration of $5x10^{-3}$M which is the highest concentration used in the experiments described in this work.

Calcium imaging

Imaging setup

Experiments were performed at approximately 25°C. Fluorescence was measured under two different alternating excitation wavelengths, namely 340 nm and 380 nm, corresponding to the characteristics of the employed fluorescent dye FURA-2. Using two excitation wavelengths enables ratiometric measurements. Excitation was performed using

a 410nm dichroic mirror; emitted fluorescence was detected through a 440nm long pass filter.

Images were recorded with a sampling rate of 6Hz using a TILL-Photonics Polychrome II imaging setup (Till Vision, Gräfelfing, Germany), mounted onto a fluorescence microscope (Axioskop, Zeiss, Oberkochen, Germany). The setup was controlled via a PC running the TillVision software (TILL-Photonics, Gräfelfing, Germany). Exposure time for each wavelength was adjusted for each animal according to the quality of the obtained signal.

Measurements started 2s before odor onset and lasted for 10s resulting in 60 double frames per measurement. Neuronal activity was recorded either through a 20x0.95 W dip objective or through a 60x0.9 W dip objective (both objectives Olympus, Tokyo, Japan) with a CCD camera (Visicam, Visitron Systems GmbH, Puchheim, Germany). CCD-resolution was 160x120 pixel (4×binned on chip). The spatial resolution was 2.2x2.2µm/pixel using the 20x objective or 0.7x0.7µm/pixel using the 60x objective resulting in an imaged area covering 350 µm x 260 µm or 112 µm x 84 µm, respectively.

KC somata and dendrites were imaged on the accessible, anterior surface of the MB calyx in the bee brain.

Odor stimulation

Odors were delivered to both antennae of the subjects using a computer controlled, custom made olfactometer (adapted from Galizia et al., 1997). Odor application was synchronized to frame 13 of the imaging process.

Odor loaded air was injected from the Pasteur pipettes into a permanent airstream. The main permanent airstream had a volume of 1000ml/min; the stimulus airstream had a 100ml/min volume implying that the odor got diluted in the permanent airstream by 1:10. When switching on the odor stimulus, a second, minor, permanent airflow of 100ml/min injected into the first one was switched off in order not to change the total airflow and to avoid mechanical stimulation by increasing the air volume. Stimulus duration was 3 seconds if not mentioned otherwise (chapter III). A LOGO! stimulus controller (Siemens, Germany) was used for all experiments except those, where two successive stimuli were applied. The air was permanently exhausted.

Presentation of 13 different odors: All odors plus control stimuli and the sucrose stimulus were delivered to the animal in a pseudo randomized order; presentation order was repeated 3 times.

Presentation of odor concentration series: The effect of a series with increasing or decreasing concentration was tested. After finding no effect, experiments were performed with an ascending concentration series.

Presentation of odor mixtures: the single components and the mix were delivered in a pseudo-randomized order, each stimulus 6 times.

Sucrose stimulation

The response to sucrose was tested as well. Using a wooden tooth pick, a 30% sucrose solution was applied to one antenna if not mentioned otherwise.

In all experiments, the interval between 2 measurements was 1.5 minutes.

Confocal microscopy and neuroanatomy

Since the fixable dye tetramethylrhodamine-dextran was always injected together with the calcium sensitive dye FURA-2, a later confirmation of the imaged structures could be undertaken using a confocal laser scanning microscope (Leica TCS SP2, Leica, Wetzlar, Germany).

Therefore, bees were sacrificed after the experiment; brains were removed and fixed in 4% PFA in PBS overnight at 4°C, then rinsed in PBS, dehydrated in an ascending ethanol series, and cleared in methyl salicylate (Roth, Karlsruhe).

Scans were performed at a laser scanning microscope using different objectives (all from Leica). Image resolution was 1024x1024 pixel.

Selected confocal stacks were further processed by importing them into the 3D AMIRA 4.1 software (Visage Imaging, Berlin, Germany); structures were reconstructed to visualize stained cells.

Data processing and analysis

While performing the experiments, images could be inspected on the PC using the recording software. Later processing of imaging data was performed with available custom written routines in IDL (RSI, Boulder, CO, USA).

First, a movement correction was performed if necessary using an IDL routine.
Changes in the calcium concentration were measured as absolute changes of fluorescence; a ratio between the images taken with the two excitation wavelengths 340 nm and 380 nm is calculated afterwards. One characteristic of the used calcium sensitive dye is that under an excitation of 340 nm the fluorescence increases with increasing calcium concentration; under excitation light of 380 nm the fluorescence decreases with increasing calcium concentration. Thus, a ratio between data from both measurements can be calculated to evaluate the relative change in the calcium concentration irrespective how high background fluorescence or baseline calcium concentration is. Ratiometric measurements improve the quality of the signal and make bleaching corrections needless. To compare different animals, the background fluorescence before odor onset is subtracted leading to ΔF with $F = F340/F380$.

For visualization of activity, false color coded pictures are generated: For each pixel the mean change in fluorescence over a certain time window is displayed. If not mentioned otherwise, the mean over 6 frames (according to 1 second, frame 13 to 18) after odor onset was calculated and the mean over 6 frames (frame 4 to 10) before odor onset was subtracted. A spatial low pass filter of 3x3 pixel was applied to reduce noise.
For calculating time traces, a region of interest (ROI) is defined by visual inspection on the basis of the false color coded pictures. Traces were calculated for the respective region by averaging pixel, no filter was applied here. From each frame, the background (mean over frames 4 to 10) is subtracted.
Changes in ΔF are approximately proportional to changes of the intracellular calcium concentration. Their absolute values, however, are influenced by several experimental parameters, such as amount of intracellular dye, background fluorescence of the tissue and light exposure time.
Quantitative data analysis and statistical analysis were done in Microsoft-Excel and MATLAB (Mathworks Cooperation, Natick, USA).

2.2 Electroporation experiments

Bee preparation

Honeybee foragers *Apis mellifera* were caught from the hive entrance, immobilized on ice, fixated in a metal tube using adhesive tape, and fed with a 30% sucrose solution. Several hours later or on the next day, electroporation was performed after fixating the head more carefully.

Electroporation and plasmid injection

Using an electroporator (CUY21EDIT, NEPA GENE, Japan) *in vivo* electroporation on honeybee brains was performed.

Either a pair of parallel needles (platinum, CUY567, NEPA GENE, Japan) were inserted into the bee's eyes (Figure 2-2 B) or custom made platinum wire electrodes were inserted directly into the brain between the central brain and the optic lobes (Figure 2-2 A).

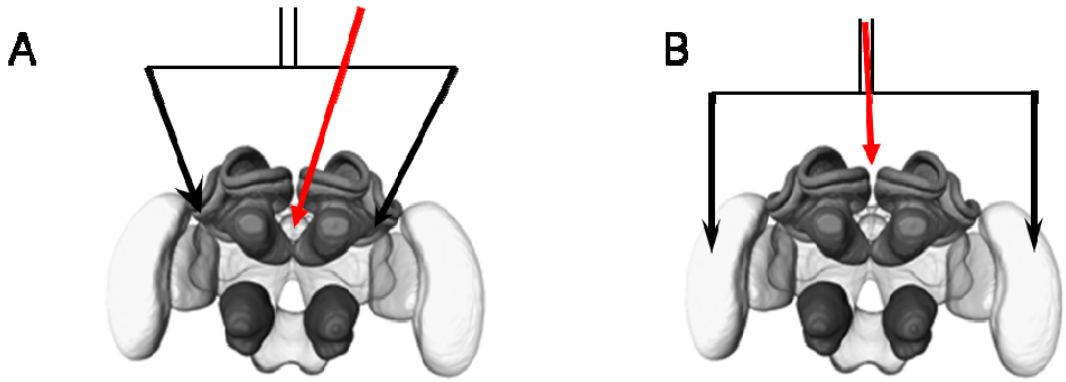

Figure 2-2 : different methods used for injecting the plasmid and electroporation
A : head capsule opened, application of plasmid on brain surface, insertion of wire electrodes through window in head capsule
B : plasmid injected through ocellar tract, parallel needle electrode inserted into eyes

Honeybees were injected with approx. 260 nl of plasmid solution (peGFP-C1, Clontech, Mountain View, CA, USA). The peGFP-C1 plasmid contains the GFP gene under a CMV – promoter. The used solution had a plasmid concentration of 2 µg/µl.

Injection was conducted 5 minutes before electroporation. When electrodes were inserted into the eyes, the solution was injected through the median ocellar tract (Figure 2-2 B, indicated by red arrow) down to the region of the mushroom bodies using a micro-injector

(Picospritzer II, General Valve Cooperation (Fairfield, New-Jersey, USA) or Pneumatic pico Pump PV820, WPI (Sarasota, Florida, USA). Therefore, a hole was pricked in the cornea of the median ocellus with an acupuncture needle before insertion of a fine glass capillary filled with the plasmid solutions.

When electrodes were inserted directly into the brain after opening the head capsule, the plasmid solution was applied right onto the brain surface (Figure 2-2 A, indicated by red arrow).

Pulse duration was 50 ms with inter stimulus interval of 950 ms (1 Hz). Voltage was 50V or 100 V; three or four pulses were applied.

Bees were sacrificed two days later to confirm successful electroporation. Until that bees were kept for 2 day in a humid chamber at 18-20 °C and fed once a day till saturation.

Evaluation was done by histological methods or by biochemical analysis.

Histology

Immunostainings were performed to enhance GFP signal.

After sacrificing the bee, the brain was dissected and fixed in 4% PFA in PBS. The sample was rinsed in PBS and embedded in 6% low melting agarose (Sigma Aldrich, Germany). After that slices of 100 µm were made using a vibratom (Leica VT1000S, Leica, Wetzlar, Germany). Slices were washed in PBS with 0.25% TritonX (Sigma Aldrich, Germany, PBS-T) for 4x30 min at RT, blocked with 10% normal goat serum in PBS-T for 1 hour and incubated with the primary antibody (mouse anti GFP, Invitrogen, USA, 1:400 in blocking solution) for 2 days at 4°C. Before application of the secondary antibody, slices were rinsed in PBS-T for 2 hours at RT. Incubation with the secondary antibody (goat anti mouse - CY5 conjugated, dianova/Jackson Lab, 1:500) was performed overnight at 4°C. Next day, samples were rinsed, dehydrated in an ascending ethanol series and embedded in methyl salicylate.

Scans were done with a confocal laser scanning microscope as described before.

Western blot analysis

After sacrificing the bee, the brain was dissected. The central part of the brain was removed and homogenised in 50 µl PBS with 2 mM EDTA, 2 mM EGTA plus 12.5 µl 5xSDS sample buffer (0.225 M Tris pH 6.8, 50% glycerol, 5% SDS, 0.05% bromphenol

blue, 0.25 M DTT) using a teflon-glass homogenizer. Homogenates were stored at -80°C until analysis.

After thawing, samples were denaturized in a thermo cycler at 95°C for 5 min.

Fifteen µl of a probe were loaded in a lane of a SDS – polyacrylamide gel, electrophoresis was performed (SDS-PAGE), and the gel got transferred onto a nitrocellulose membrane. The membrane was blocked in 1x PBS, 0.1% Tween-20 (Sigma Aldrich, Germany), 5% non-fat milk powder for 1 hour at room temperature (RT). Then, the membrane was incubated with the primary antibody (goat anti GFP, 1:500 in blocking solution, abcam, Cambridge, UK) overnight at 4°C. Afterwards, it was washed with 1x PBS, 0,1% Tween-20, 3 times for 10 min at RT, and incubated with the secondary antibody (rabbit anti goat IgG - Peroxidase conjugated, 1:160,000, Sigma, Saint Louis, USA) in 1x PBS, 5% non-fat milk powder for 1 hour. The membrane was washed again and developed by Western Lightning Plus Chemiluminescence reagent (Perkin Elmer, Boston, USA); a Kodak-film X-Omat AR (Sigma Aldrich, Germany) was exposed with signals.

3. Results

3.1 Characterization of Kenyon cell activity

Kenyon cells (KC), the principle cells of the mushroom bodies, are critical for odor coding and processing. The first levels of the olfactory pathway, the receptor neurons and antennal lobe neurons, were intensively studied and are fairly well understood. Recently, there are an increasing number of studies on the mushroom bodies ongoing; however, the coding principles and the physiology of the mushroom body intrinsic cells are still far from being deciphered. To extend the knowledge about this important group of neurons I focused on a subgroup of KCs which is essential in olfactory processing – the clawed KCs. At first, some of their general features were addressed.

Clawed Kenyon cells as subjects of this work

In Figure 3-1 the fine structures in the lip of the MB calyx are shown. KCs of type II, termed clawed KC, which are the subject of this work, can be seen. Figure 3-1 A shows a projection view of an image stack of a central bee brain after dye injection, scanned with a confocal laser scanning microscope (CLSM). Figure 3-1 B illustrates a scan with higher magnification from the same preparation. It shows a zoomed view of the region marked in A. Due to the limitations of the objective, some deeper parts were missing in the scanned stack and, consequently, the projection view looks slightly different from the one in A. The scanned stack in B was used for 3D reconstruction of KC somata and individual dendrites of some cells using the reconstruction software AMIRA. The result of this reconstruction is shown in D. KC somata which also can be seen in B were illustrated as well as some reconstructed dendritic parts of individual cells. The Figure 3-1 C shows the honeybee standard brain (http://www.neurobiologie.fu-berlin.de/beebrain/) including the registered display of KC somata and reconstructed dendrites. The MBs are displayed in red, the lip is bright red. Since the somata of the stained KCs are located outside of the calyx, they could get allocated to KCs type II. Due to limitations of the objective used in the scanning process, only the brain surface could be scanned whereas the deeper axons were not visible.

The somata of this type of KCs are arranged at one end of the cell, next to their dendritic input sites with typical claw-like extensions which could hardly become reconstructed due

to the mass staining of cells and limited resolution. This dendritic input region of KCs embraces the MB lip. On its other flank, the KC axons originate in the dendritic input region and project inside the calyx into the peduncle and further into the lobes. The large number of somata visible in the figure suggests that many cells got stained using the backfill technique.

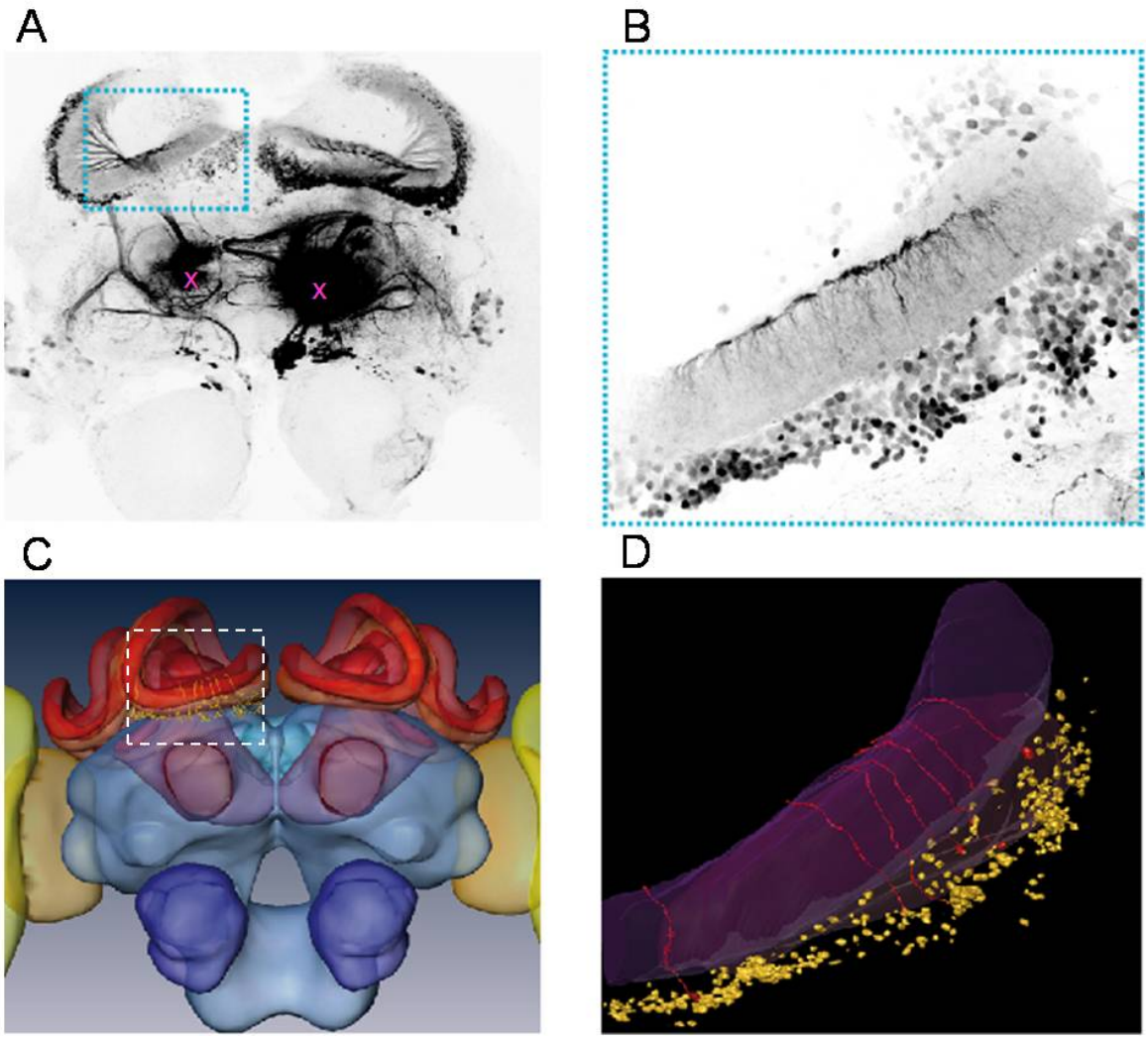

Figure 3-1 : Reconstruction of KC somata and dendritic region
A: Central honeybee brain with rhodamine staining accomplished by backfill via the α-lobe, magenta cross indicate injection sites, scanned with 10x objective at CLSM
B: Scan with 40x oil objective of the region marked in A, smaller z-range included
C: Honeybee standard brain with registered data from D: the MB are red, the lip neuropil is bright red.
D: Original data before registration into standard brain. Many somata of KCs lie outside the cup-shaped calyx. Somata are displayed in yellow, some individual somata and their dendritic region are demonstrated in pink, a cutout of the lip neuropil is purple.

Odor responses in Kenyon cells measured by calcium imaging

When performing a calcium imaging experiment, the calcium sensitive dye is often widely distributed in the lip neuropil after staining. This neuropil was optophysiologically imaged to perform the experiments described in this work. In Figure 3-2 A the calcium response in the frontal part of a median MB calyx is displayed as false color coded activity. The lip neuropil was imaged over a time period of 3 minutes. The whole frontal surface of the lip region of the calyx is visible which account for approximately 30% of the whole perimeter of the lip. In Figure 3-2 B response kinetics of different regions - marked in A - are plotted. The red lines indicate the duration of one odor pulse lasting for 3 seconds. I could observe an odor evoked response all over the lip. However, no strong, overall spontaneous activity was observed. Small excitatory events, arising from excitatory input from PNs could not be distinguished from noise.

Note, that in Figure 3-2 B the trace for region 0 is less noisy due to the large size of the marked area. Region 4, which was apparently outside the activated area, still shows a response which is due to the scattered light. However, this response is rather noisy.

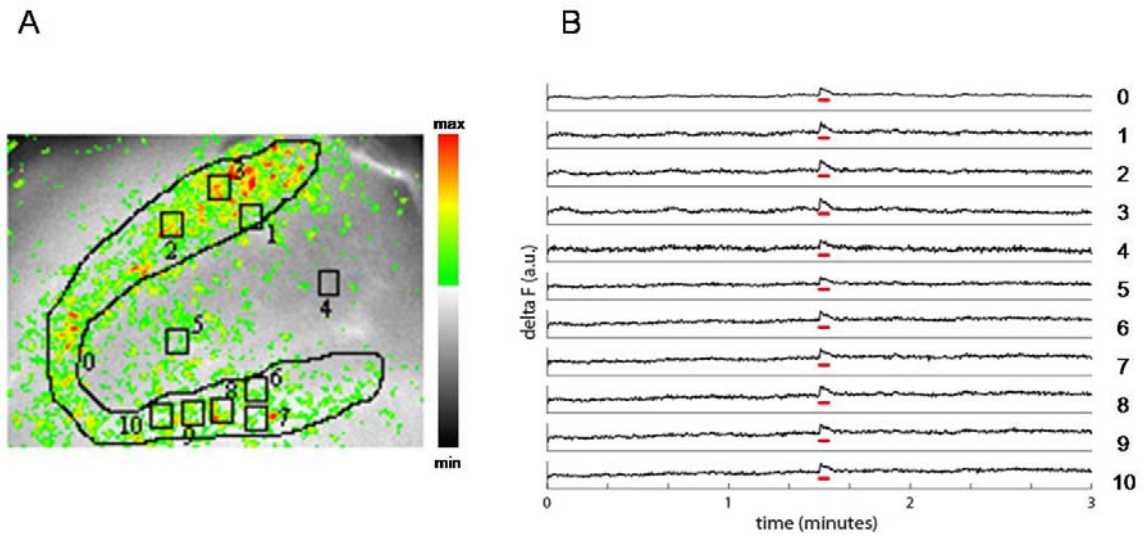

Figure 3-2 : Odor evoked calcium response in a median calyx
A: Averaged response during first second after stimulus onset, the activity is false color coded, imaged with a 20x objective; black squares indicate ROI 1 to 10, black line encircling the lip neuropil indicates ROI 0. Colors indicate activity measured as fluorescent change: red is highest activity.
B: Time traces of different regions of interest (ROI) as indicated in A over a time window of 3 minutes, odor pulse for 3 seconds (octanol) (a.u.: arbitrary units)

In my experiments, I measured the change of intracellular calcium concentrations as an indicator for activity in KCs. The response kinetic exhibited the characteristic phasic

response at odor onset (Szyszka et al., 2005) with a rather fast calcium increase and a slightly slower decay.

Neither inhibitory responses nor spontaneous activity have been described for KCs, but they probably get excitatory input arising from spontaneously active PNs since PNs emerging from the AL and projecting onto KCs show spontaneous activity (Abel et al., 2001;Krofczik et al., 2009).

Some, odors evoked additionally another response with a smaller peak after odor offset (also see Figure 3-4) referred to as off-response. The following figure (Figure 3-3) shows a characteristic odor response in clawed KCs.

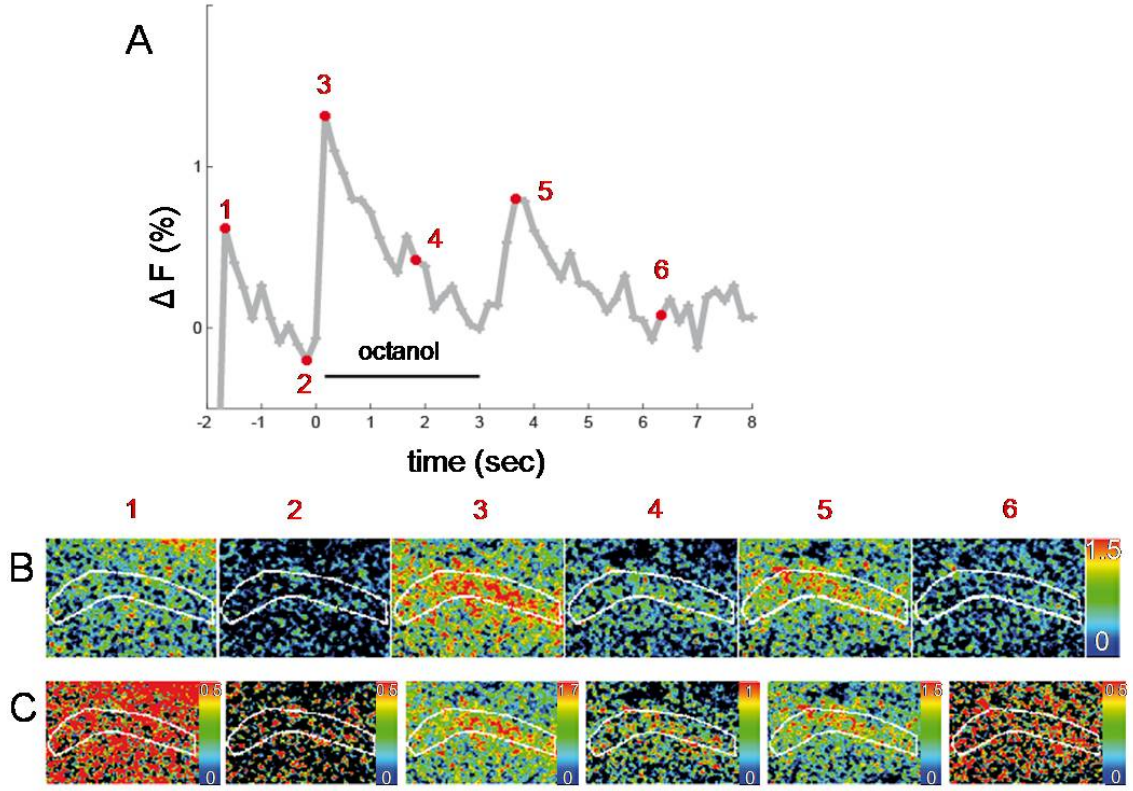

Figure 3-3 : Typical calcium response observed in the lip neuropil
A: Typical response kinetic of octanol-evoked response, red dots indicate time points corresponding to color coded pictures in B; Activity was measured over 10 seconds with a 6 Hz sampling rate, a 3 second odor stimulus was applied.
B,C: Color coded pictures indicating activity, single imaging frames, ROI (white) corresponds to the outline of the lip neuropil of a median calyx (ventral is up); B: all pictures are scaled to same min and max value, highest response after odor onset and odor offset; C: all pictures are individually scaled, here it becomes clear that the response at light onset is not limited to ROI but distributed over the whole display window

Figure 3-3 A shows a time trace calculated as mean over all pixels located inside the region of interest (ROI) indicated in white in all pictures in B and C. This region corresponded to the stained lip of the median MB calyx. At the beginning of the recording,

also a short phasic response at light onset was measured. In Figure 3-3 B and C, false-color-coded pictures show activation patterns inside the imaged area. They correspond chronologically to the red numbered dots plotted onto the time trace in A. In B, all false colors were scaled to the same range (ΔF ranging from 0 to 1.5 %). In the second row (Figure 3-3 B C), each picture was color coded to its own minimum and maximum.

The first images in B and C show that during response to light onset the evoked patterns were different from those patterns evoked by odor on- and offset: The response was not limited to the outline of the MB lip but rather dispersed over the whole imaged field. Additionally, one can see very similar response patterns to the odor stimulus' on- and offset, unfortunately it is impossible to track down the responses to identifiable cell populations because of the rather rough spatial resolution. The highest response was in both cases clearly limited to the lip region which is easily distinguishable due to its characteristic shape. The responses observed in the lip only differed in their absolute strength. This points out that at odor onset and odor offset cells from the same population or even the same cells were active, whereas the responding cells at light onset were different.

Response to odors of different chain length or functional group

The next experiments investigated the question if systematic response differences can be unveiled. Sachse et. al. (Sachse et al., 1999) compared odors having different chemical structures including varying chain length and different functional groups when imaging the AL. They found that the differences in the spatial pattern of odor responses are correlated with those parameters. These spatial patterns even lead to the establishment of an atlas of the honeybee AL.

When measuring the calcium activity over the accessible part of the MB lip neuropil, odor evoked activity was found for all tested odors. The following dataset was obtained from 4 animals, all measured in the lateral calyx. The odors used here were from different functional groups: primary and secondary alcohols, aldehydes, and ketones, having 6, 7, or 8 carbon-atoms in the carbon chain; in addition I used linalool. Most of these odors can be found in the bouquets of flowers. Linalool, for instance, is a main component of linden tree blossoms (*Tilia spec.*) and therefore of high ecological relevance for honeybees.

Each of the odors was applied three times; paraffin oil (PO) and clean air were used as control stimuli. Further, sucrose was applied as a stimulus.

Figure 3-4 A illustrates mean response kinetics of these different odors. All traces look rather alike except some showing a response peak after odor offset in addition to the on-response.

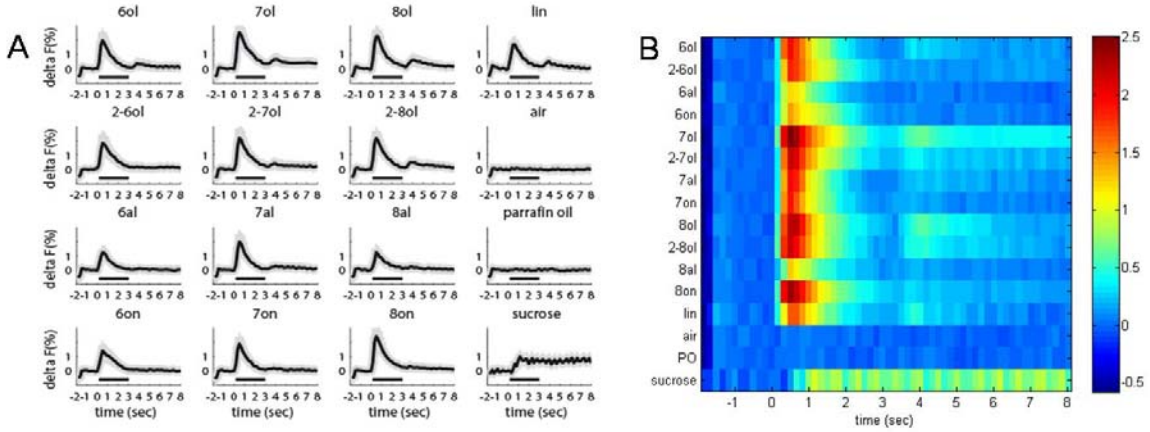

Figure 3-4 : Response to different odors
A: Response curve for different odors, mean, grey shaded: SEM (n = 12 trials from 4 bees, always lateral calyces)
B: Same data plotted as false color coded time course showing off-responses occurring in response to some odors

All primary alcohols (6ol, 7ol, 8ol) evoked an off-response; likewise did the secondary alcohols with 7 and 8 carbon atoms and the tertiary alcohol linalool. The controls with pure air stimulation and PO stimulation, the solvent for odor dilutions, did not evoke a response. Sucrose application evoked a long lasting response. Figure 3-4 B shows the same data as A but enables better comparison of signal strength and duration. Primary and secondary heptanol and octanol as well as octanone evoked a rather strong response; hexanal and octanal evoke only weak response here.

Comparing this data with findings from Hähnel (Hähnel, 2009), obtained in MB extrinsic neurons, it is apparent that response traces with different curve progressions were not found in KC. In extrinsic neurons some odors evoked only an off– but no on-response. But it is noteworthy that Hähnel used different odors than I tested in my work.

In Figure 3-5 a set of principal component analyses (PCA), which was performed on data from the same 4 animals, is illustrated.

For this analyses, based on the response kinetics, only data starting from 1 second before odor application until 4 seconds after switching off the odor loaded airstream was used, in total 8 seconds. Before running a first PCA, shown in Figure 3-5 A, the values of three

repetitive trials of the same odor per bee over 4 bees were averaged (n=12 measurement) in order to enhance the reliability of the data. The analysis revealed (**Figure** 3-5 A) that all odors cluster together, while the controls, air and paraffin oil, formed their own cluster and the sucrose response was separated as well from both other clusters. In Ai only the first and second component were used to plot data, in Aii data was displayed 3-dimensional with the first three components as axes of the coordinate plane. Here, different odors were marked by different colors/markers. All responses differed mostly in their absolute response strength and in the occurrence of an off-response. Variance in the data is already to 71.2% explained by the first principle component, and 24.9% by the second one, that means the first two components explained more than 96% of the variance. On the axis for the first component, odors evoking an off-response appeared on the negative side of the axis, odors not evoking an off-response on the positive side. This corresponded with the tendency that odors with 8 carbon atoms were further in the negative span on the axis and odors with 6 carbon atoms were in the positive span (Ai).

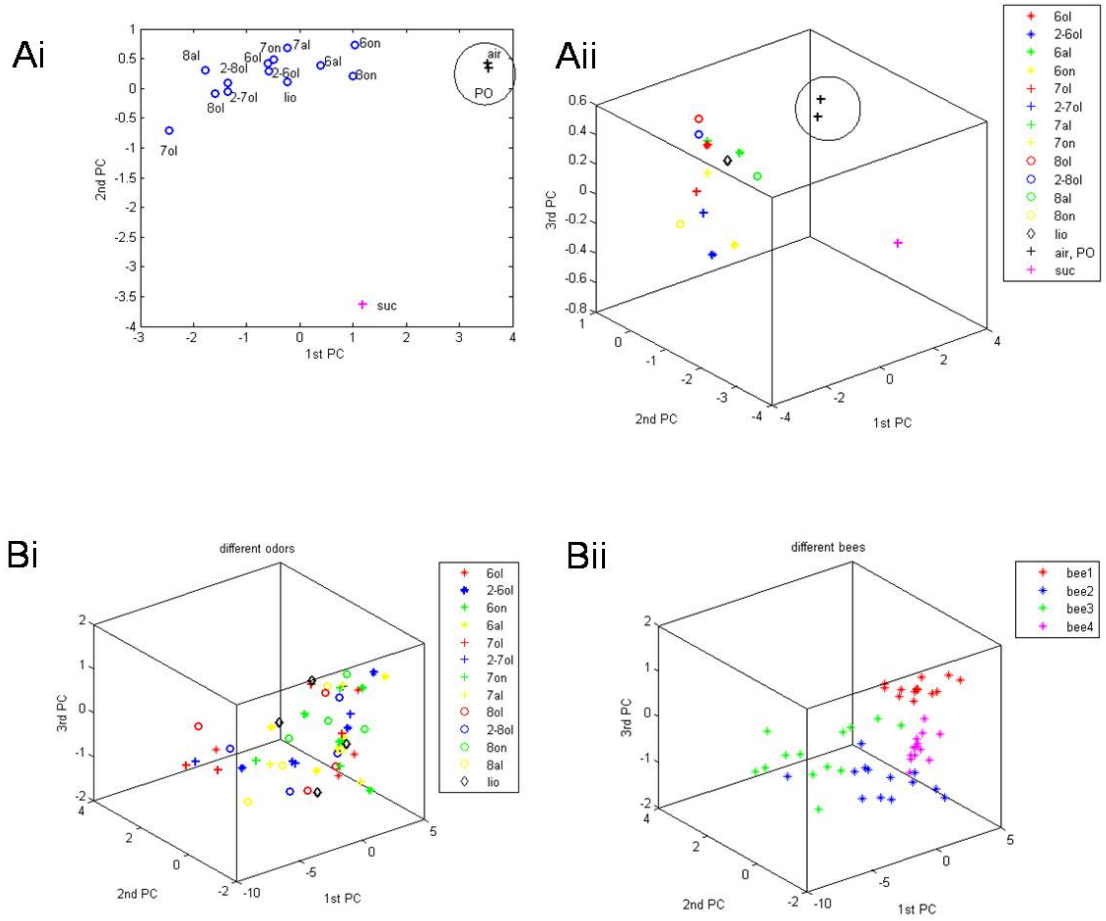

Figure 3-5 : Principal Component Analyses
A: Mean odor responses (averaged over 4 bees with 3 trials each) cluster in a PCA. The first two components explain 96% of the variance. Ai: two-dimensional display, Aii: three-dimensional display
B: Individual odor responses per bee averaged over repetitive trial cluster for the same bee (Bii) as can be seen in differently colored clusters, but do not cluster for the same odor (Bi).

In **Figure** 3-5 Bi and Bii, traces for individual bees (averages over three repetitive trials per odor, not pooled from different bees) were used for calculations. When looking at the three dimensional plots showing the first three principal components, it was found that data points cluster according to the different bees (Bii) but not according to different odors (Bi). This implies that responses to different odors within one bee are more similar than responses to the same odor in different bees. To investigate how homogenous responses to different odors are within one animal, I analyzed each bee separately.

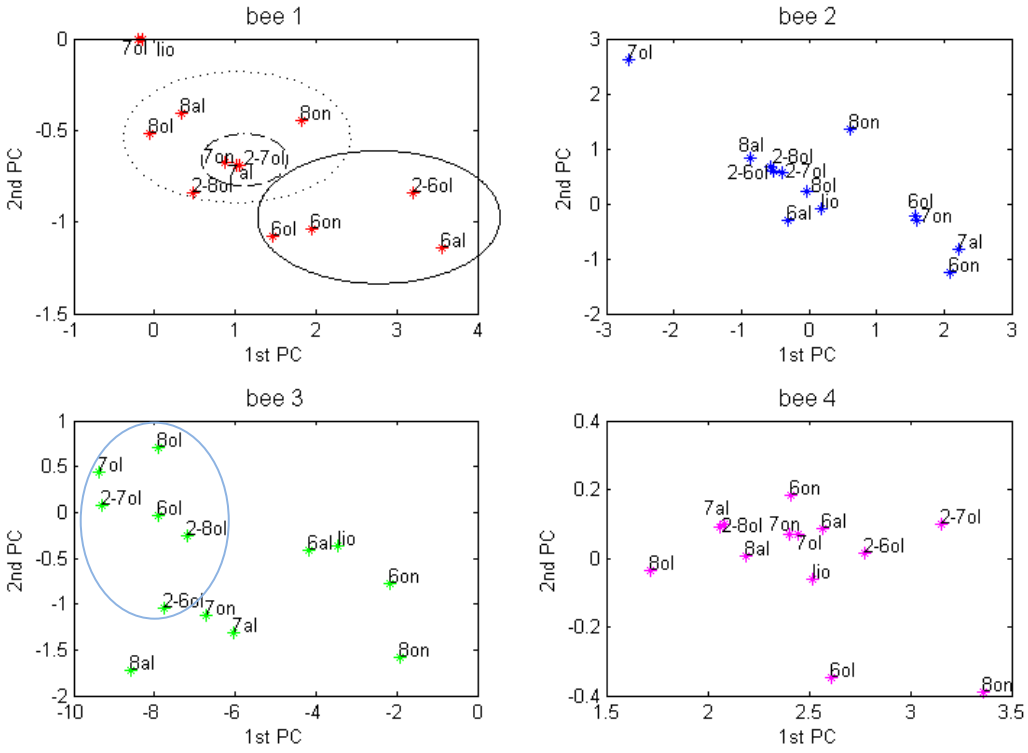

Figure 3-6 : Principle Component Analyses over odors per bee
For each bee a PCA was performed to compare odors within animal
Bee1: Solid line encircles odors with 6 carbon atoms, dashed line encircle 3 out of 4 odors with 7 carbon atoms, dotted line encircles odors with 8 carbon atoms.
Bee 3: All alcohols are encircles with solid blue line.

This analysis showed (Figure 3-6) that response to different odors were widely distributed over the whole sheet for each bee and odors were intermingled. Only for bee 1 and 3 clusters could be found: in bee 1 all odors with 6 carbon atoms clustered in the upper part of the positive span of component 1 and were separated from other odors; in bee 3 all alcohols were clustered in the lower part of the spectrum of component 1. No common pattern for all bees was found.

Figure 3-7 represents an illustration of another PCA showing trajectories over time. In A trajectories were grouped by chain length; in B measurements of odors that have the same functional group were put together in each respective plot. This analysis was conducted with a time window ranging from 1 second before, 3 second during, and 1.5 seconds after stimulus application. After that time, all trajectories have again reaches the starting point close to zero.

The plots show that all odors yield rather similar trajectories. Aldehydes (green in A and Figure Biii) tended to evoke a weaker response and therefore the slope of time trajectories was smaller. The three primary alcohols differed slightly in their maximum response.

Outstanding differences could be observed neither between different functional groups nor between different chain lengths.

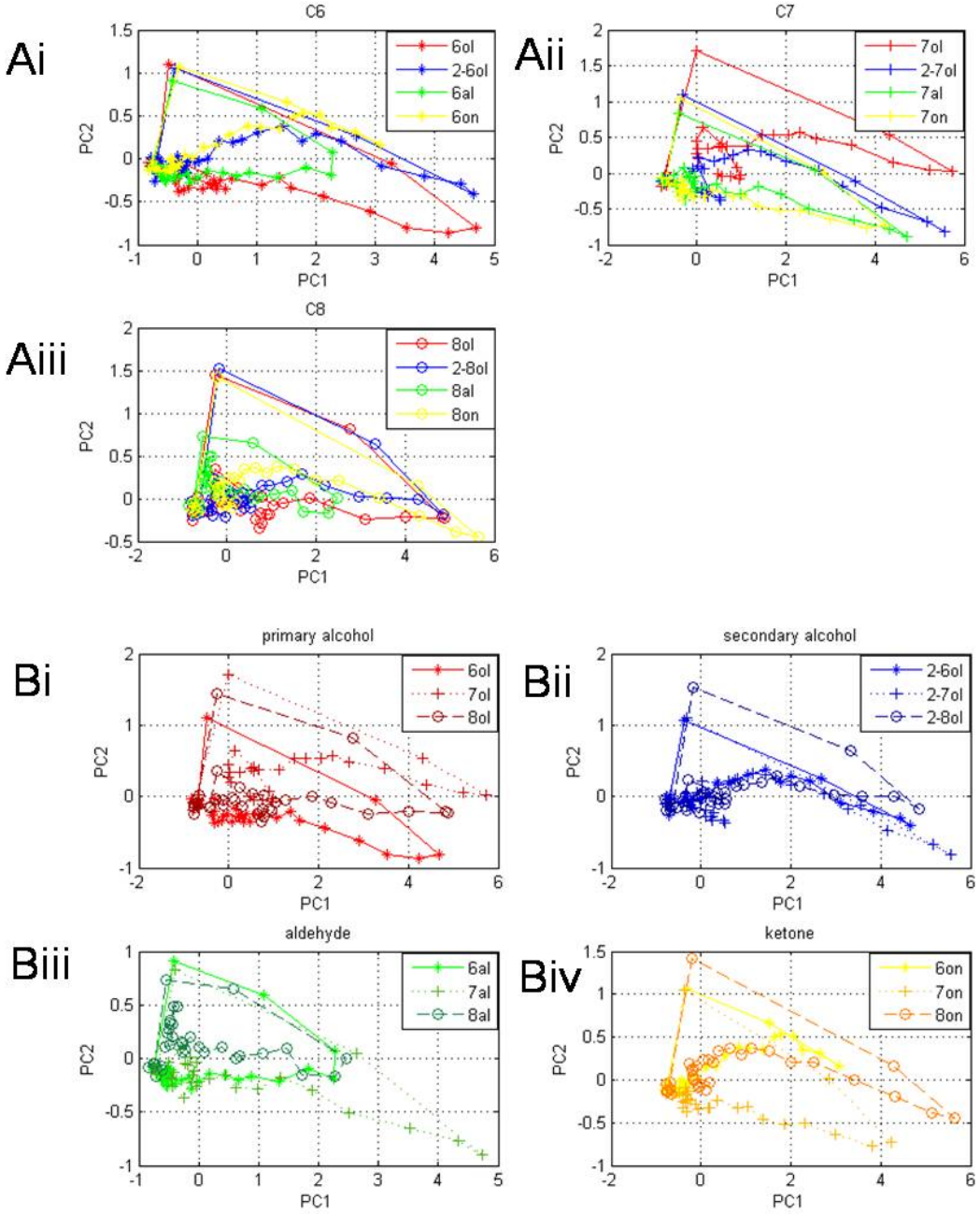

Figure 3-7 : Time trajectories
A: Combined depiction of trajectories for odors with same number of carbon atoms
B: Combined depiction of trajectories for odors of same functional group

Off-responses in Kenyon cells

As already demonstrated in the previous experiments, some measurements showed an increased intracellular calcium concentration after odor offset. This was true for most alcohols.

Off-responses were also known from other cells in the olfactory pathway. In the honeybee's antennal lobe, for instance, some glomeruli respond at odor onset, other glomeruli at odor offset (Sachse and Galizia, 2002). Off-responses were also seen in KCs of other insects (Ito et al., 2008).

Figure 3-4 showed a plot of the mean responses to different odors over a time frame of several seconds, so the off-responses could also be seen: alcohols tended to show off-responses whereas aldehyds and ketones did not. Off-responses to hexanol were smaller than to heptanol and octanol.

I never observed a calcium response that is dominated by the off-response as Hähnel was able to show for benzaldehyde and 1-nonanol in MB extrinsic neurons (Hähnel, 2009).

Responses to non olfactory cues

As already shown in Figure 3-3, there is also light evoked activity in the MB. While performing calcium imaging, the light switched on when the measurement started, beginning with a 340 nm light pulse of about 10 msec. The spatial activation pattern during this light evoked response looked different than during odor supply, indicating that other cells are responding to light than to odors.

Figure 3-8 shows another example of a preparation were a prominent response at light onset can be seen. In A an overview from the imaged brain is shown indicating the region where imaging was performed. This image proves the successful staining of KCs, since axon bundles in the peduncle and in the β-lobe are clearly visible. However, somata of type II KCs were barely stained. The ROI 1 in Figure 3-8 B corresponded to the lip neuropil, ROI 2 was located inside the calyx where KCs type I have their somata. For light onset, the same response strength in both regions could be observed, whereas for odor onset the response was much stronger in ROI 1 - the lip of the calyx. This finding matches the fact that sensory input from the visual system enters the calyx not in the lip but in its collar region.

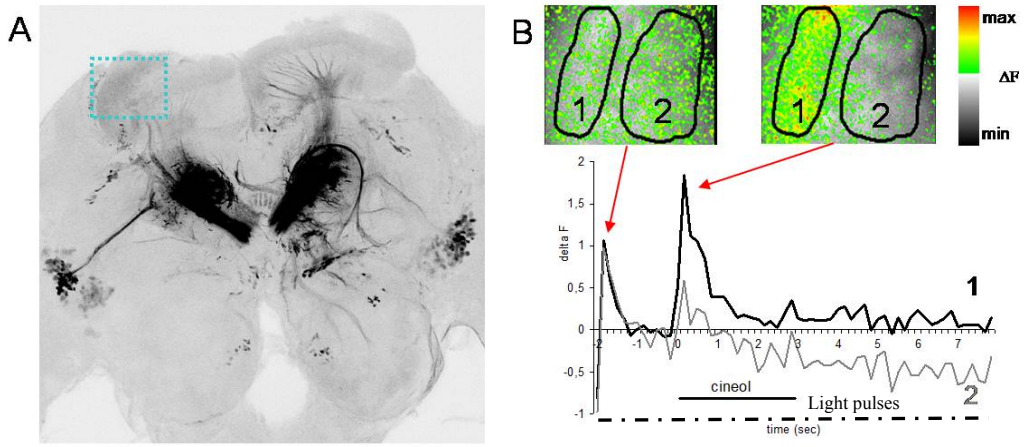

Figure 3-8: Example showing response to light onset
A: Scan from CLSM indicating monitored region, KC axons are clearly visible in the β-lobe and in the peduncule.
B: False color coded pictures of light onset (left) and odor onset (right), two ROI are selected.
Response amplitudes over time of two ROI are plotted. Both regions showthe same response during light onset, during odor onset the ROI 1, which corresponds to the dendritic input region, shows higher response.

A representative example for a response curve, measured in KCs in the calyx after applying sucrose as a stimulus, is shown in Figure 3-9.

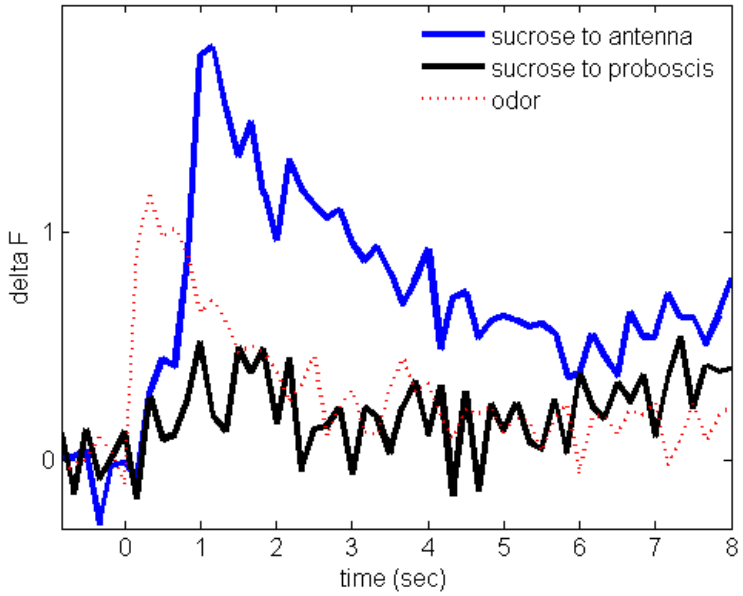

Figure 3-9 : response in KCs to sucrose application
The response measured in KCs when applying sucrose to one antenna is displayed in blue, the response when applying sucrose to the proboscis is black
For comparison: the red dotted line shows response to odor application (octanol), note that sucrose responses start with little delay due to manual application by experimenter

The stimulus was either given to one antenna or to the proboscis; concentration of the sucrose solution was 30%. The response to antennal stimulation was much higher (blue line), while only little response could be seen to proboscis stimulation (black line). For comparison I also plotted the response at odor application (red dotted line, octanol in a 1% concentration + further dilution in permanent airstream). The sucrose evoked response was higher than the odor evoked response. The temporal delay is due to the handling by the experimenter.

3.2 Effects of odor intensity on Kenyon cells and influence of GABA

3.2.1 Odor intensity is coded in Kenyon cells

Correlation between odor intensity and calcium response in Kenyon cells

Using calcium imaging techniques it was shown that the response in olfactory PNs is correlated with odor intensity (Sachse and Galizia, 2003;Yamagata, 2008). But, how odor intensity is coded in the brain, is still unknown. Also it is unknown, how different intensities of the same odor are processed in KCs.

Odors of different intensities can be distinguished and learned by bees (Wright et al., 2009), as well as other insects (Yarali et al., 2009). Since MB are involved in olfactory learning, KC, the MB intrinsic cells, should also sense odor intensities. Individual KCs are described as responding very sparse and odor specific. It is also possibly that they respond concentration specific (Stopfer et al., 2003). Thus, the question of how honeybee KCs deal with different odor concentrations is addressed here.

When testing different concentrations of the same odor, I applied the concentrations in an ascending or descending order.

I tested if the increasing or decreasing row of concentrations has any influence on the response, which might be due to adaptation or a repetition effect and found no differences for either increasing or decreasing odor concentrations in the sequence of odor

applications (data not shown). Thus, given the experimental conditions (ISI 1.5 min) the direction of the sequence does not influence response intensity.
In the following experiments, I measured concentration sequences starting with the highest dose. I applied six concentrations of odors ranging from pure odor to a 5 times logarithmic dilution (10^{-5}, -5). Note, that each concentration gets further diluted in the permanent airstream by 1:10.

For all tested odors (hexanal, 1-hexanol, 2-heptanon, 1-octanol) a positive correlation between concentration and calcium activity in MB KCs was found when performing calcium-imaging of the dendritic region of KCs in the calyx. Time courses of calcium responses to different dilutions of the same odor are shown in Figure 3-10 for two odors: hexanal (A) and 1-octanol (B).
Lateral and median calyces were subject to my investigations. Although to my knowledge no functional differences between the two calyces of a MB were described, I analyzed the data separately. Figure 3-10 Ai and Bi show traces measured in median calyces, Aii and Bii show responses in lateral calyces. This figure illustrates that time courses in response to different odor concentrations look similar, however, they differ in their amplitude's maximum: With increasing odor concentration the response amplitude increases. All responses show a phasic response with fast rise and slower fall of the signal. For the lowest concentration, a dilution of -5, still a small response is observed. At high odor concentrations there are higher amplitudes observed in the lateral calyces compared to the median calyces. The mean responses are higher for hexanal than for octanol.

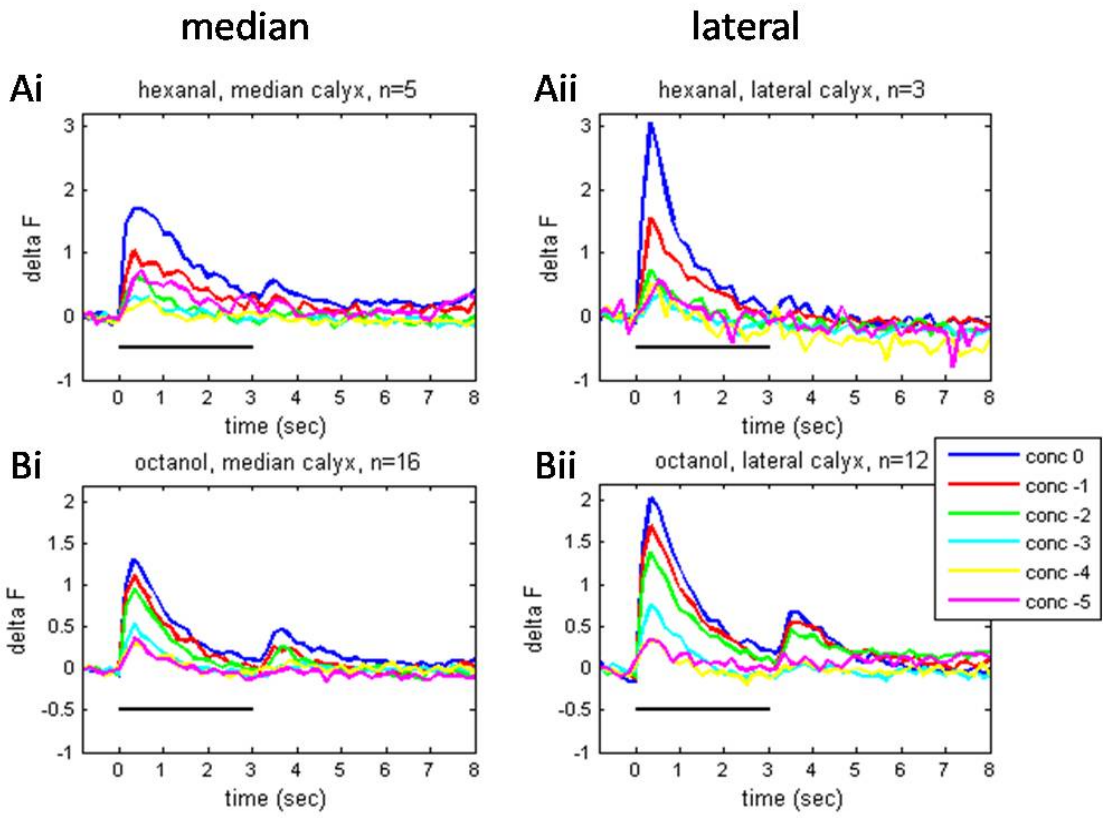

Figure 3-10: Time courses of responses to different odor concentrations in the median and lateral calyces
In each experiment the bee was exposed to 6 different concentrations of odor ranging from pure odor (conc 0) to a logarithmic dilution of -5.
Ai, Bi: Mean responses in the median calyces to hexanal (Ai) and octanol (Bi)
Aii, Bii: Mean responses in the lateral calyces to hexanal (Aii) and octanol (Bii)
Black bars indicate odor stimulus

To quantify the time courses, I calculated the mean response over the three seconds of odor application (Figure 3-11 Ai and Aii) and the mean over the first second only of odor stimulation (Figure 3-11 Bi and Bii), since most of the response is confined to this first second after odor onset. This allowed me to plot dose response curves over six different odor concentrations; dose response curves for different odorants are shown (Figure 3-11).

The curves do not reach saturation level. For hexanal (blue curves in Figure 3-11) exponential curves were obtain; the dynamic range is between undiluted odor and dilution -3. For lowest concentration (-5) in both, median and lateral calyces, the response strength slightly increases compared to the -4 dilution.
For octanol (red curves) I found for both calyces sigmoid curves with a dynamic range between -2 and -4.

A small increase at lowest concentrations was observed for lateral calyces (Aii, Bii).
For hexanol only data for the lateral calyces were available. The dose response curve was rather linear. Between the -3 and -1 dilution, the curve ran very similar to the one for hexanal. However, for the highest concentration the increase in response strength was smaller. It reached maximal values similar to octanol. Using the odorant heptanone, the response in the median calyx was measured obtaining a sigmoid curve reaching a maximal value, at highest dose, similar to hexanal.

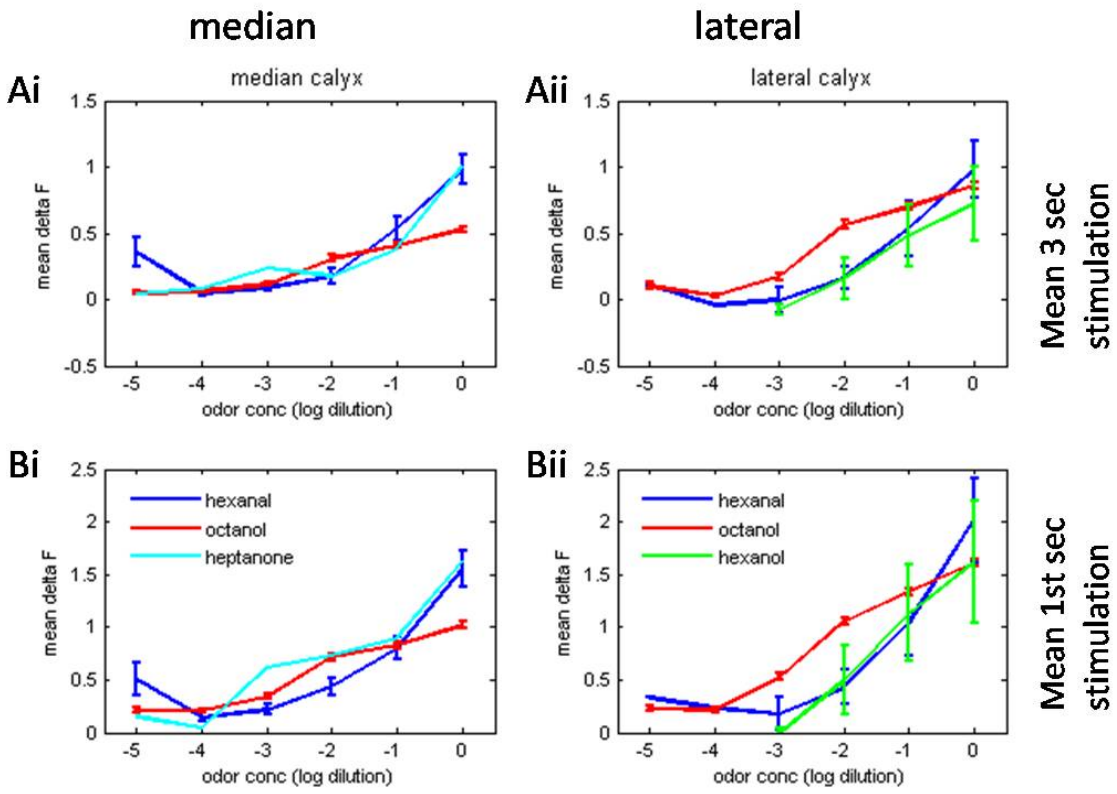

Figure 3-11: Dose response curves to four different odors in median and lateral calyces
Left: median calyx, right: lateral calyx
Hexanal (blue) median: n=5, hexanal (blue) lateral: n= 3, octanol (red) median: n=16, octanol (red) lateral: n=12, heptanone (light blue) median: n=1, hexanol (green) lateral: n=3; Mean, SEM

There was no difference between the curves calculated from the first three or just the first second of odor stimulation, except that the values calculated from the first second were higher. This demonstrates, as already could be seen from the time courses, that most calcium activity occurs during the first second of odor application. Therefore, further quantitative analysis is based only on this first second after odor onset.

Odor sensitivity in the median and in the lateral calyx

When comparing response curves of the median and the lateral calyces, I found that the response signals in the lateral calyces were on average higher, compared to median calyces, when applying highly concentrated odors. This was already visible in the previous figures. To visualize this, I plotted curves for the median and lateral calyces of the same odor in one figure (Figure 3-12 Ai and Aii).

For stimulations with the odor 1-octanol, I applied a statistical analysis (Two-sample t-test, n=16 for median, n=12 for lateral). A significant difference between lateral and median calyx at the two highest odor concentration (p=0.0052 and p=0.0098 for concentration 0 and -1 respectively) was found when calculating the response over the first second after stimulus onset (Figure 3-12 Aii). Even when averaging over the whole 3 seconds of odor supply, the difference is still significant (p=0.019 and p=0.028 for concentration 0 and -1 respectively, curves not shown).

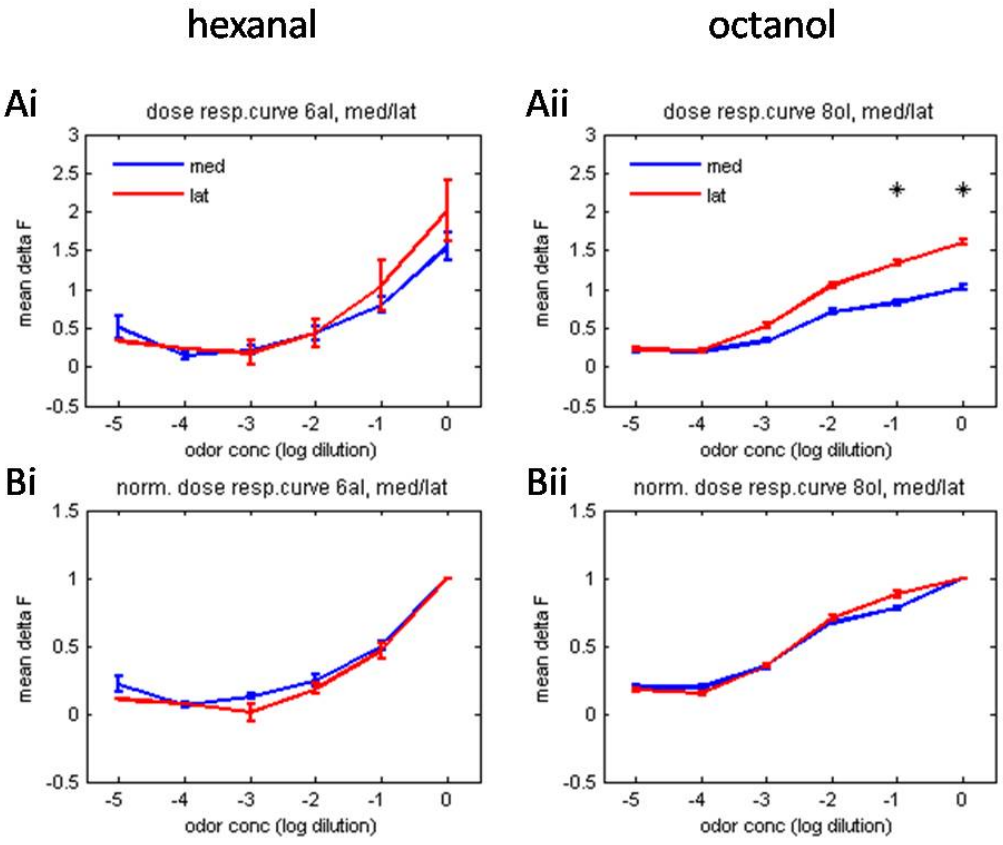

Figure 3-12: comparing dose response curves of median and lateral calyces
Left: hexanal, right: octanol
Ai, Aii: averages dose dependent responses in lateral (red) and median (blue) calyces.
Bi,Bii: data as in A but normalized to response to highest dose
octanol: n=12(lateral), 16(median), 6al: n= 5(median), 3(lateral), Mean, SEM
Two-sample t-test for octanol: p=0.0052 (odor conc 0), p=0.0098 (odor conc -1)

For hexanal no statistical test could be performed due to the small number of animals, but the effect is visible here as well.

When normalizing the dose-response curves to the highest odor concentration (Figure 3-12 Bi and Bii), curves ran very similar, the response dynamics were the same in the lateral and the median calyx and the curves are in each case exponential for hexanal and sigmoid for octanol.

Concentration sensitivity of single cells

To understand the principle of intensity coding in KCs one also has to look at the level of individual cells. Using calcium imaging, this can be done by investigating the response in single somata.

In Figure 3-13 an example of two responding somata within one preparation is shown. Both somata responded to octanol. One soma, marked with a blue arrow (ROI 1), is activated upon stimulation with octanol when applying different concentrations ranging from dilution 0 (100%) to dilution -3 (0.1%). For another soma (magenta arrow, ROI 2) a response was measured for concentration ranging from dilution 0 (100%) to -2 (1%).

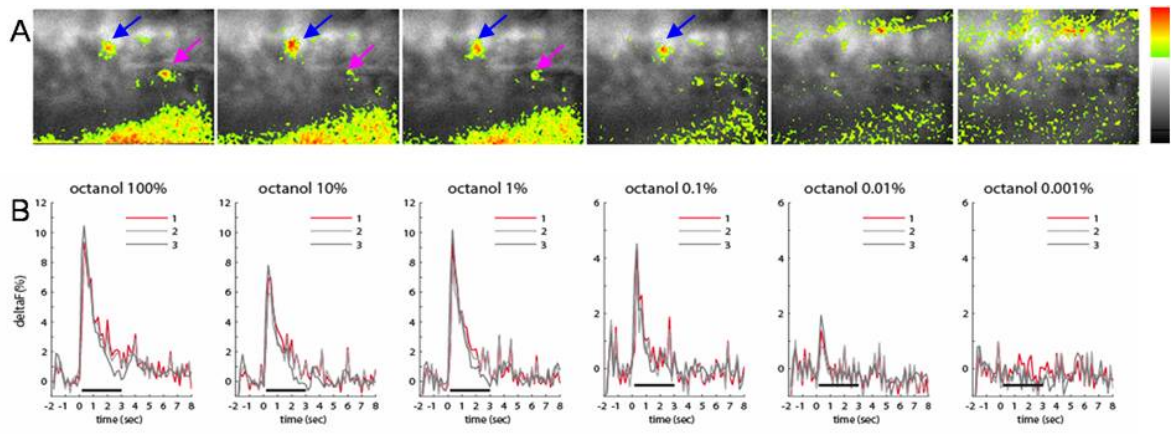

Figure 3-13: Soma responding to different concentrations of the same odor
A: All pictures are scaled to individual min and max value. Pictures become noisier with smaller response. Soma in ROI 1 (blue arrow) is responding to the 4 highest concentration of octanol
The soma in ROI 2 (magenta arrow) responds to 100%, 10%, and 1 % odor concentrations
B: time traces for ROIs, ROI 3 corresponds to the neuropil at the bottom of the picture, note differences in y-scale with decreasing odor concentration

Thus, somata are not specific for a certain concentration but rather have an effective range covering several orders of magnitude. Different cells have different activating dose ranges.

One soma in the example was already active from a dilution of -3 onwards, the other one only from -2.

The calcium response in the respective soma was always correlated to response amplitude in the neuropil (ROI 3). Here, the absolute increase in calcium concentration depended on odor intensity.

Correlation between odor intensity and off-responses in Kenyon cells

Some odors evoke responses at odor onset and odor offset. Such responses were described in the previous chapter. In Figure 3-10 of this chapter it can be seen that not only responses at odor onset are dose dependent but also responses at odor offset are sensitive for odor intensity. In Figure 3-14 dose response curves for off-responses calculated from the time traces shown in Figure 3-10 are shown. Again higher responses in the lateral calyx were found. Also in the lateral calyx, increasing responses at low doses were found for stimulation with octanol.

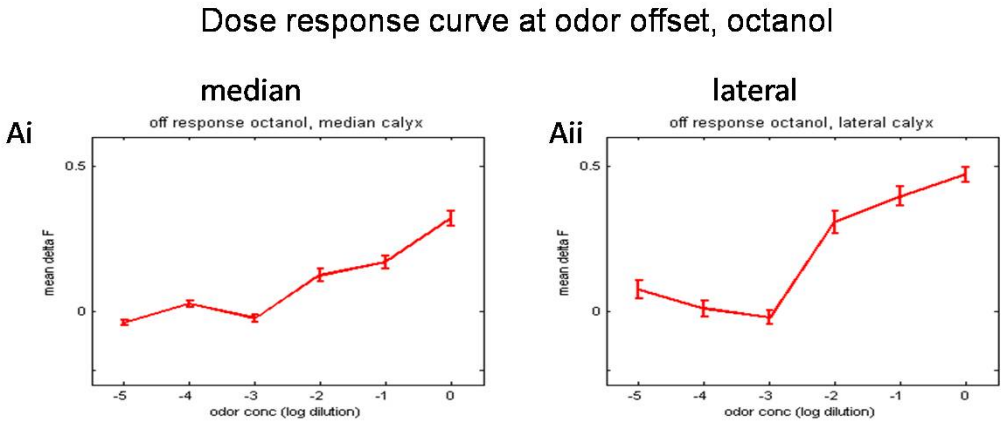

Figure 3-14: off-responses show dose dependency
Calculated over 1 second after odor offset, mean (median n=16, lateral n=12), SEM

3.2.2 Influences of GABA on Kenyon cell response

Impact of $GABA_A$ receptor blocker picrotoxin on Kenyon cell responses

As I have shown in the experiments by applying different odor concentrations, the response amplitude changes with odor intensity. The used concentrations span several orders of magnitude. Compared to this wide range, the increase in response strength with

increasing odor intensity is low. This points to a gain control mechanism by inhibitory synaptic input (Assisi et al., 2007;Stopfer, 2005).

In PN boutons, which are presynaptic to KCs, many inhibitory events were measured with the calcium imaging technique (Yamagata, 2008). These two facts lead to the question whether GABA-mediated inhibition has an impact on KC responses.

Therefore, I investigated in the next step how GABA influences response of KCs by using GABA receptor antagonists. I asked how the amplitude changes when not only the odor concentration varies, but also the GABA-mediated inhibition in the honeybee brain in blocked.

First I used PTX, a $GABA_A$ receptor blocker. I tested different concentration of the drug: 10^{-6}M, 10^{-5}M, and 10^{-4}M.

The lowest dose had no or only a little effect on the response, 10^{-5}M had a strong effect (Figure 3-15). The highest of those concentrations, 10^{-4}M, completely abolished signal (not shown).

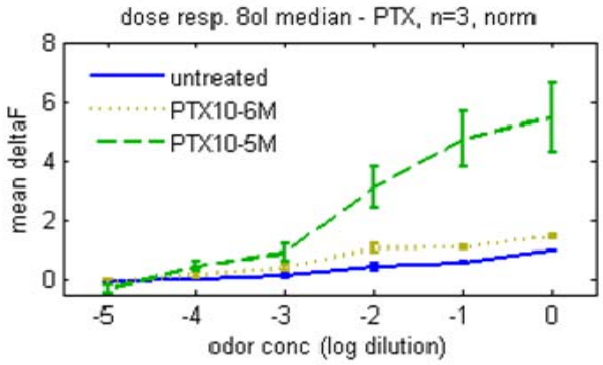

Figure 3-15: Effect of different concentrations of picrotoxin on dose response curve, applied odor was octanol
Responses of KCs before and after treatment with 2 concentrations of picrotoxin, data normalized to response at highest odor concentration in the untreated run (n=3 animals, mean, SEM)

Bath application of PTX in a 10 µM (10^{-5}M) concentration leads to a highly increased response amplitude at higher odor concentrations, as can be seen in Figure 3-16. This figure shows response traces measured in a MB calyx before and after treatment with 10^{-5}M PTX when the animal was exposed to different odor concentrations of octanol. It is noteworthy that in spite of PTX application, the concentration dependency is still apparent.

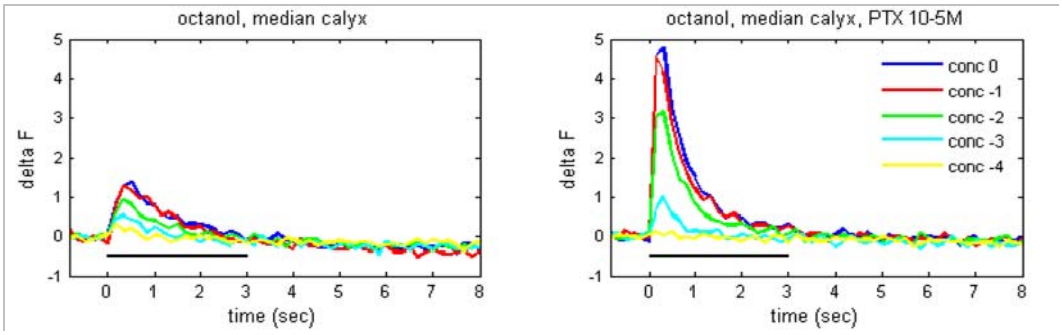

Figure 3-16: Example of one bee before and after PTX application
Five different concentration of octanol were applied, left: before treatment, right: after treatment with 10^{-5}M PTX

This applies for both, lateral and median calyces. In the bee shown in the next figure (Figure 3-17) the odor 1-octanol was used as the stimulus. In the median calyx (Figure 3-17 Ai) the increase in response strength is significant for the three highest odor concentrations (left-tailed paired t-test, p=0.0063, p=0.0067, p=0.027 for odor concentrations 0, -1, and -2 respectively). The odor concentration -2 (1% odor in Paraffin oil) is normally used for odor coding experiments. For the lateral calyx no statistical test could be performed due to the limited number of bees, but the effect can clearly be observed here as well, although less strong (Figure 3-17 Aii).

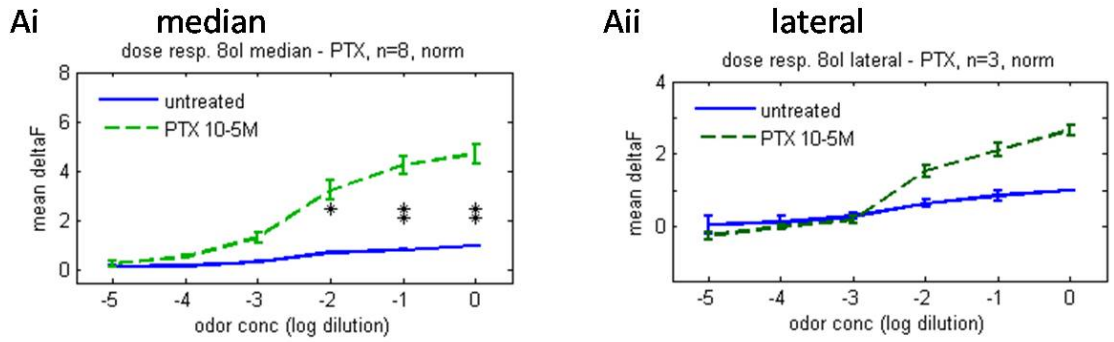

Figure 3-17: Effect of picrotoxin on dose response curves in median and lateral calyx
(mean, SEM)
Ai: Dose response curves for octanol before and after treatment with PTX, median calyx, n=8, left-tailed paired t-test, p=0.0063, p=0.0067, p=0.027 for odor concentration 0, -1, and -2 respectively)
Aii: Dose response curves for octanol before and after treatment with PTX, lateral calyx, n=3

While in the first set of experiments it was observed that responses to high odor intensities are generally stronger in the lateral calyces, now it was found that the PTX mediated increase in response strength is higher in the median calyx. Due to small number of bees, a statistical test could not be applied.

Similar effects can be observed when using other odors; hexanal and heptanone were tested (data not shown).

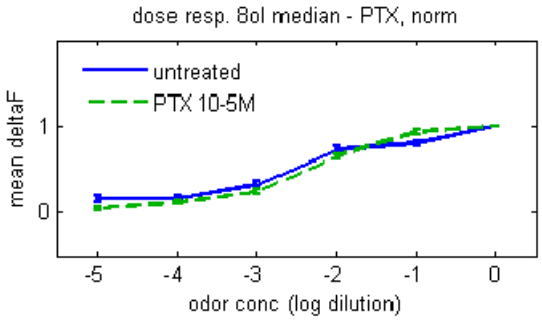

Figure 3-18: Dynamic range not changed by picrotoxin
Dose response curves for octanol before and after treatment with PTX, median calyx, n=8, curves mormalized to highest response (mean, SEM).

When normalizing both, the dose response curve for untreated bees and the curve after PTX treatment, the curves look rather similar suggesting that the response dynamic does not change (Figure 3-18), the curve is stretched between -3 and -1 odor concentration when applying PTX and response is approaching saturation at the -1 dose.

Impact of $GABA_A$ receptor blocker bicuculline on Kenyon cell responses

Bicuculline methiodide (BMI) is another blocker of $GABA_A$ receptors which probably acts via another target or mechanism.

In KC, an application of 10^{-5}M BMI increases calcium response to odor stimuli of a concentration of -2 and higher (Figure 3-19). The dose response curve is saturated at high odor concentration. BMI has its strongest effect at an odor intensity of -2. The absolute increase of calcium response when BMI is applied is much smaller compared to PTX application.

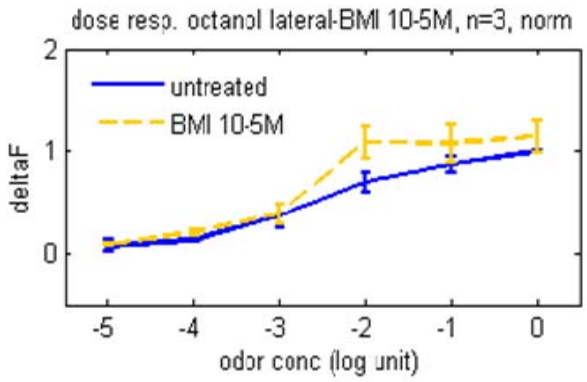

Figure 3-19: Effect of BMI on dose response curve
Dose response curves for octanol before and after treatment with BMI 10^{-5}M, n=3, mean, SEM
Only data from lateral calyx available

Impact of $GABA_B$ receptor blocker CGP 54626 on Kenyon cell responses

In a next experiment, I applied CGP54626 which is a blocker of $GABA_B$ receptors. $GABA_B$ receptors are metabotrophic receptors. This drug has been shown to be effective in honeybees and other insects (Gühmann, 2007b;Root et al., 2008;Wilson and Laurent, 2005;Rotte et al., 2009).

I tested two concentrations and found $5x10^{-4}$M to be the most effective one (Figure 3-20). A $2x10^{-5}$M concentration of CGP54626 does not cause any effect.

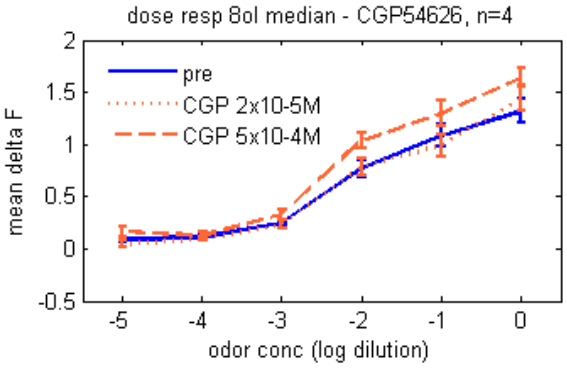

Figure 3-20: Effect of different concentrations of CGP54626 on dose response curve
Dose response curves for octanol before and after treatment with different concentrations of CGP54626, n=4, median calyx, mean, SEM

Also this receptor blocker has an impact on the signal amplitude in KCs. When administering a 500 µM ($5x10^{-4}$M) concentration, a significant increase in response amplitude at higher odor concentrations is found. The difference (median calyx) before

and after treatment is significant at the three highest odor concentrations (left-tailed paired t-test, n=6, p=0.0437, p=0.0333, p=0.0092 for the odor concentration 0, -1, and -2 respectively).

Similar results can be obtained in the lateral calyx, but no statistical tests could be applied due to the smaller number of tested animals (n=3 bees, all animals show same effect).

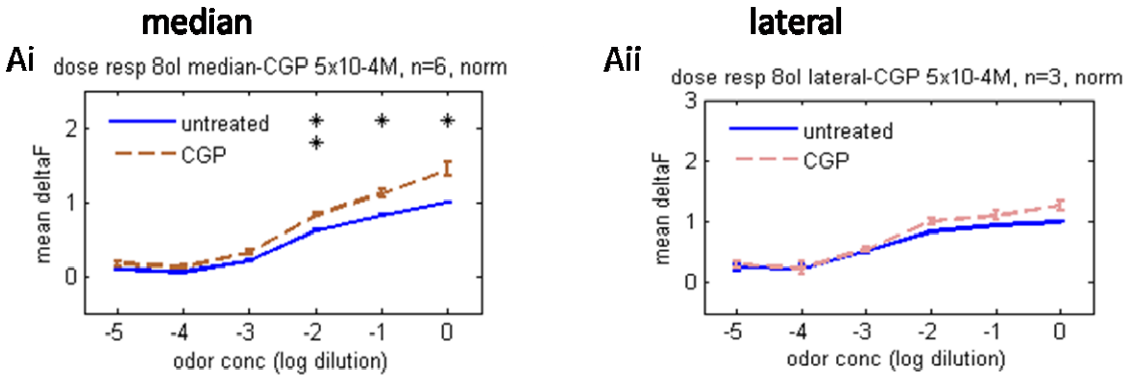

Figure 3-21: Effects of CPG54626 on dose response curve for median and lateral calyces, octanol
mean, SEM
Ai: Dose response curves for octanol before and after treatment with 10-4M CGP54626, median calyx, n=6, left-tailed paired t-test, p=0.0437, p=0.0333, p=0.0092 for odor concentration 0, -1, and -2 respectively)
Aii: Dose response curves for octanol before and after treatment with 10-4M CGP54626, lateral calyx, n=3

The absolute increase in calcium response evoked by CGP54626 is on average smaller compared to PTX effects. In Figure 3-22 a series of false color coded images of responses to different odor concentrations before and after application of CGP54626 is shown exemplarily. In this animal the drug had a clear impact on KC response.

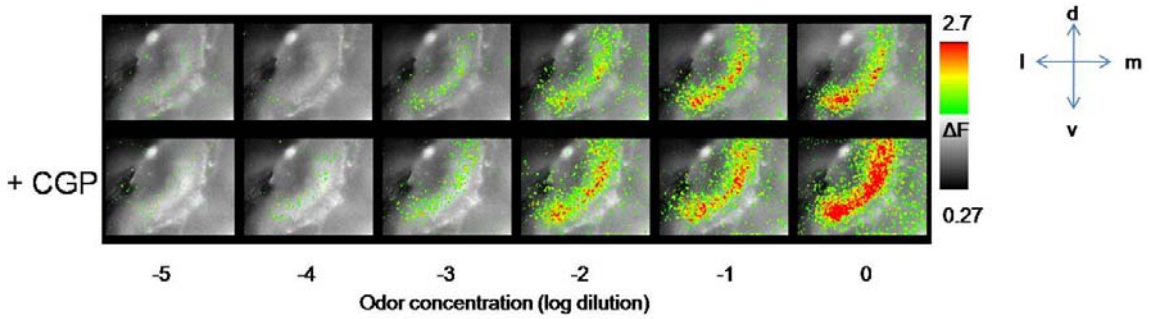

Figure 3-22: Effect of $GABA_B$ blocker CGP54626 on calcium response, example from a lateral calyx
False color coded pictures illustrate response after odor onset of different concentrations of octanol before and after application of CGP54626.

The effect of CGP54626 is reliable and significant. Mean response at highest odor concentration is doubled after CGP54626 application (about 4 times higher after applying PTX).

The same effect was found using other odors: the following figure shows the effect of CGP54626 when using the odor hexanal as olfactory stimulus. The curve after treatment is still an exponential function, whereas the curve for the odorant octanol before and after drug treatment is a sigmoid curve (see Figure 3-21).

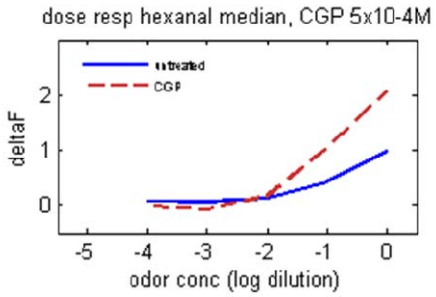

Figure 3-23: Example for effect of CPG54626 on dose response curve for median calyces using hexanal as odor stimulus

Impact of $GABA_A$ receptor blocker picrotoxin on off-responses

The impact of PTX on the response at odor onset was already shown before. Now I reveal how the $GABA_A$ blocker influences the response at odor offset.

In the Figure 3-24, four examples are displayed where off-responses could be measured before PTX treatment. The responses to three different odor concentrations before and after application of 10^{-5}M PTX are plotted. In A two examples (bee 1 and 2) are shown, in which the median calyces were investigated. After applying 10 µM (10^{-5}M) PTX to these bees, the off-responses increase as the on-responses do. In fact, both parts of the responses show drastic increases.

Further, it was found that dose response curves for odor on- and offset within one animal are very similar (not shown) implying that the concentration evoking the highest on-response also evokes the highest off-response.

In B, two examples (bee 3 and 4) from lateral calyces are shown. After PTX treatment, the response to odor offset disappears or is clearly decreased (Figure 3-24 Aii, Bii) although responses at odor onset increase.

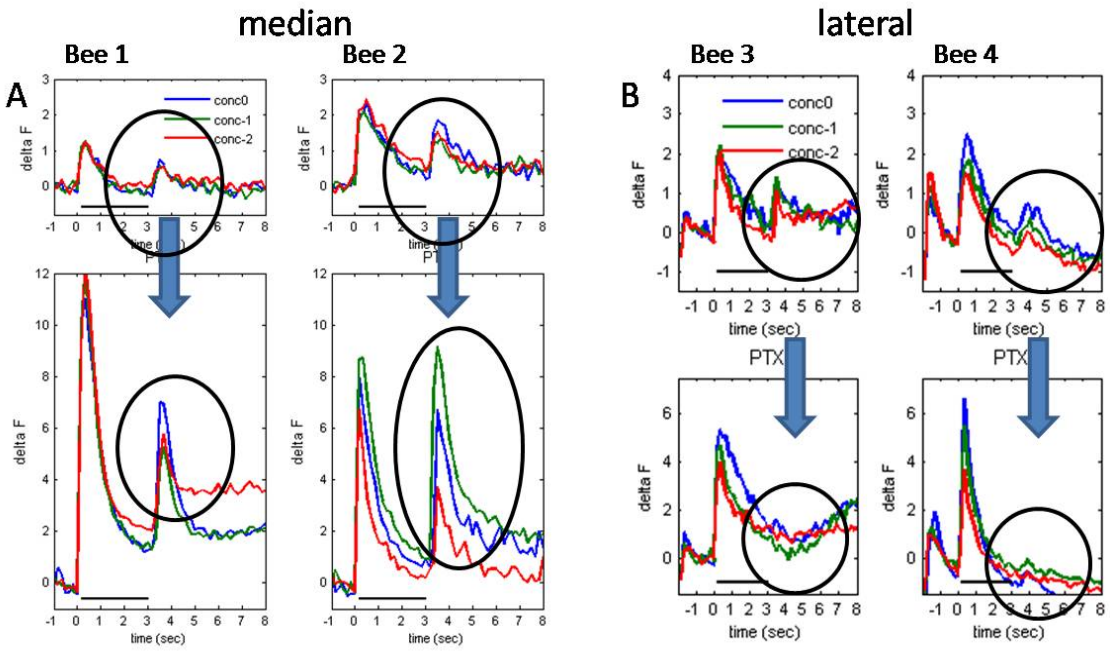

Figure 3-24: Off-responses change with application of picrotoxin
Four examples are shown, 2 from median (A) and 2 from lateral calyces (B)
All show off-responses before treatment (upper row). Response after treatment (10^{-5}M PTX) is shown in the bottom row.
A: In the median calyces off-responses increase after PTX treatment.
B: In the lateral calyces off-responses disappear after PTX treatment.

When applying BMI or CGP54626 to the bee brain, off-responses were not found to change after blocking a GABA receptor.

Impact of GABA receptor blocker on optic responses

As described in the previous chapter, in some bees the time traces start with a very prominent response peak at the onset of light excitation. This phenomenon is called an optic response to the light stimulus; this response is not restricted to the lip neuropil.

The strength of this optic response is independent from the olfactory stimulus, but it is also sensitive to GABA blockers as it is shown in Figure 3-25.

One representative example shows a decrease of this signal after applying BMI, another example shows an increase of the signal after PTX application. In the PTX-example, the change is in the same direction as odor on- and off-response change, namely increasing after drug treatment. In the BMI example it is the opposite case: the optic response vanishes while olfactory response increases.

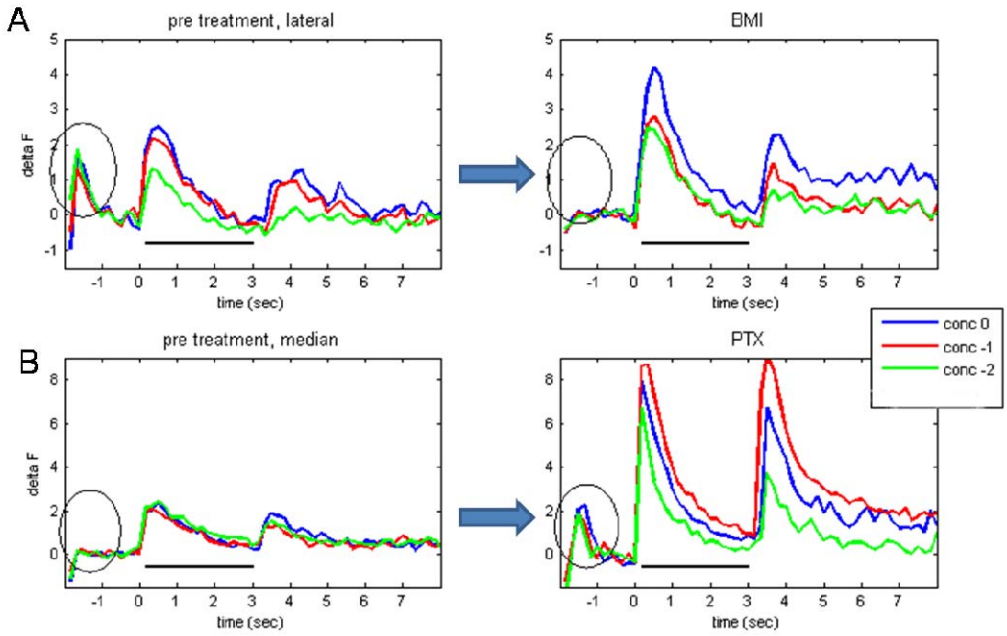

Figure 3-25: Examples for GABA inhibition influencing responses to light stimulation
A: BMI application on a lateral calyx, left: before treatment, right: after treatment: optic response disappears after BMI application
B: PTX application on a median calyx, left: before treatment, right: after treatment: optic response increases after PTX treatment
Three highest odor concentrations shown, influence of inhibitors on odor evoked stimulus also observable

Impact of DMSO on Kenyon cell responses

All the drugs applied here were diluted in DMSO. To exclude that the drug effects are evoked by the solvent rather than by the drug, I applied the highest used concentration of DMSO, a concentration of $5x10^{-3}$M, to three animals and compared the response with the succeeding application of 10^{-5}M PTX. As result, no effect could be observed as demonstrated in the examples in Figure 3-26: the response after DMSO application (red line) is similar to the response before treatment (blue line). The response increases clearly After PTX application.

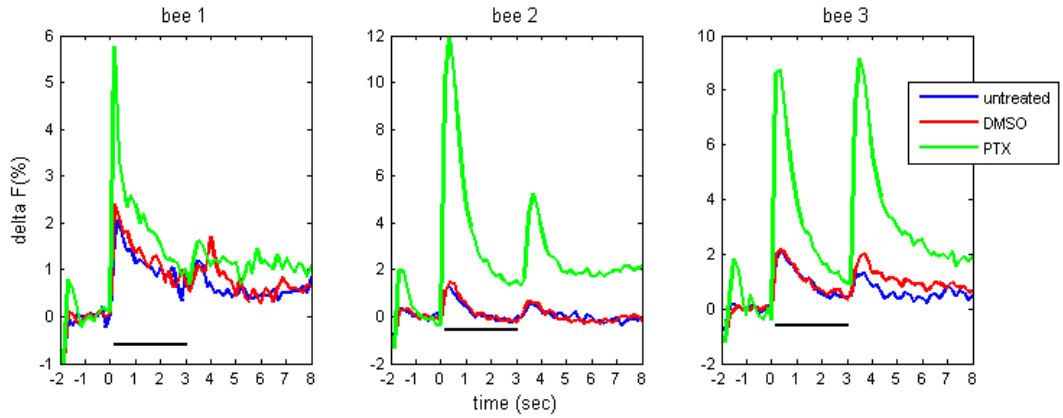

Figure 3-26: DMSO has no effect on on-response amplitude
Three examples are shown, responses were measured with Ringer application (untreated, blue), DMSO application (red), and 10^{-5}M PTX application (green)
A 10% odor concentration was used; odor stimulus was either hexanal or octanol.

In this section it was shown that the activity of a population of KCs is correlated with odor intensities when measuring the activity in the dendritic region of the cells. It was further exemplarily shown that individual somata respond to more than one concentration, implying that they are not very specific for a small range of odor intensity.

In addition, it was shown that different GABA receptor blocker influence odor sensitivity in KC, but to different extend. Different impact on lateral and median calyces and differences in the impairment of off-responses were detected.

3.3 Temporal Dynamics in mushroom body Kenyon cells

Odors are coded as spatial and temporal patterns in the olfactory bulb of vertebrates (Spors et al., 2006) as well as in the antennal lobe of insects (Galizia and Szyszka, 2008;Fiala et al., 2002;Carlsson et al., 2005).

In the locust, temporal coding and synchronicity between PNs has been demonstrated to have a high impact on odor coding (Mazor and Laurent, 2005;Laurent et al., 1998;Laurent et al., 1996;MacLeod and Laurent, 1996).

For the honeybee AL Galizia et al. (Galizia et al., 2000) have shown that the characteristic spatial activation pattern of the glomeruli in the AL is a dynamic pattern which changes within a time window of 2-3 seconds after stimulus onset. During odor stimulation some glomeruli show a tonic, some a phasic-tonic, and others a slow phasic response pattern. The differences between the response patterns increase within 2 seconds. The odor representation becomes more distinct over time.

For the next level of olfactory cells, the KCs, it was shown in the first part of this work that responses are short and phasic and do not last for longer than 2 seconds. Similar observations were described by Szyszka et al. (Szyszka et al., 2005).

Temporal representation of single olfactory stimuli

In this chapter, I address the question of temporal coding properties of KCs and compare them with PN, further I investigate the impact of GABA antagonists on temporal features of the responses since it is proposed that GABA influences temporal sparseness (Szyszka, 2005;Yamagata, 2008).

I applied stimuli of different length and measured calcium responses in PNs within the antennal lobe as well as in the dendritic region of KC, to compare the data obtained from the same setup and under same experimental conditions. In Figure 3-27 recordings of PNs in their input region, the AL glomeruli, are plotted. Responses from the glomeruli 17, 33, and 52, as indicated in Figure 3-27 A (all innervated via antennal nerve tract 1) are shown. The glomeruli were identified according to the honeybee antennal lobe atlas (Galizia et al., 1999). All three glomeruli responded with excitation to the applied odor octanol. Odor stimuli were applied for 1, 2, or 3 seconds. The calcium responses are displayed in Figure 3-27 B as false color coded time courses and as time traces for all three glomeruli.

The response traces over time reflect the stimulus length with great precision. All glomeruli show a tonic or phasic-tonic response. The calcium level decreases after stimulus offset. In glomerulus 17 this decrease is less dramatic; calcium level stays up until the end of the measurement.

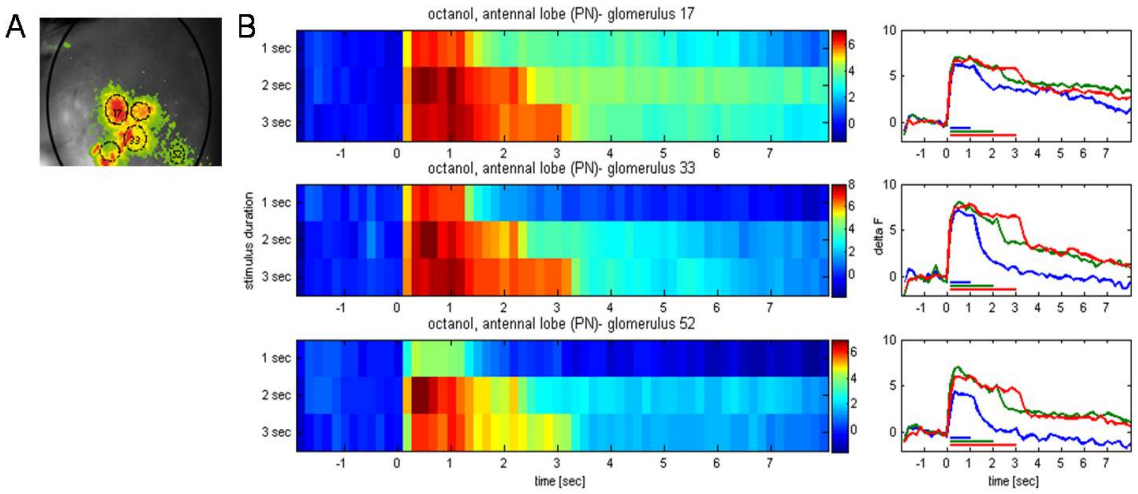

Figure 3-27 : Different stimulus durations affect response length in AL
A: Raw fluorescence image of the antennal lobe, with false color coded responses during odor application, a subset of glomeruli numbered: 17, 33, 52
B: For each glomerulus (17, 33, 52) the response to an either 1, 2, or 3 second stimulus is shown as false color coded response traces, and as line plot (blue: 1 sec, green: 2 sec, red: 3 sec)

In the glomeruli 33 and 52, the calcium concentration quickly decreases back to baseline level after a 1 second odor stimulus. After a 2 or 3 second odor stimulus the baseline level was not reached again within several seconds after stimulus offset.

In contrast to this finding in AL PN, I found no differences between short (0.5s) and longer (3s) stimuli in KCs (Figure 3-28).

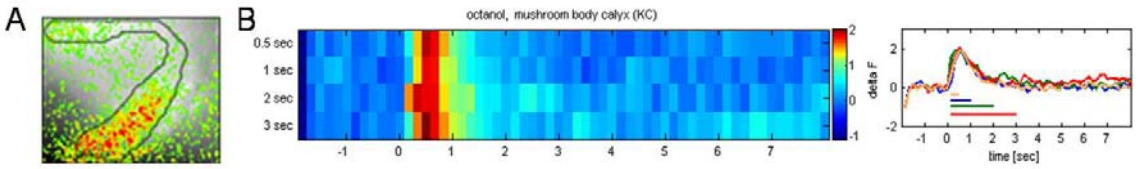

Figure 3-28 : Different stimulus durations do not evoke different response length in KC
A: Raw fluorescence image with overlaid false color coded response, the outline of the lip is drawn.
B: Response to an 0.5, 1, 2, or 3 second stimulus is shown as false color coded response traces, and as line plot (orange: 0.5sec, blue: 1 sec, green: 2 sec, red: 3 sec)

The calcium response recorded in the calyx was in all cases a brief phasic response at odor onset with a characteristic slope. This implies that the calcium response in KCs does not reflect the length of an odor application. Even shorter stimuli, ranging from 0.1 to 0.3 seconds, evoked the same response as shown in Figure 3-29.

However, this figure also shows that the occurrence of an off-response depends on stimulus length. In the experiment shown here, the odor linalool was applied as a stimulus of varying length. Here, it was observed that an off-response is not generated when stimuli last less than 3 seconds.

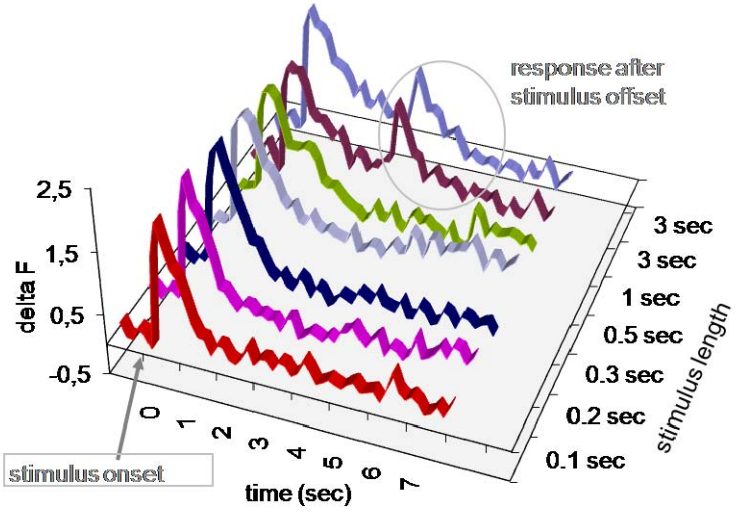

Figure 3-29: Response traces in KCs
At odor onset always the same time course appears independent from stimulus length; the occurrence of off-responses depends on stimulus length

Influence of GABA inhibition on temporal sparsening

I have demonstrated in this work that Kenyon cells exhibit a very characteristic and a rather short response. The calcium response typically lasts for about 1.5 seconds under our experimental conditions. For a stimulus longer than a few hundred milliseconds, the response in KCs is temporally shorter compared to their upstream cells in the olfactory pathway, the PNs. This phenomenon is referred to as temporally sharpening or sparsening (Szyszka et al., 2005).

It was proposed that a reason for the relatively fast decay of the signal could be GABA mediated inhibitory input. To verify this idea, different blockers of GABA-receptors were used in a pharmacological assay.

In the previous chapter I analyzed the impact of GABA blocker on the response amplitude and found that the response strength increases after application of a GABA inhibitor. Especially the $GABA_A$ blocker PTX was found to be very potent. Figure 3-30 demonstrated that PTX did not change the temporal dimension of the response. I stimulated the animal with odor stimuli of different length, ranging from 0.5 sec to 3 sec, before and after systemic application of 10^{-5}M PTX. The effectiveness of the drug was verified by the increased amplitude. However, I did not find any change in the temporal domain.

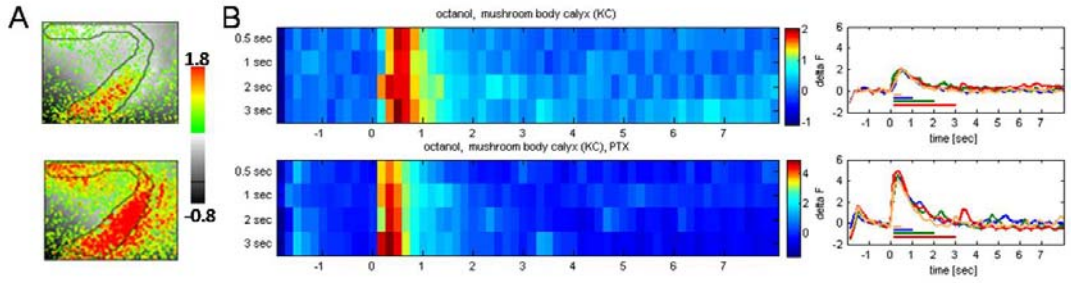

Figure 3-30 : Picrotoxin does not influence response length
A: Raw fluorescence image with overlaid false color coded odor response before and after 10^{-5}M PTX application, the outline of the lip neuropil and ROI for calculating traces is drawn.
B: Response to an either 0.5, 1, 2, or 3 seconds odor stimulus is shown as false color coded response traces, and as line plot before and after PTX application (orange: 0.5sec, blue: 1 sec, green: 2 sec, red: 3 sec).
Note that false color coded response traces are scaled to different maxima.

The typical phasic response did not change when applying the $GABA_A$ blocker PTX.

Next, I tested 10^{-5}M bicuculline as a second $GABA_A$ receptor inhibitor (Figure 3-31). Again, an increased calcium response was found, but no temporal elongation in the response could be seen upon application of a 3 second odor stimulus. In fact, in the example in Figure 3-31 the response looks even shorter showing a more drastic dip.

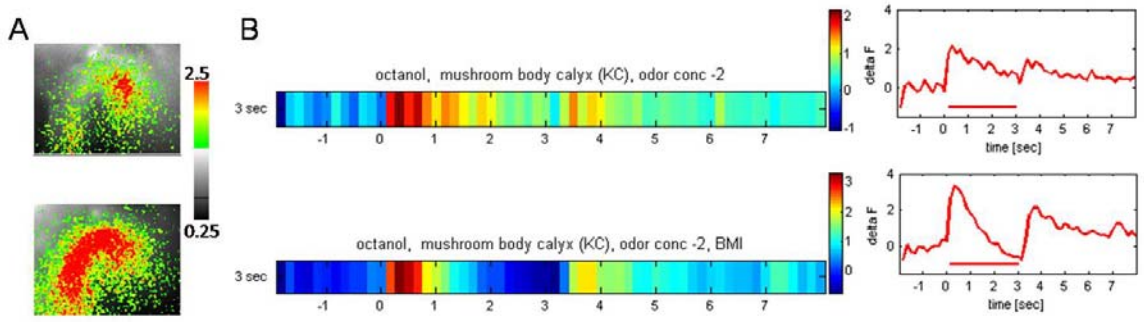

Figure 3-31 : BMI does not influence response length
A: Raw fluorescence image with overlaid false color coded odor response before and after 10^{-5}M BMI application.
B: Response to a 3 seconds odor stimulus is shown as false color coded response traces and as line plot before and after BMI application.
Note that false color coded response traces are scaled to different maxima.

Further, I tested the $GABA_B$ receptor blocker CGP 54626. I applied an odor stimulus lasting 3 seconds and found no elongated response after application of $5x10^{-4}$M CGP54626 (Figure 3-32). Also, in this example the calcium activity was increased.

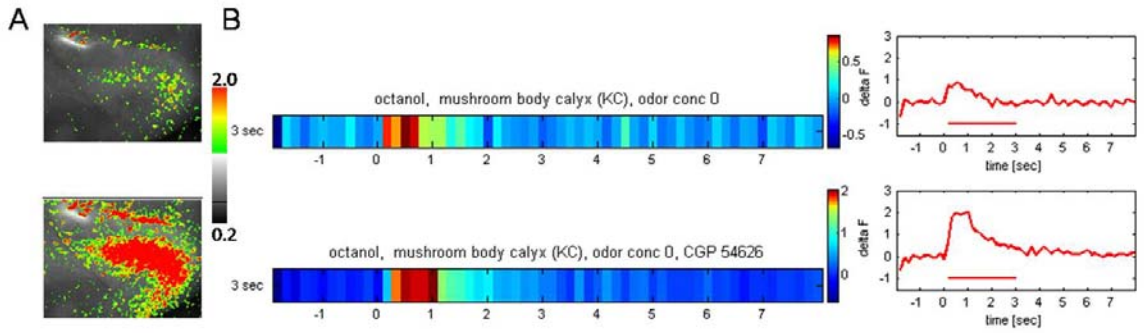

Figure 3-32: CGP54626 does not influence response length
A: Raw fluorescence image with overlaid false color coded odor response before and after $5x10^{-4}$M CGP 54636 application.
B: Response to a 3 seconds odor stimulus is shown as false color coded response traces, and as line plot before and after CGP 54626 application.
Note that false color coded response traces are scaled to different maxima.

In the last three figures individual bees, treated with different GABA receptor blockers, were displayed. In Figure 3-33 pooled data from several animals are shown; response traces before and after drug application were normalized to the maximal response.

A

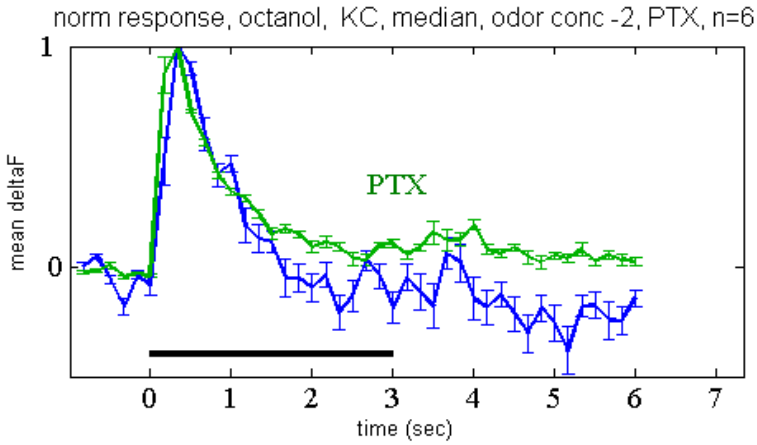

B

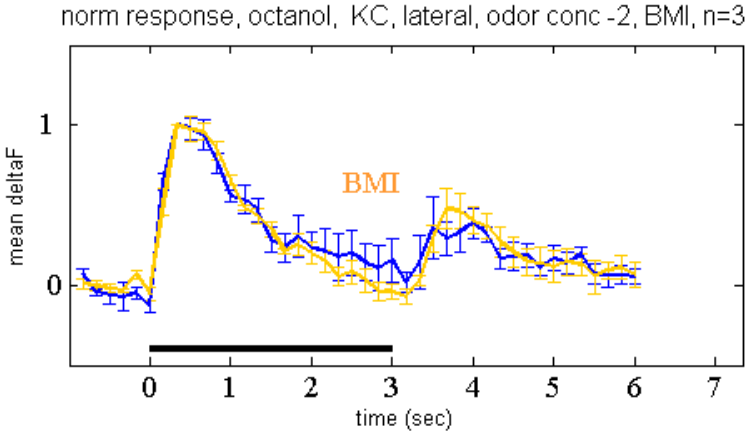

C

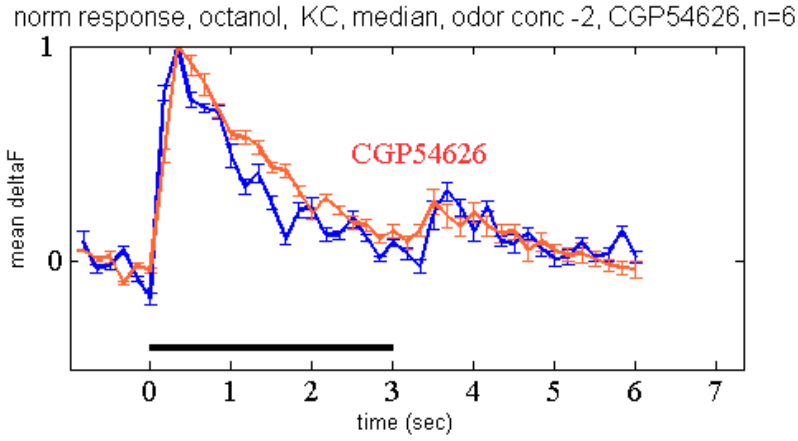

Figure 3-33: normalized response curves of KCs before and after treatment with GABA receptor blocker

The blue line always corresponds to the measurements before drug application
A: Green: response after PTX treatment, n=6 bees, median calyx, mean, SEM
B: Yellow: response after BMI treatment, n=3 bees, lateral calyx, mean, SEM
C: Orange: response after CGP54626 treatment, n=6 bees, median calyx, mean, SEM
Black bar indicated the 3 seconds odor application, all traces normalized to maximal response

For none of the used drugs a change in response length can be observed. Only in the PTX treated group (Figure 3-33 A) the response did not fully reach baseline as long as measurement lasted. In Figure 3-33 B and C one can observe that BMI and CGP 54626 application did not influence the off-responses which is in accordance with findings from the previous chapter of this work.

Representation of successive olfactory stimuli

The experiments described before revealed that the temporal sparseness of KC responses is not mediated by GABA inhibition.

Subsequently, I addressed the question how KCs respond to sequenced odor pulses. First, I again tested responses in AL PNs to compare results from similar experimental conditions.

In Figure 3-34 a representative example is shown: the calcium response in an AL glomerulus was recorded while applying two successive stimuli with different inter-stimulus intervals. For 1 second stimulus / 1 second break rhythm a decreased response to the second stimulation can be observed. (Note, that each stimulus was applied here for one second. Therefore, the ISI of 1 second corresponds to a frequency of 0.5 Hz).

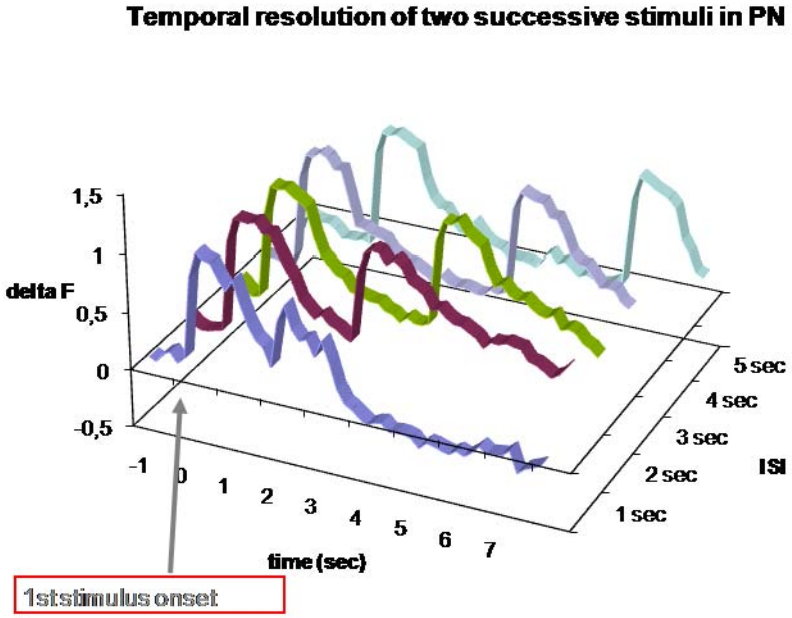

Figure 3-34 : Response in AL projection neurons (glomerulus 33) after application of two stimuli with different inter stimulus intervals (ISI)
Each stimulus applied for one second, both stimuli are the same odor (octanol)

An inter stimulus break of two seconds results in an equally large response during the second stimulus. This is in accordance with findings from Sachse et al. (Sachse and Galizia, 2002) who showed for AL glomeruli that the calcium response follows a repeated 2 second stimulus / 2 second break rhythm, implying that 2 seconds are sufficient to "reset" the system.

When performing the same experiment in KC, as shown in Figure 3-35, I found that an inter stimulus break of only 0.1 seconds (which in fact is an ISI between onsets of 1.1 sec) is sufficient to evoke the same maximal response for stimulus two, but in this case a clear response peak could not be observed, since baseline was not reached before the onset of the second stimulus. Using an ISI of 0.5 seconds is sufficient to evoke an equally high response peak during the second stimulus; even increased response amplitudes after a 2 or 3 second ISI were observed. With a 4 or 5 second ISI, both stimuli evoke equal responses.

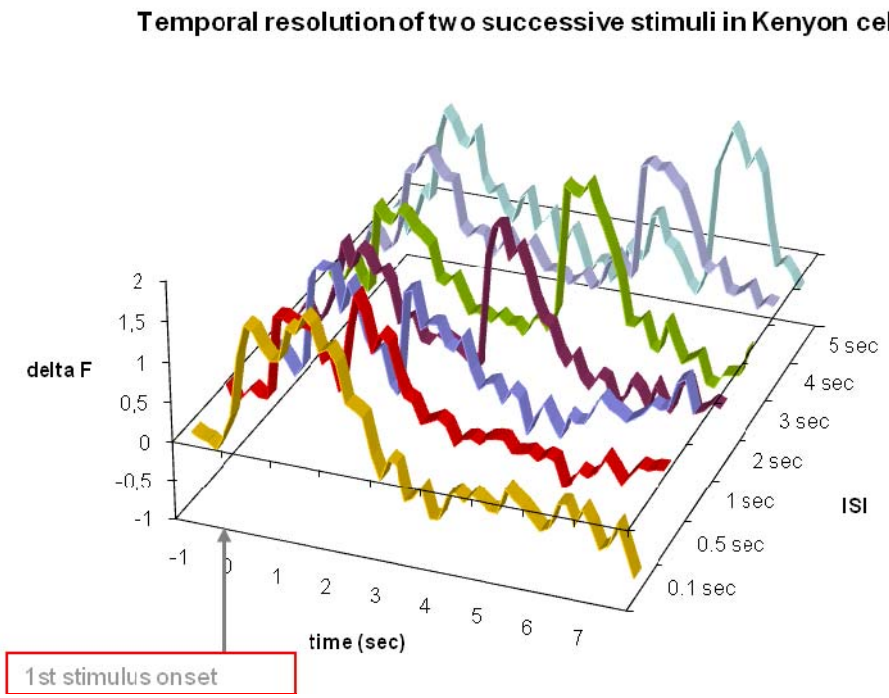

Figure 3-35 : Response in Kenyon cells after application of two stimuli with different inter stimulus intervals (ISI)
Each stimulus was applied for one second, both stimuli were the same odor (hexanal).
The curves were normalized to the odor onset of the first stimulus.

Influence of GABA on reduced response to a succeeding stimulus

In the next experiment, I investigated how the resolution of successive stimuli in KCs is influenced by GABA. Therefore, I used an ISI of 0.5 seconds between two successive stimuli of the same odorant; stimuli were applied for only 333 ms (2 frames of a 6 Hz imaging protocol) resulting in an ISI between odor onsets of 833 ms which is less than what was used for the previous example.

Under this conditions the second response is significantly smaller than the first one (individual time traces shown in Figure 3-36 A, first and third column; pooled data in Figure 3-36 B, n=10, Wilcoxon-signed-rank-test, p=0.006). Different odors were used (linalool, octanone, hexanal, and octanol) as indicated in the following graphs in A.

Next, I combined the application of two successive stimuli with application of 10^{-5}M of the $GABA_A$ receptor blocker PTX. The response trace after PTX application is shown in the columns 2 and 4 of Figure 3-36 A. As already described in the previous chapter, the amplitude of the calcium response increases significantly for both stimuli (see Figure 3-36 B; $p(1^{st}/1^{st}$ PTX stim) = 0.004, $p(2^{nd}/2^{nd}$ PTX stim) = 0.004). It becomes apparent that also after PTX application the response to the second stimulus is significantly weaker than during the first stimulus (p(1st PTX /2nd PTX stim) = 0.004).

In order to compare the two odor stimulations, I calculated a ratio of the first and second response for untreated and for PTX treated measurements. The ratios before and after PTX treatment do not differ (p=0.7). Thus, no change in the relation between first and second stimulus can be found; I could not observe any increase of the response during second stimulus after PTX application relative to the first stimulus. In fact, for bee 2 and 4 it can rather be observed that the second stimulus is responded to with relatively smaller amplitude. This way I have shown that the decreased response during the second stimulus was not due to a GABA inhibition via PTX sensitive receptors.

A **Time courses for successive stimuli**

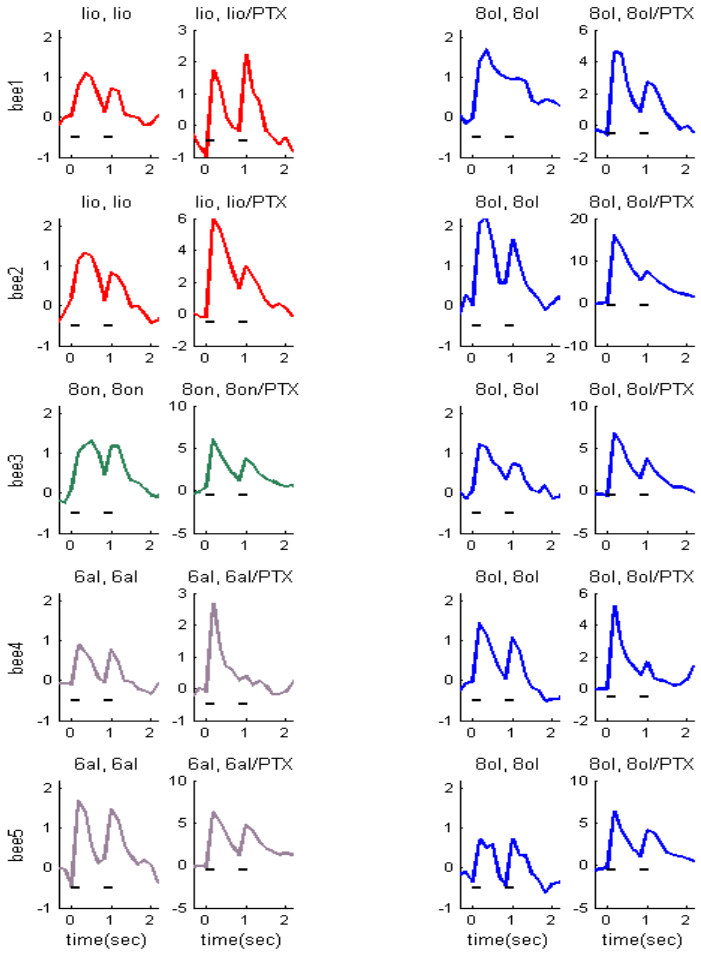

B **Responses during successive stimuli**

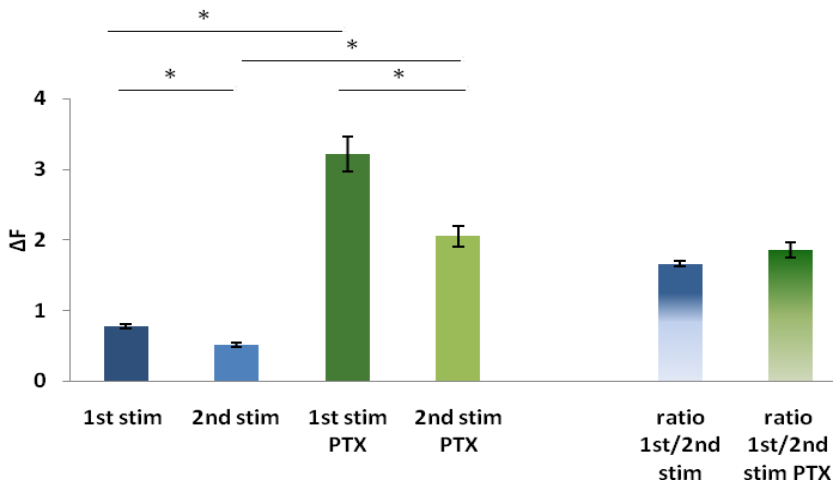

Figure 3-36 : Influence of $GABA_A$ inhibition on two successive stimuli in KC
Stimulus duration: 333 ms each, ISI 0.5 s
5 bees tested: bee 1-4 in median calyx, bee 5 in lateral calyx, two different odors were tested in each bee, odors indicated in plots, sequenced stimuli were of the same odor
A: time traces for two successive stimuli are plotted: Column 1 and 3: before drug treatment; Column 2 and 4: after applying 10^{-5}M PTX
B: pooled response strength for all measurements (averaged over 5 imaging frames after stimulus onset); n=10 measurements from 5 bees; blue columns: responses before PTX application, green columns: after PTX application; Wilcoxon signed-rank test, p(1^{st}/2^{nd} stim)=0.006, p(1^{st}/1^{st} PTX stim)=0.004, p(1^{st} PTX /2^{nd} PTX stim)=0.004, p(2^{nd}/2^{nd} PTX stim)=0.004

In the following figure time course of the application of three successive stimuli were shown (Figure 3-37). In Figure 3-37 A one can see the same effect as in the previous figure: a second stimulus shows a reduced response after an ISI of 0.5 seconds. However, a third stimulus with the same ISI evokes a response which is smaller than the first one but higher than the previous one.

Three successive stimuli with an ISI of 1 second (Figure 3-37 B) evoke constantly decreasing responses. When using an ISI of 1.5 seconds (Figure 3-37 C), all stimuli evoke the same response amplitude.

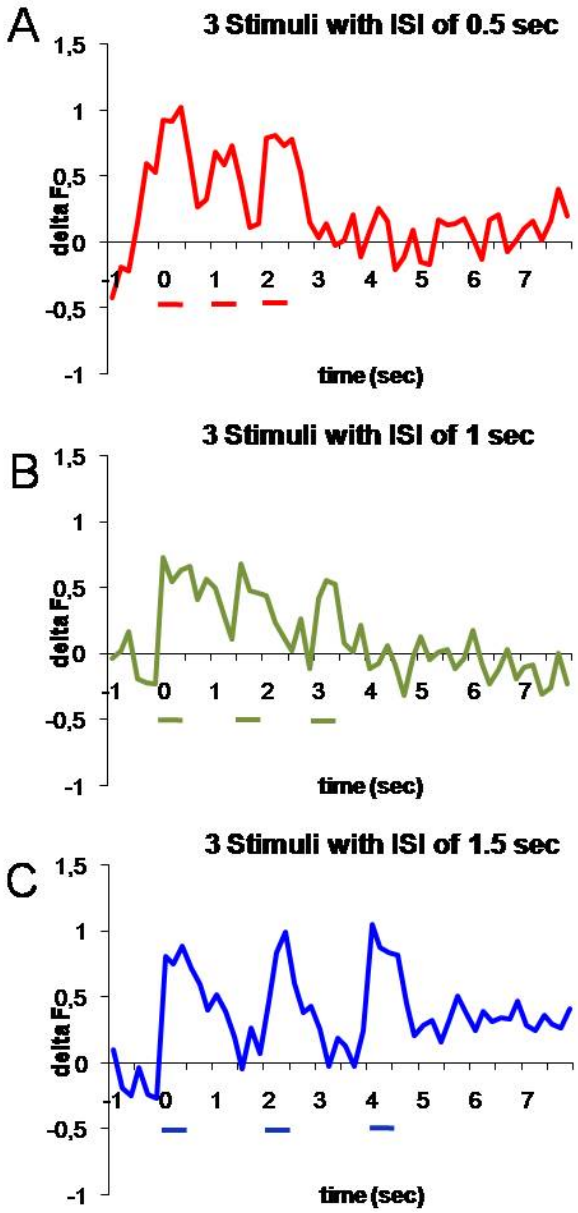

Figure 3-37 : Three successive stimuli of the same odor (hexanal)
Odor stimuli lasted 0.5 seconds, stimuli indicated by bars
A : ISI of 0.5 seconds ; B : ISI of 1 sec ; C : ISI of 1.5 sec

3.4 Response in individual Kenyon cells and spatial patterns in the dendritic region

Responses in Kenyon cell somata

A mass staining technique as it was performed in the experiments described in this work results in a large number of stained KCs since their axons are rather thin and densely packed. So far, large populations of cells were summarized, in particular at their overlapping dendritic input regions. On the dendritic level it turns out to be impossible to reliably resolve dendritic fields of individual cells when using wide field imaging combined with mass staining. Cells are not only densely packed in a two dimensional way, but also they are stacked in depth which means there are cells closely under the upper most layer of cells which are also stained and might as well respond to stimulation. Therefore, imaging the somata of KCs would help to learn about single cell characteristics. This would also be necessary to answer how sparse individual cells respond.

In *Drosophila* stereotype responses in KC somata were shown (Wang et al., 2004) using an optical imaging technique. In honeybees somatic responses in KC were investigated too, but reliable responses from KC somata are rather rare for different reasons (Szyszka et al., 2005).

In Figure 3-38 and Figure 3-39 two examples of measured calcium responses in KC somata are shown. The first example is from a lateral calyx, the second from a median one. The somata belong to KCs type II, since their somata lie outside the calyx (Figure 3-38 B, Figure 3-39 B) ventrally and also anteriorly (note that dorsal is up in false color coded images).

In the false color coded pictures of Figure 3-38 C potentially responding somata are visible in the octanol and hexanal response images (ROI 1 -3 in B). When calculating response kinetics for these somata and other regions of interest (D), it becomes clear that it is difficult to identify whether the lighting up in the image is in fact a somatic signal or caused by artifacts. Only for the response to octanol one can be confident that the indicated soma (ROI 3 indicated in Figure 3-38 B, magenta arrow) is responding with a somatic calcium increase. Here, the calcium response signal is surmounting the response from other regions in amplitude.

For hexanol it is also very likely that the soma in ROI 1 (blue arrow in C) is responding specifically to this odor since the response amplitude is as high as, or slightly higher, than in the neuropil. The soma in ROI 2 shows a very noisy response and would therefore be described as a movement artifact of a well stained soma (dotted line in D).

Such movement artifacts can be accounted to rather slight movements of structures located right on the border between bright and dark structure. This way, slight movement of the brain result in enormous changes in fluorescence in the respective area which can easily be misinterpreted as changes in the calcium level. A movement correction was performed using a custom written routine, but this correction can only be used for corrections in x- and y- direction but not for correcting movements in the z-dimension.

In the example from Figure 3-38 none of the somata is responding to more than one of the five presented odors.

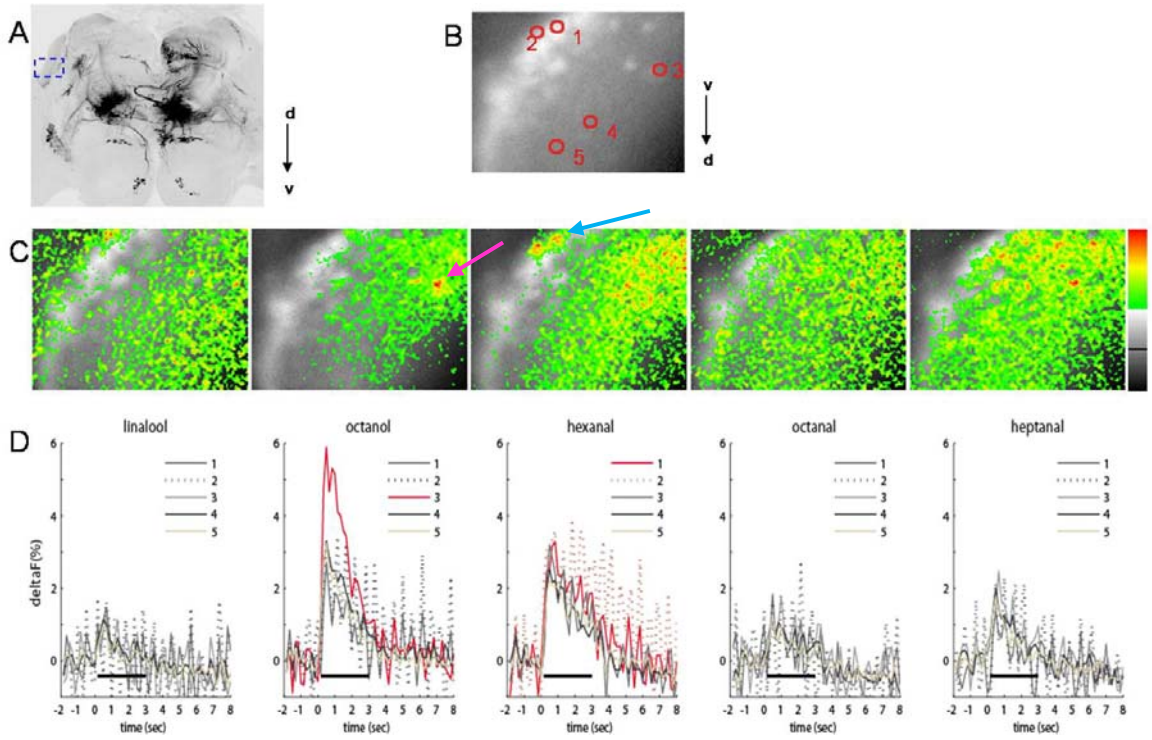

Figure 3-38 : Measuring response in a soma of the lateral calyx
A: Overview of central brain scanned with CLSM, the calcium imaged area is marked with a blue rectangle.
B: Raw florescence image of recorded region, stained somata and the lip neuropil of the right lateral calyx are clearly visible. 5 ROI are marked with red circles, 60x objective was used, dorso-ventral orientation inverse from A
C: False color coded image of activity during odor application, different odors were tested, the second picture shows response to octanol, a responding soma is marked with a magenta arrow; in the third picture, showing response to hexanal, a potential responding soma is marked by a blue arrow
D: Response kinetics for the 5 different ROIs for each odor, respective traces corresponding to marked soma in C are indicated in red when showing the time course for different ROIs
The active soma during octanol application is the only time a clearly higher response amplitude than in neuropil was observed.

In a second example from a median calyx shown in Figure 3-39 (imaged region indicated in A) there is one soma (ROI 1 indicated in B, blue arrows in C) responding to 2 out of 5 odors, namely linalool and octanol. The pictures are individually scaled to min and max value. Since heptanone is hardly evoking a response, the image appears very noisy.

A calcium response spread over the whole visible lip neuropil can be seen (ROI 3).

In the response kinetics for the hexanal application (Figure 3-39 D), the effect of light scatter is very obvious since the highest amplitude occurs for ROI 3, the neuropil, and response amplitude decreases with increasing distance to the dendritic region, the putative source of activity (ROI 2, ROI 1).

Another effect described by Szyszka et al. (2005) can also be found in both examples, namely a slightly slower decrease of the calcium signals in the soma compared to the dendritic region (see previous Figure 3-38 D, response to octanol and hexanal; and Figure 3-39 D, response to linalool).

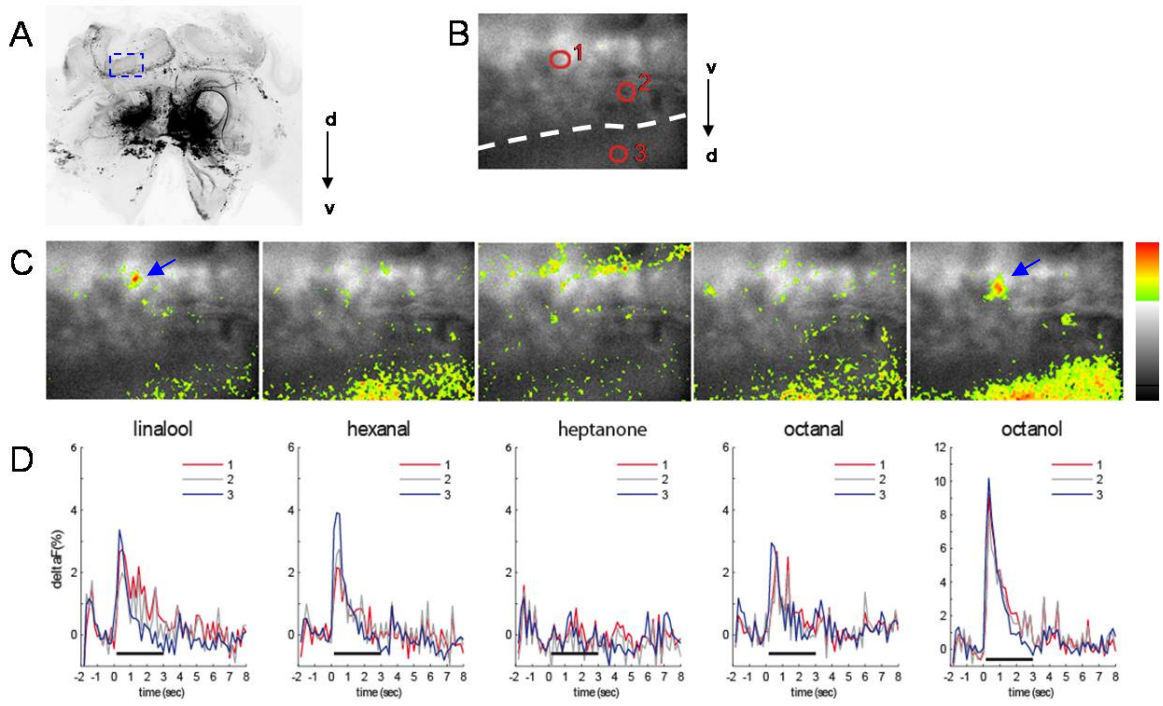

Figure 3-39 : Measuring response in soma of the median calyx
A: CLSM scan of central brain, blue rectangle is indicating the imaged region at right median calyx, KCs type II are stained.
B: Raw fluorescence image of recorded area, stained soma visible, ROIs are marked as red circles, 60x objective, dorso-ventral orientation inverse from A
C: False color coded images of responses during odor application overlaid on raw fluorescence image, one soma corresponding to ROI 1 is responding to 2 out of 5 odors namely linalool and octanol. Since pictures are individually scaled to min and max value and heptanone is not evoking a response, image appears noisy.
D: Kinetics of ROI indicated in B, note: scale changes for octanol, for the soma (ROI 1) the kinetic shows a slower decay, also for hexanal the kinetic show a response in ROI, this is due to light scatter; off-response seen for octanol
Odor pulse is indicated by the black bar below the traces.

Somatic responses of individual cells were obtained rarely. Therefore, the focus of this work was on the calcium activity in the dendritic input region, the MB lip.

Spatial response patterns in the mushroom body calyx

The same work that had shown reliable responses of KC somata in *Drosophila* also demonstrated patterns of responses in the calyx (Wang et al., 2004). This is raising the question whether one can also find a spatial pattern in the lip region of honeybee calyces without resolving individual cells. Spatial pattern in the olfactory path are known from the antennae and the AL, and recently also from uniglomerular PN target areas in the calyx: a stereotype representation of sensory input in the calyx was for instance shown for *Drosophila* larvae (Masuda-Nakagawa et al., 2009a).

KCs have their dendritic fields perpendicular to PN axons spanning across the lip of the MB calyx (Rybak and Menzel, 1993;Strausfeld, 2002;Szyszka et al., 2005). Hence, I investigated whether such dendritic fields could be distinguished as column like patterns in my calcium imaging experiments.

False color coded response pattern obtained with optical imaging of the calyx appear very homogenous. To unveil any “hidden” response pattern in the lip neuropil, two approaches were used: The first one is based on comparing images of different measurements to find differences between different stimulus conditions, namely different odors. The second approach is based on correlating quantitative data, i.e. the response traces of small sub regions.

Results of the first approach are shown in figure Figure 3-40. Individually scaled false color coded pictures (A) showing calcium activity during odor stimulation were taken. Each odor was presented three times. I filtered for pixels with highest 20% of response, those pixel are shown in B. The images of these pixels showing the highest response were merged and screened for overlap (C and D).

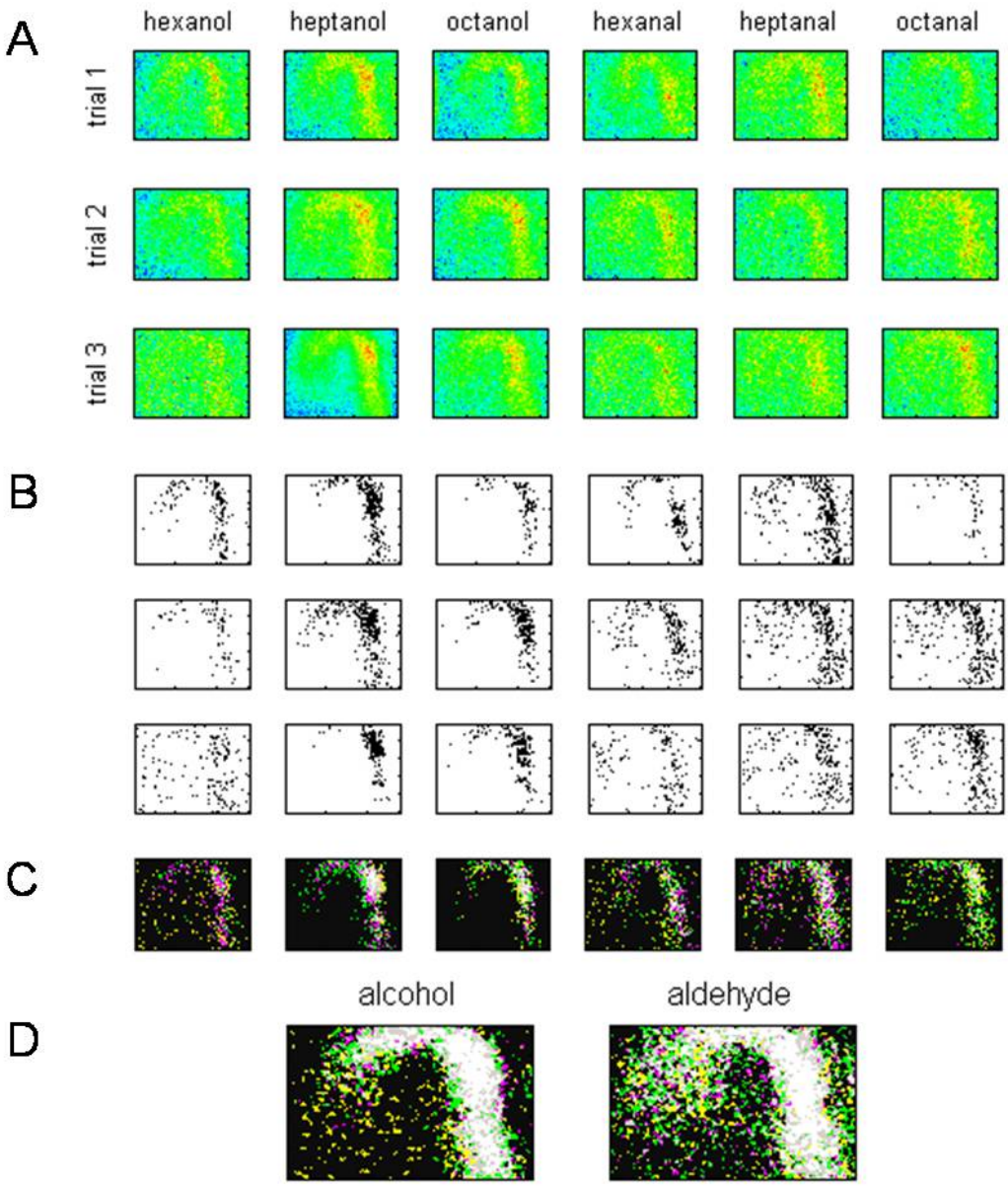

Figure 3-40 : Pattern analysis based on images
A: False coded picture for each measurement
B: Pixel with highest grey values (above 200 on red channel)
C: Overlay of three trial for each odor (magenta: trial 1, green: trail 2, yellow: trial 3; white and grey: overlay of all three or two trials)
D: Overlay of three odors (primary alcohols hexanol, heptanol, and octanol or aldehydes hexanal, heptanal, octanal) after averaging three trial for each odor (magenta: hexanol/al, green: heptanol/al, yellow: octanol/al)

First, the overlap between measurements of the same odor was compared which means that responses of the three trials of one odor got merged (Figure 3-40 C). Each trial is shown in a different color, shared pixels are displayed white. The overlays demonstrate that the highest activity is always within the same area, namely the outline of the lip. On a more detailed level the overlap is rather imperfect for repeated applications of the same odor.

In the next step the overlay of stimulations with different odors were compared. For Figure 3-40 D pictures of the three trials per odor were averaged, then this averages were overlaid including either the three alcoholic odors or the three aldehydes. As a result it was found that already the averages of three trials look very homogeneous (not shown). Therefore, overlaying several odors results in a big area which is common for the response pattern for each odor. Only at the more noisy edges of the lip there are pixels which are exclusively activated by one odor.

This lack of patterning might be a result of a too low magnification. Therefore, a similar analysis for measurement imaged with a 60x objective was performed; five different odors were presented in a median calyx.
The respective false color coded images are shown in Figure 3-41 A. Again, those pixel showing highest responses (B) were selected and overlays of two odors (C) were conducted, thus comparing each odor with every other. This time, no averages of repeated trials were used in order not to cover any patterns.
Not many white pixels were found which would indicate a relatively high calcium response in both compared odors at the same spot. Still, images look very much alike, except overlays with linalool. Linalool already has an outstanding image in the original false color image (A) because of a very strong response on the right edge of the imaged region. It can be concluded from this finding that there is a soma, which lies on the lip surface, responding specifically to linalool (blue arrow in A).

To further compare quantitative information from the measurements, the images were divided in different ROI of the same size from which response kinetics were calculated for each odor. A mask for this ROIs is shown in Figure 3-41 Dii or Fii, respectively. First, the area was divided in horizontal layers (Dii), second in vertical columns (Fii).
The calculated traces (Di) for the horizontal ROIs show a rather homogenous signal for each odor stimulus. In E the mean response during 3 seconds of odor stimulation is plotted.
When looking at Figure 3-41 Di and E a tendency was found showing an increasing signal from the most ventral region (ROI 1) to ROI 4 and a dip in ROI 5, the most dorsal one (the soma laid ventral from the lip neuropil, dorsal is the transition of the dendritic site to the axons projecting into the peduncle). That means, the response is highest in the more

dorsal part of the lip. One has to note that response to linalool is by far highest and that here ROI 4 shows the highest activity. This is the layer where the identified soma is located.

In a second step, when dividing the image in vertical columns (Figure 3-41 F and G), even more homogeneity within time courses for each odor is found. Comparing response to different odors, obvious differences can be observed. This could be an indication for some odor specificity. In the 1-octanol measurement there is a higher response in ROI 2+3 and ROI 6+7 what could also be guessed from the colored images in A. The linalool measurement shows again the highest response in all regions but in particular in ROI 2, where the identified soma is located.

Besides, it is found that 1-octanol and nonanol evoke off- responses whereas other odors do not (Di, Fi). Although some differences between odors can be seen, it cannot be concluded from these findings that there are odor specific patterns.

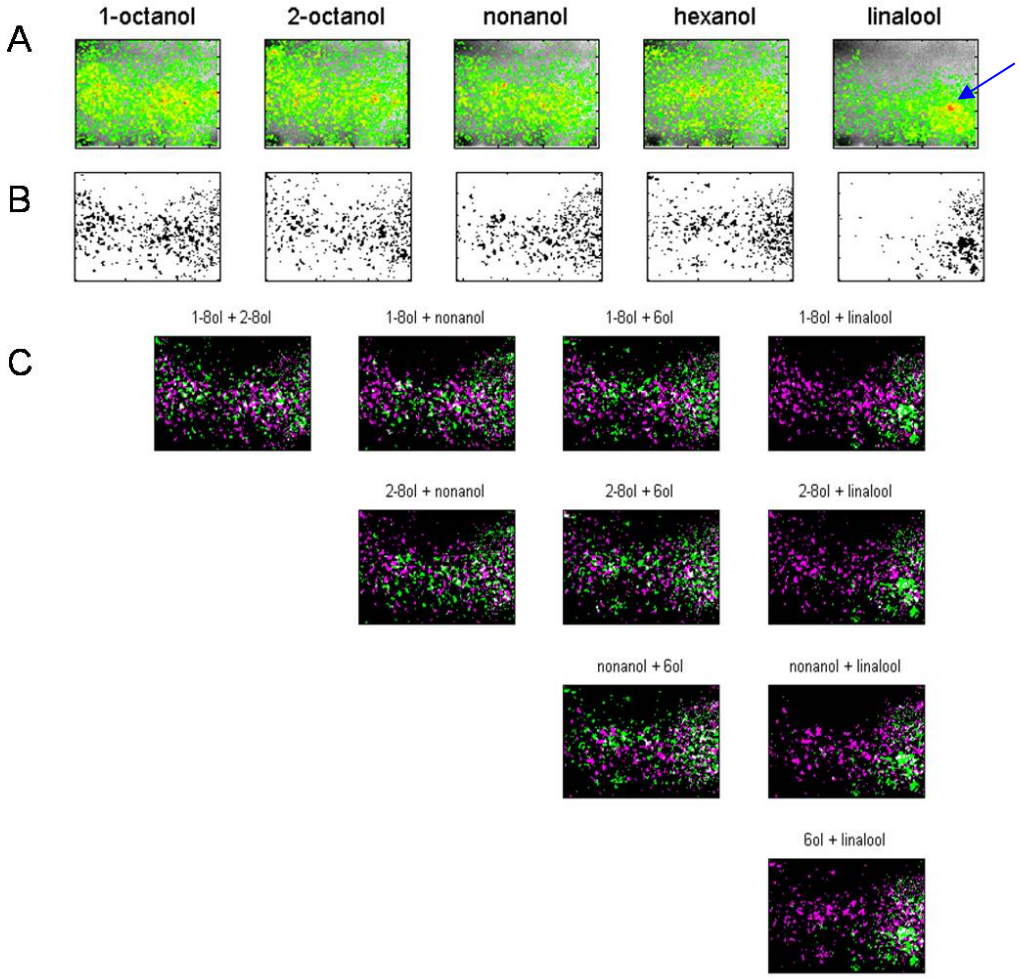

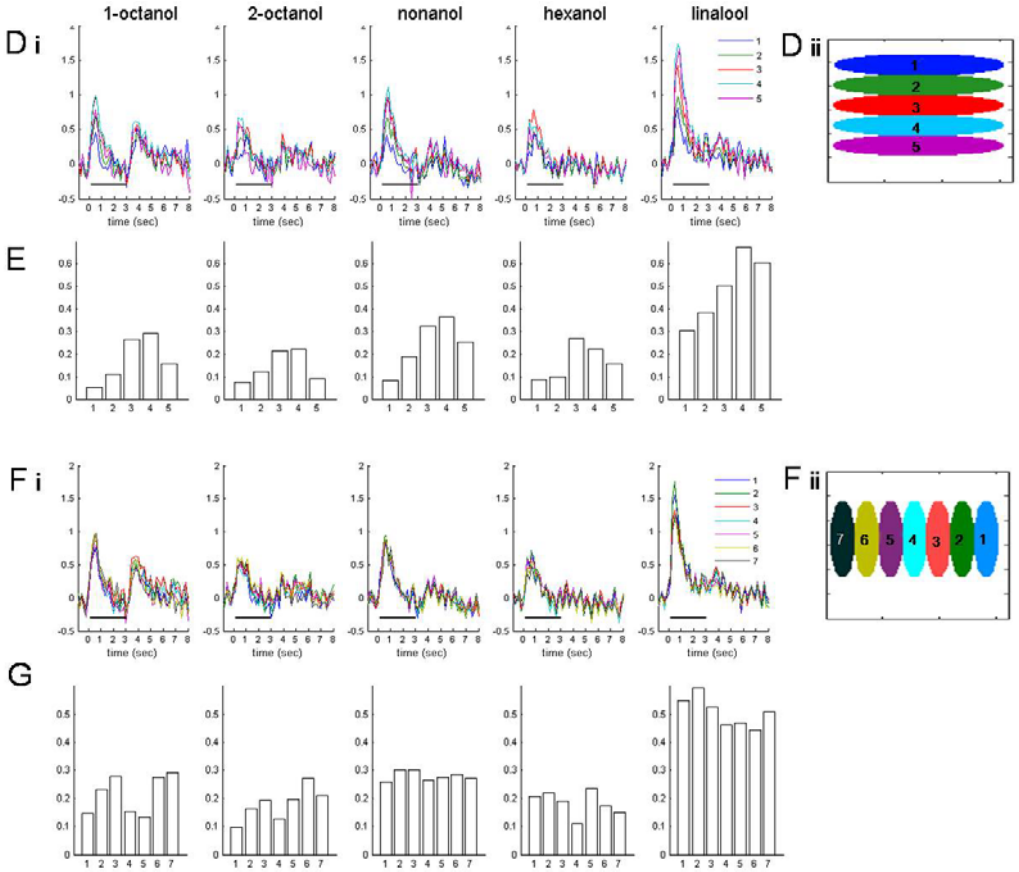

Figure 3-41 : Pattern analyses based on images and kinetics
A: False color coded images of responses to different odors
B: Pixel with highest grey values (above 200 on red channel)
C: Overlap of two odors (magenta and green: both odors; white and grey: overlap)
Di; Fi: Time course of ROIs indicated in Dii/Fii, each plot for a different odor, black bar: time of odor stimulus
E,G: Mean response during 3 seconds odor application, Histograms derived from the graphs in Di and Fi

Subsequently a correlation analysis was performed based on the time courses in order to investigate potential spatial patterns. To do so, 27 coordinates or ROIs (numbered from coor 0 to coor 26) were picked on the basis of the color coded pictures of the imaged structure, the lip of a lateral calyx, and response kinetics were correlated. Each ROI covered 5x5 pixel.

In Figure 3-42 A the response for each single measurement is shown as a false color coded image. In B one enlarged image shows the location of all individual ROIs. In Figure 3-42 C each plot displays one measurement: the false color coded time courses for all coordinates are plotted (every line corresponds to one coordinate). Every odor was three times applied, thus every row of plots corresponds to the first, second or third trial, respectively. Already when looking at the color coded traces in C it becomes clear, that for each measurement the response in different coordinates is very similar except for the coordinates 22 to 26. These coordinates lie outside the active region as can be seen in figure B. The different plots for different odors show some dissimilarity: For some odors, hexanal and octanal, the response strength was low which leads to noisier pictures in A and in C.

To investigate how high the correlation between different regions of the lip neuropil is, or, in other words, whether some distinct areas with higher correlations can be found, time courses of all coordinates for every measurement were correlated with each other (Figure 3-42 D). One sees in these plots that correlation (Pearson correlation coefficient) in general is rather high (coded in red and orange) for most coordinated. That means the response kinetics for all parts of the imaged areas are very similar. Exceptional are again the coordinates 22 to 26, being located outside the lip, at the lower and right edges of the correlation matrix.

Comparing all correlation matrices for first trial odor applications in D with those from third trial one can find that correlation slightly increases.

In a next step, the different time courses obtained from various measurements but the same coordinate (E) were correlated. Rather high correlations were found again except between sucrose applications and odor stimulations. (Sucrose applications are always the last stimulations in a row of ten stimuli, 3 trials each). This fact is in part caused by a temporally delayed sucrose application accomplished by the experimenter and in part by a different response kinetic, which does not show the typical sharp response as can be seen in C.

This analysis also revealed that for the 5 outlying coordinates (coor 22 to coor 26) the correlation is low.

Comparing correlations of different regions within a measurement with correlations of different odor responses in one particular region, one will find that the correlation between regions is higher. That means, when applying an odor stimulus to the bee and recording the calcium activity of the lip neuropil, a rather homogenously distributed response within the respective area is obtained. There are some differences in responses to different odors. These differences can be found mainly in the amplitude of the response. But these varieties are reflected in the whole neuropil.

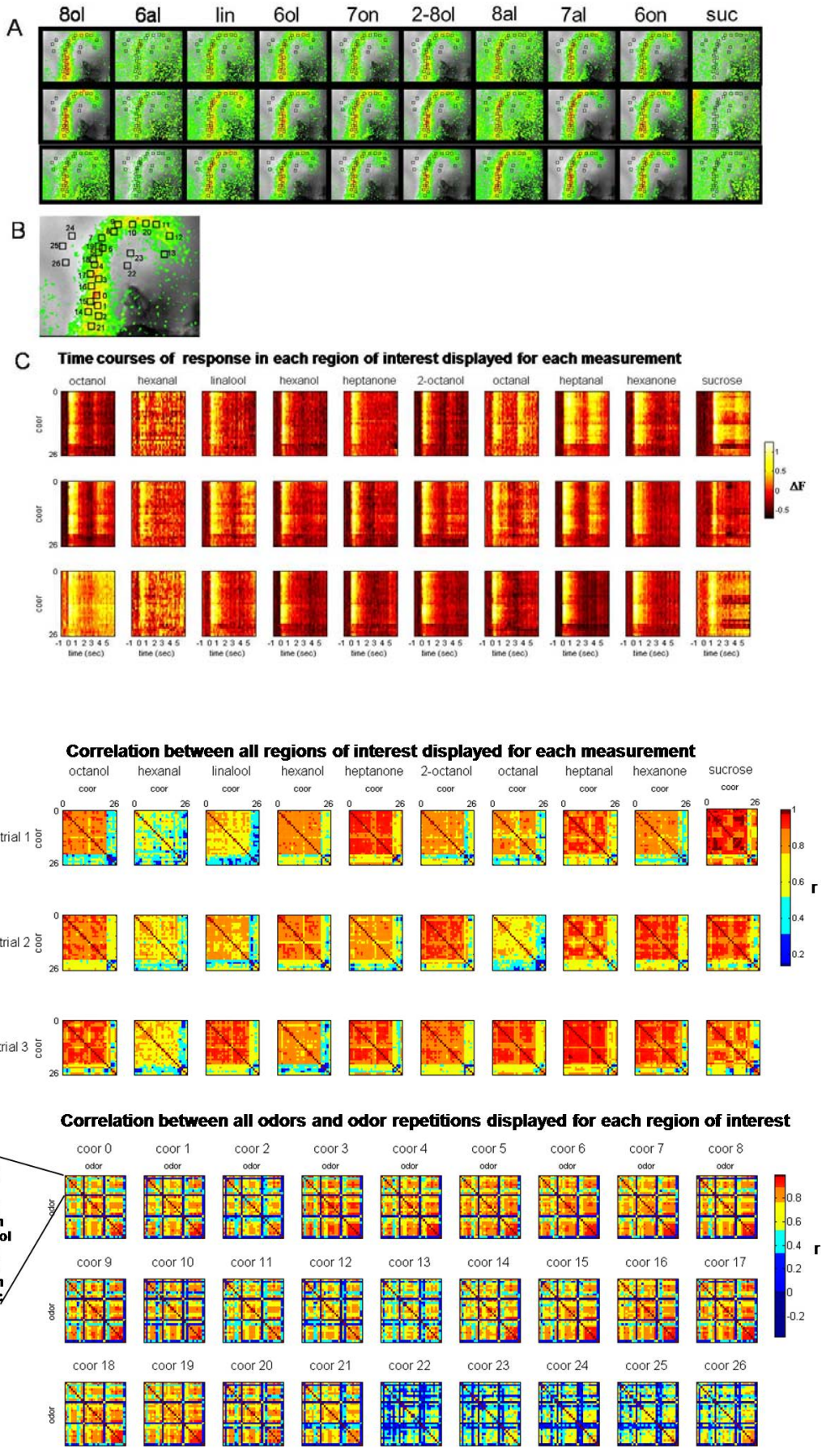
A
8ol
6al
lin
6ol
7on
2-8ol
8al
7al
6on
suc
B
C
Time courses of response in each region of interest displayed for each measurement
octanol
hexanal
linalool
hexanol
heptanone
2-octanol
octanal
heptanal
hexanone
sucrose
coor
time (sec)
ΔF
D
Correlation between all regions of interest displayed for each measurement
trial 1
trial 2
trial 3
r
E
Correlation between all odors and odor repetitions displayed for each region of interest
Trial 1
8ol
6al
lin
6ol
7on
2-8ol
8al
7al
6on
suc
odor
coor 0
coor 1
coor 2
coor 3
coor 4
coor 5
coor 6
coor 7
coor 8
coor 9
coor 10
coor 11
coor 12
coor 13
coor 14
coor 15
coor 16
coor 17
coor 18
coor 19
coor 20
coor 21
coor 22
coor 23
coor 24
coor 25
coor 26

Figure 3-42: correlation between spatial coordinates versus correlation between repeated measurements, recorded in a lateral calyx
A: False color coded pictures averaged over three frames after odor onset, each odor was given three times (3 trials)
B: One picture (2-8ol, trial 1) with marked coordinates (= regions of interest), each 5x5 pixel
C: Time courses for all coordinates ranging from 1 second before odor onset to 3 seconds after odor offset (odor applied for 3 seconds, starting at time point 0)
D: For each measurement (nine different odors+sucrose application, three times each) all the time courses per coordinate were correlated with each other and displayed per measurment, pearson correlation coefficients depicted in a matrix
E: For each region of interest all 30 measurements were correlated with each other and displayed per coordinate, pearson correlation coefficients depicted in a matrix. Note that the sucrose application does not correlate with odor application, this is mainly cause to time delayed application by the experimenter or by temporally extended response

---

It was demonstrated on this section that activity in the whole imaged area is rather homogenous, under the used methodological conditions, as long as there is no soma responding to the stimulus. For quantification of calcium imaging data, the majority of the analyses within this work will focus on the calculation of responses from a big region of interest spanning the visible part of the MB input region, the lip (as done by Szyszka et al., 2005).

3.5 KC responses to odor mixtures

Another approach to address the question of odor specificity in KCs, is the use of odor mixtures. In the following experiments, tertiary mixtures were applied as they were used by Krofczik et al. while performing intracellular recordings from l- and mACT PNs in honeybees (Krofczik et al., 2009). Two tertiary mixtures and their single components were used. Mix A was a mixture of 1-hexanol, 2-heptanone, and nonanol; mixture B consisted of pentanal, nonanal, and cineol. Single odors were used in a 1:10 dilution, further diluted in permanent airstream.

The mixtures were of the same concentration (v/v) as single components, i.e. a mixture of the three components was 1:10 diluted in the solvent.

For each mixture, a set of 4 animals were tested. In all animals, the median calyx, either right or left, was investigated.

In 6 out of 8 animals, a 60x objective was used to obtain higher magnification. However, single somata responding to odor stimulation could be observed in none of these animals.

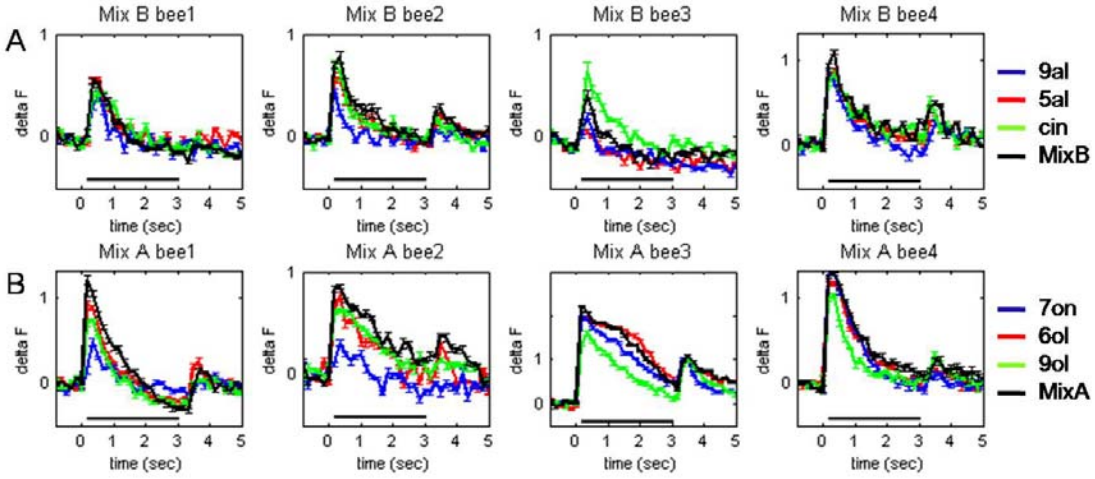

Figure 3-43: single components and their tertiary mixture in different animals
8 animals, Each curve is a mean of six trial within one animal, SEM
A: Mix B and single components applied (nonanal, pentanal, cineol)
B: Mix A and single components applied heptanone, hexanol, nonanol)

In these experiments, I found in 7 out of 8 animals that the response to the mixture was as high or slightly higher than the response to the strongest odor (hypoadditivity). This refers to both odor mixtures. Only in one example, bee 3 in Figure 3-43 A, a different effect could be observed: the mixture presentation lead to a response which was smaller than for the salient component cineol (suppression).

The hyperadditivety-effect cannot be explained by a concentration effect since single components were not summed up in the mixture; rather the mixture is of same v/v concentration.

The temporal dynamics for all four stimuli were very concordant within each bee.

Odor mixtures also evoked off-response. Those occur only when at least one single component also evoked them. In return: if at least one single odor was responded to with an off-response, also in the mixture an off-response is found.

3.6 Electroporation of honeybee brains

The staining method via backfill results in a very large population of stained cells which hinders a resolution of individual cells. Another disadvantage performing backfills is that the cells get injured at the insertion site and only retrograd staining can be done.

In *Drosophila*, the calcium imaging technique is today usually performed using fly lines expressing calcium sensitive proteins in a certain cell population (Fiala et al., 2002;Wang et al., 2004). In honeybees, genetic lines are not available. Another way of inserting and expressing an exogenous gene within cells, for instance coding for a dye protein, is the import of a vector via electroporation. This technique was already successfully performed in honeybee brains (Kunieda and Kubo, 2004). Such method offers some new approaches for selectively staining small cell populations and for assuring for vitality of the stained cells.

Thus, I aimed to establish this method in our lab, adapting in part the protocol by Kunieda and Kubo (2004). First, the electroporation technique was applied using a plasmid, peGFP-C1, which carried a GFP gene. In this plasmid, the GFP gene was expressed under the control of the human CMV (cytomegalovirus) promoter. Different parameters such as different electrodes, different pulse lengths and intensities, and different insertion points for the electrodes were tested.

To evaluate the success rate, manipulated brains were either homogenized two days after electroporation in order to perform western blot analysis or they were prepared to perform immunohistological investigations.

For both approaches, primary antibodies directed against GFP were used to inspect for the expression of the GFP protein.

With both methods, the presence of GFP could be attested.

In Figure 3-44 two different examples are displayed showing KCs that expressed the GFP protein. In A, KCs having their somata outside the calyx are stained as well as some dendritic branches in the lateral calyx. For this sample, the plasmid was applied onto the brain surface, platinum wire electrodes were inserted into the brain, and three pulses of 50V were applied lasting for 50 ms each (ISI 950 ms). In B, KC somata inside the calyx as well as their dendrites are stained. This bee was electroporated with a parallel needle

electrode inserted into the eyes after injecting the plasmid through the ocellar tract, three pulses of 100V were applied for 50ms each (ISI 950 ms).

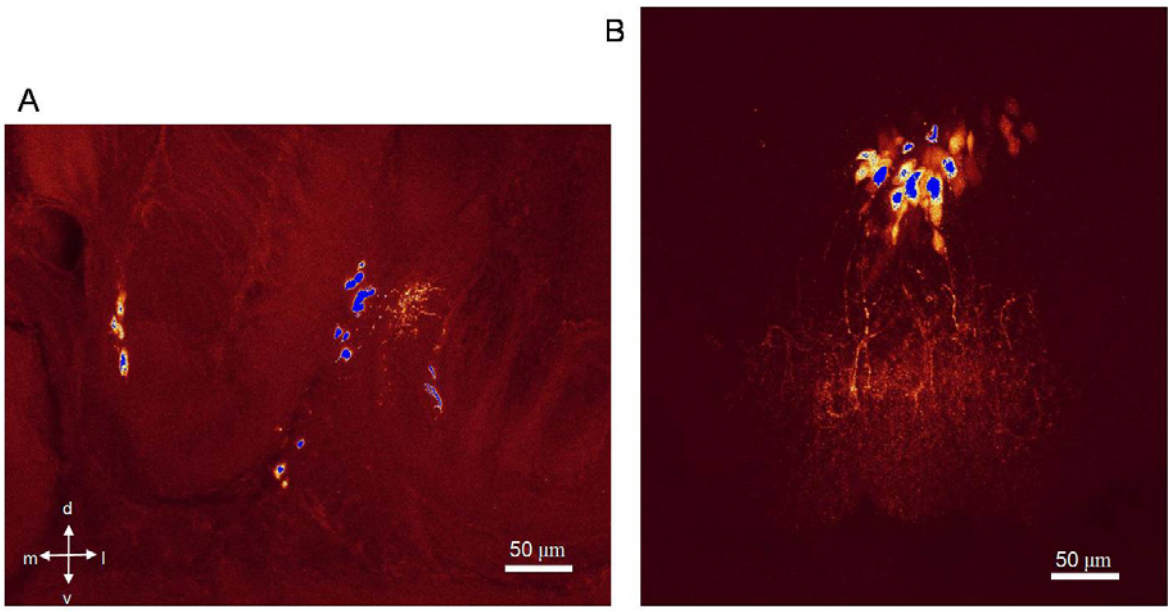

Figure 3-44 : GFP staining in Kenyon Cells after electroporation
Expressed GFP two days after plasmid injection and electroporation
A: Clawed KCs at lateral calyx with stained dendrites in the lip, platinum wire electrode placed between central brain and optic lobes, 3x50V pulses of 50 ms (ISI 950ms)
B: KCs class I inside the median calyx, dendrites are visible in the lip, parallel needle platinum electrode placed into the eyes, 3x100V of 50 ms (ISI 950 ms)
In Both preparation GFP was enhanced with an antibody staining: mouse anti GFP, goat anti mouse-CY5

In Figure 3-45 the results of two western blots are shown. Different electrodes were used for the results shown in A and B. In A, both animals (lane 1 and 2) got the plasmid solution applied onto the brain and were electroporated with the custom made platinum wire electrodes inserted into the brain (3x50V, 50ms per pulse, ISI 950ms). Both have the GFP protein expressed which can be recognized by the detected band at an apparent molecular weight of 36 kDa which is approximately the expected size. In B, the protein can be found in two out of four animals (lane 3 and 4). For this experiment, a pair of parallel platinum needles was inserted into the eyes (4x100V, 50ms per pulse, ISI 950ms); the plasmid was injected through the ocellar tract.

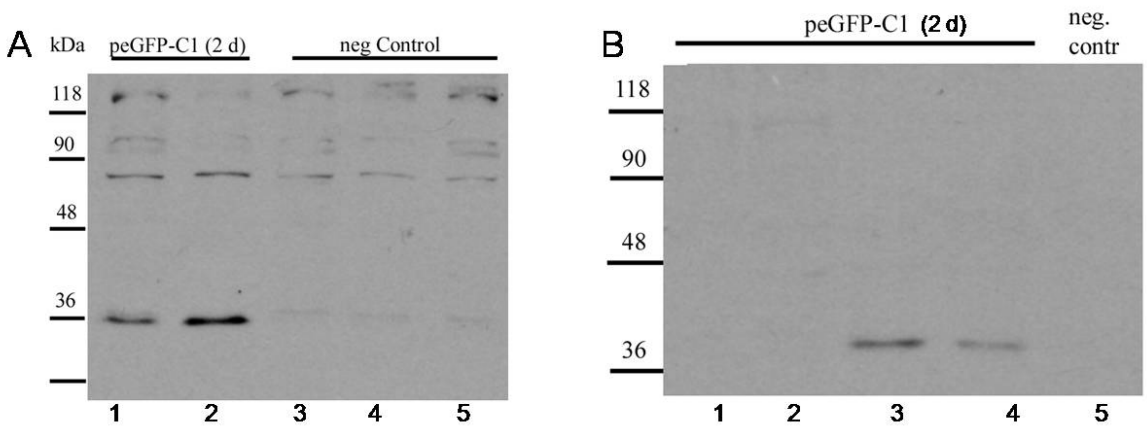

Figure 3-45 : Detection of GFP in Western blot after infection of GFP-carrying (peGFP-C1) plasmid and electroporation
Brains were dissection 2 days after manipulation
A : Platinum wire electrodes, 3x50 V pulses of 50 ms (ISI 950 ms) used, electrodes were inserted between optic lobes and central brain, plasmid was applied on brain surface, detected signals in lanes 1and 2; lanes 3, 4, 5 contain negative controls
B : Parallel platinum electrodes were inserted into eyes, 4x100V pulses of 50 ms (ISI 950 ms) were applied, injection through median ocellar tract, detected signals in lanes 3 and 4; negative control in lane 5
Detection of protein with goat anti GFP antibody.
Negative controls were injected only with plasmid solution without electroporation; negative control without injection but with electroporation were done as well but did not show a signal either (data not shown).

The results shown in Figure 3-44 and Figure 3-45 prove that the plasmid peGFP-C1 under the CMV promoter works in honeybee KC and the electroporation technique is applicable.

This approach needs to be further developed.

4. Discussion

4.1 Characterizing Kenyon cells

Subject of this work were higher order interneurons of the olfactory pathway, the clawed Kenyon cells of honeybee foragers, also termed KCs type II. These cells get dendritic input from olfactory PNs in the lip neuropil of the calyces, the input regions of the MB. I reconstructed the dendritic input region of some individual clawed Kenyon cells and their somata. The reconstruction shows that the dendrites lie on the outer surface of the MB lip and do not span over other regions of the MB calyx. This is in accordance with an example shown by Rybak (Figure 10 in Rybak and Menzel, 1993).

Activity in olfactory neurons

When performing optical imaging at the dendritic input region of a rather big cell population, one can measure calcium activity in response to nearly all olfactory stimuli, although individual KCs are described as responding in a sparse manner and not being easily excitable. They rather need simultaneous synaptic input from several synaptic sites to generate an AP themselves (Laurent, 2002). In fact, it is unclear whether the measured calcium increase is caused by actual firing of KCs or by EPSPs evoked at their postsynaptic sides.

However, measuring the calcium responses in the lip, the signal extends over the whole visible neuropil. This is in consistence with the morphology of olfactory PNs in the honeybee, which are known to innervate the whole lip neuropil of the calyx (Kirschner et al., 2006;Müller et al., 2002;Krofczik et al., 2009), whereas some individual PNs exhibit unequal innervations within and between the two calyces (Abel et al., 2001). There are also differences in the terminal arborization patterns of both ACT tracts: mACT neurons innervate the whole lip with different densities, lACT PNs innervate the central core of the lip region and leave an outer cortical layer non-innervated (Kirschner et al., 2006). This would lead to the assumption that mostly signals from mACT are recorded when imaging the anterior part of the lip, especially when the calcium activity is caused by EPSPs. Since KC dendrites span the whole lip and they get most likely input from both ACTs, the

calcium activity caused by intrinsic spikes distributes in the whole dendritic region and thus, transmitted signals from both tracts are measurable. The fact that calcium signals in stained KCs can be measured all over the lip neuropil is also in accordance with the distribution of KC dendrites which are densely packed and, this way, form the calyx neuropil. Compared to other cell types in the olfactory path, KCs exist in enormous number, but they are characterized as responding sparse implying that only a little portion of cells is active at a certain stimulus. This might lead to a spatial activity pattern visible in the region of interest while performing optophysiological measurements. But no such spatial patterns could be observed for active KC dendrites during this work (Figures 3-39, 3-40). In fact, when defining several small regions of interest distributed over the whole imaging field, the calculated traces are rather homogeneous for the same stimulus. This was also affirmed by correlation analyses (Figure 3-42).
The only inhomogeneity over the lip was found when dividing the region in horizontal layers. Then, the dorsal part of the lip neuropil shows slightly higher activity than the ventral part which is closer to the somata (Figure 3-41). This could be causes by spikes generated far away from the soma at the distal side of the dendrites.

However, the olfactory receptor neurons and PNs show a stereotype spatial organization in terms of morphology and odor evoked activity. Information from a glomerular unit of the AL is transferred by uniglomerular PNs towards the MB calyces. Thus, one might presume that a spatial code is transferred to the next neuropil and each PN innervates a distinct area. Such transmission of a spatial code has been found in the calyces of *Drosophila* adult flies, although the integration of PNs in the calyx is describes as less stereotyped than in the lateral horn (Jefferis et al., 2007). Also for *Drosophila* larvae, some data was published showing that PNs innervate the calyx in a stereotype manner and transfer information from olfactory sensory neurons via PNs to distinct areas in the calyx. In contrast, subsets of KCs show no clear spatial preference here (Masuda-Nakagawa et al., 2005;Masuda-Nakagawa et al., 2009b). In the adult fly at least some subsets of KCs show apparently non-stereotypic responses to odors (Murthy et al., 2008). ON the contrary, by other authors a stereotype spatial pattern was described over several animals on the level of the MB calyx in *Drosophila* using an optical imaging approach (Wang et al., 2004). This latter finding could not yet been approved by others (Fiala, A, personal communication) which might be due to differing methodological approaches. Also data

from the zebrafish OB as well as downstream areas being homologue to the olfactory cortex confirm that odor-evoked activity patterns become more widespread downstream of mitral cells and a topographic organization of mitral cell activity patterns is not maintained. Thus, the transformation of odor representation does not underlie strict topographic constraints (Yaksi et al., 2009).
Nevertheless, the question of stereotype spatial organization of KC activity is yet not answered concluding.
When asking why odor representation is spatially so well organized at early stages of olfactory processing but not at the later stages, there are different possible explanations. 1) Response spectra of higher order neurons are too complex to be mapped along a low number of dimensions with available methods. Conventional imaging only allows observations of the surface, patterns occurring in the depth (z-dimension) cannot be addressed. 2) Topographic organization is not according to obvious features but according to other variables which are still unknown. 3) The chemotopy of glomerular maps within the OB or AL arranges interactions best for local processing of activity patterns but the spatial pattern has no "meaning" per se. 4) Since MB are known to be involved in learning there might be no stereotypy across individuals since each animal has experienced different events and undergone different synaptogenesis. Maturation of synaptic circuitry is likely to occur after adult emergence (Ganeshina et al., 2006). There is probably a high degree of plasticity in the MB which would not allow a stereotype pattern (Heisenberg et al., 1995;Brill et al., 2008).

One has to take into account that the number of KCs is by far exceeding the number of PNs which leads to the assumption that the code is not just transmitted but reorganized in some way. Each KC gets input from several different PNs and each PN synapses onto many KCs; this leads to a rearrangement of any spatial code. The wiring from PNs to KCs is presumably highly complex and spatial and temporal information get integrated into a high dimensional space. Another possibility is that a spatial code would be found only in KCs class I whereas clawed KCs show a higher degree of plasticity and inhomogeneity.

Representation of structurally similar odors

In behavioral tests it could be shown that the degree of generalization between odors also depends on similarity between odorants, for instance in the moth *Maduca sexta*

generalization is a function of the carbon chain length as well as the functional group (Daly et al., 2001). In accordance to such findings, the AL shows spatial patterns being more similar for similar odors (Ditzen, 2005).

In my work I investigated similarities between responses to odors having similar molecular structure like the same functional group or the same number of carbon atoms. Since spatial patterns could not be found in the calyx, I could not compare such patterns but looked at the response traces over time. It was observed that odor responses in the dendritic region of KCs have very similar time courses (Figure 3-4). The main differences between odors found were the response strength and the occurrence of off-responses for some odors, mainly the alcohols.

Applying a PCA analysis (Figure 3-5 et seq.), I could show that all odor responses form a cluster which is distinct from the control stimuli air and paraffin oil and from stimulation with sucrose.

When comparing responses to different odors or odor-evoked responses in different bees, it was found that all responses to different odors within one animal are more alike than odor specific responses from different animals. Looking at data from only one animal, no clustering of odors having either the same number of carbon atoms or the same functional group could be seen. The responses in the lip do not show different types of response traces according to the characteristics of the stimuli.

For analyzing imaging data, especially with respect to spatial patterns, more advanced analyses needs to be applied allowing objective separation of different functional neuronal groups and simultaneous analysis of the time courses of these groups. Artifacts caused by movement or camera noise need to be identified and subtracted from raw data. An example for such an analysis was demonstrated for the olfactory bulb and somatosensory cortex of mice using spatial independent component analysis (sICA) (Reidl et al., 2006). Further analyses of KC imaging data are in progress in cooperation with Dr. M. Schmucker.

Olfactory responses in Kenyon cell somata

To understand the combinatorial coding and read out of KCs, single cells or small functional units need to be investigated. Also sparseness can be investigated best on the level of individual cells. With our methodological limitations I could not resolve

individual dendrites or branches, therefore it is recommended to look at somatic responses (Szyszka et al., 2005).
Such measurements are based on the assumption that KC activity is measurable in the somata and that this is a reliable indicator for cell activity. Somatic calcium increase in KCs occurs presumably as a result of back propagating spikes, probably generated close to the dendrites. Also depolarization events at the postsynaptic membrane can passively be transferred. In fact, it is unclear if all evoked spikes propagate back all the way to the soma, or if activity can only be seen when the excitatory input to a KC is very strong and coming from several input sites distributed across many dendritic sites as it is shown for *Drosophila* PNs (Gouwens and Wilson, 2009). It is also unknown where exactly the action potential is generated in KCs. For PNs in *Drosophila* it was recently shown that APs initiate at a location distant from the soma, in the proximal portion of the axon (Gouwens and Wilson, 2009).

In a uniglomerular honeybee PN odor-evoked calcium responses in the soma and in the dendritic region, the glomerulus, were compared after intracellular staining of the neuron. Both parts of the neuron responded to the odor, the signal in the glomerulus is rather strong and weaker in the soma. The calcium increase is much faster in the dendrites; also the decay is fast here. Calcium concentration stays up in the soma for at least 5 seconds (Galizia and Kimmerle, 2004). Also, in AL neurons of the Silkmoth *Bombyx mori* somatic responses of different cells were measured recently (Fujiwara et al., 2009), as well as in the honeybees' MB extrinsic neurons (Hähnel, 2009). The latter author could show that a calcium response is measurable in the dendritic region as well as in the somata cluster. The temporal dynamics as well as response strength in the two regions are similar.

I measured a few individual somata showing odor-evoked activity; I could not observe an outstanding slower decay of the signal in a KC soma, only a slightly delayed one. When a somatic response in a KC was measured, the response trace was very similar to those recorded from the dendritic neuropil, just having a slightly slower decay of the signal, an effect shown before (Szyszka et al., 2005).
In MB extrinsic neurons and in the PNs of the AL, the two investigated regions, soma and dendrites, are clearly spatially separated. In clawed KCs, soma region and neuropil are very close and partly overlapping. Therefore, scattered light from the neuropil is also

measured in the region enclosing the soma when many cells are stained and activated simultaneously. If the signal in the soma is weaker than in the neuropil as described for honeybee PNs, it would be hard or even impossible to reliably distinguish it from light scatter emitted by the dendritic region. The response showing the slower decay could represent an overlap of the neuropil response and a slightly delayed response of the soma. I could measure only one somatic response which was stronger in fluorescence change than the response in the neuropil (Figure 3-38).

Some recordings from single somata unveiled odor evoked responses (Figures 31-5, 31-6, 31-8). Out of four investigated somata in different bees, three responded to only one out of 5 odors, one soma showed a response to 2 out of 5 odors (linalool and octanol). This finding is in accordance with previous findings from other publications where 92.2 % of clawed KC somata respond to one out of four odors and 6.5% somata respond to two out of four odors (Szyszka et al., 2005). Based on this result I can confirm that clawed KCs show lifetime sparseness, or in other words the odor tuning of individual cells is narrow. This is in accordance with findings in other models where sparseness of KC was extensively described (for instance: Broome et al., 2006;Ito et al., 2008).

To answer the question of odor tuning for the honeybee satisfyingly, one needs to test a bigger set of different odors in individual cells.
However, the fact that somatic responses could be obtained so rarely can not only be explained by sparseness. I suggest some methodical or physiological reasons. A lack of calcium sensitive dye in the somata can be excluded since staining of somata is mostly clearly visible in the raw fluorescence images. It might be that at the soma there are less calcium channels and therefore less calcium influx occurs to protect the soma from calcium fluctuation since calcium triggers many physiological processes. Then, calcium influx might only be visible after strong excitation. Further, one has to consider that imaged somata lie at the surface of the brain. The head capsule of the bee was opened several hours before and some tracheae were moved aside. This might cause some oxygen deficiency which might lead to impaired cells at the surface.

Response to light and sucrose stimulation

KCs seem to play a significant role in the processing of olfactory information. But other modalities are also processed within the MB as it was shown for honeybee clawed KCs using calcium imaging: tactile stimuli evoke responses as well as the application of water to the antennae (Szyszka et al., 2008). This suggests that clawed KCs get multimodal input (Farris et al., 2004), or there are different subgroups among the stained KCs, each responding to a different modality. Excitation by different modalities could be either transferred via different input pathways or by olfactory PNs, which were also shown to respond to stimuli of different modalities like mechanical stimulation or stimulation with water or sugar (Homberg, 1984).

I have shown (Figures 3-3, 3-8) that light evoked responses can be measured in the MB calyx. Since in optophysiological experiments the light stimulus lasts for the whole measurement, namely ten seconds, it is not known, whether there is a permanent tonic light response on top of the measured odor responses. But assuming visual KCs have similar response characteristics as olfactory KCs, they only respond with a sharp response at light onset and no tonic response occurs. Such a short odor response with a sharp boost could often be observed when excitation light was switched on. It is likely that the occurrence of light responses depends on the stained subgroups of cells.

I have shown that the response to light shows a different spatial distribution in the imaged region, it is not restricted to the lip neuropil of the MB calyx as the odor response is. This is not surprising since the visual input from the optic lobes innervates the calyx neuropil in its collar region. The responding cells might be class I KC (in the example from chapter 3.1 stained somata of class I KC are visible) or (multimodal) clawed KC having their dendrites in the visual input area of the calyx, the collar.

I found GABA inhibitors impairing the optic response. The optic lobes of bees are also extensively innervated by GABA immunoreactive neurons (Schäfer and Bicker, 1986;Paulk et al., 2008), thus an influence of GABA antagonists on the optic responses is not astonishing. Whereas the $GABA_A$ blocker BMI leads to a diminished optic response, the application of the $GABA_A$ blocker PTX evoked an increased optic response. Thus, it seems that at least two GABA networks are involved in regulating optic responses.

The sucrose stimulation of an antenna with a 30% solution evokes a high response in MB KCs. Response is often higher than olfactory response to a 1% odor stimulus. Since tasting sugar is a primary stimulatory signal for feeding in bees, it is likely that sucrose receptors at the antennae are very sensitive, although the honeybee has only two sugar receptors genes. The genome of most *Drosophila* species contains eight sugar receptor genes (Kent and Robertson, 2009) besides the about 60 olfactory receptor genes. This is rather astonishing if one concerns the importance of sugar for a honeybee colony.
When sucrose was applied to the extended proboscis only a little calcium response could be seen since there are no receptors located on the proboscis. The little response might be cause by evaporating water exciting antennal receptors. Gustatory receptors are expressed on the antennae, the tarsi and the mouthpart of honeybees (Brito Sanchez et al., 2008).

4.2 Kenyon cells sense differences in odor concentration, the response is influenced by GABA

Kenyon cells sense odor intensity

A smell is characterized by the odor identity as well as by its intensity. In honeybees, different concentrations of one odor are not interpreted as different stimuli but as different characteristics of the same stimulus (Wright et al., 2005). Thus, odor intensity and identity are two features describing one stimulus. Odor intensities were also investigated in behavioral tests which revealed that bees actually sense differences in concentration (Pelz et al., 1997). To understand olfactory coding, it is therefore also important to learn about intensity coding.
In the glomeruli of the honeybee as well as in the relevant structures of other animals it could be shown that increasing odor intensity is reflected by response strength (Ditzen, 2005;Friedrich and Korsching, 1997;Spors and Grinvald, 2002). Also reduced latency or changed temporal features of the neuronal ensemble like elongated responses at higher stimulus intensity were shown (Zube et al., 2008), as well as modified synchronicity of neuronal firing in different PNs (Christensen et al., 2000;Spors and Grinvald, 2002).

When studying conditioned odor discrimination in *Drosophila*, it was found that the memory traces for odor quality and odor intensity are separately stored (Masek and

Heisenberg, 2008). This would lead to the expectation that information about odor quality and intensity are also processed differently.

In KCs, sparseness in the sense of stimulus specificity in response to different odors has been comprehensively described. Still, little is known about how the MB treats different odor concentrations. If individual KCs are very selective for specific odors one might also wonder whether they are also specific for odor concentrations.
Different scenarios for odor sensitivity are conceivable: 1) There are different subpopulations of cells responding at different odor concentrations, but the overall response remains unchanged. Such implementation was shown for *Drosophila* KCs. Here, different concentrations of the same odor led to different spatial patterns but the averaged amplitude of the response appeared constant over the monitored region (Wang et al., 2001). 2) The overall response changes, and is due to an increasing number of active cells. 3) The overall response changes, but is due to an intensified activity within cells without an increasing number of active cells. 4) The number and identity of responding cells remains unchanged and odor intensity is coded in the temporal domain or in the degree of synchronicity between responding cells.

I have shown in chapter 3.2 of this work that increasing odor intensities result in an increasing calcium response in the neuropil which contradicts the finding from *Drosophila* (Wang et al., 2001). Therefore, the first scenario can be ruled out for the honeybee KCs: coding for different concentrations is not realized by different ensembles of KCs. For the same reason, the fourth scenario is also unlikely, at least as the only way of coding, because of the shown increase in response strength. Anyway, temporal differences on a small time scale could not be investigated due to limited temporal resolution of our imaging technique. Odor dependent oscillations and phase locking is not sufficiently described in honeybees yet.

Application of odors with increasing concentrations leads to increased calcium responses in the MB lip. When plotting dose response curves over six logarithmic dilutions of odor intensity (figure 3-11) one finds an exponential curve with a dynamic range between undiluted odor and a dilution of -3 for the odor hexanal. At lowest odor concentration (-5) a slightly increased response is measured. Sachse and Galiza (Sachse and Galizia, 2003)

investigated the effect of odor concentrations on inhibited glomeruli and found that for the odor hexanol (hexanal not tested) at a -4 dilution more glomeruli are inhibited than at a -5 dilution or at higher odor concentrations. This could explain the increase in response amplitude at the lowest tested concentration: there are less glomeruli inhibited and therefore more PNs active which evoke a response in KCs which is slightly higher at very low odor concentrations. Thus, one can assume that low and high concentrations are processed differently as it is also proposed from behavioral tests (Wright et al., 2005).
Generally, it seems that KCs are less sensitive than PN, since Yamagata (Yamagata, 2008) found even at the lowest measured concentration (-5) a substantial proportion of boutons exhibiting excitatory responses. But, the comparison of data obtained at different experimental setups is unfavorable. Different olfactometers differ for instance in air volumes and velocity of the air stream.

The dose response curve for octanol is a sigmoid curve with a dynamic range between the concentrations -2 and -4. The dynamic response range for octanol is shifted by one order of magnitude dilution towards the lower concentrations compared to hexanal. Boutons of PNs show the same effect in calcium imaging experiments: in the range between a -2 and -4 dilution the percentage number of excited boutons for 1-octanol is higher than for hexanal. Also there the dynamic range is shifted towards lower concentrations (Yamagata, 2008).

Whereas for octanol the dose-response-function in KCs is sigmoid, it is exponential for hexanal. Similar result were shown for AL glomeruli from lACT PNs: for octanol the curve in responding glomeruli is sigmoid as well as in KCs, and exponential for hexanol, as it was found in KCs for hexanal (compare Sachse and Galizia, 2003). For all tested odors a clear positive concentration dependency was found in KC dendrites. Thus, odor intensity is also coded in KCs, they are not concentration invariant.

At the beginning of this chapter I had introduced four scenarios about how odor intensity might be coded in MB KCs. The first one, implying that for each concentration a different subpopulation is active, has already been ruled out as well as the fourth one, proposing changes in the spike timing, because an increasing calcium activity in the dendritic region was measured with a higher stimulus dose. The second and third scenario imply that with

increasing odor concentration either the number of active cells increases or active cells show higher response rate. To answer which principle is realized in KCs one would need to investigate individual cells.

Therefore, I have shown an example (Figure 3-13) in which two individual somata respond to a specific odor. Each soma shows a measurable calcium increase over several orders of magnitude in odor concentration. For one soma the effective dose range is spanning over three concentrations, for the other soma over four different concentrations. The response strength in the somata is decreasing with descending odor concentration, a result also obtained when the response strength is measured in the dendritic region.

This experiment reveals that KCs appear to respond in a odor-specific manner with diverse degrees of concentration invariance. Some KCs might respond to a narrow concentration range while others are unspecific for different intensities. This reconfirms findings in the locust (Stopfer et al., 2003).

The examples showing individual somata lead us to the assumption that the firing rate in individual cells is higher at high odor concentrations.

In this specific example, dendritic responses at low odor concentrations were still measured although the two individual somata were not responding anymore. This gives room to two different explanations: 1) the respective cells are only recruited at higher concentrations, or 2) the cells are activated also at lower concentration but only high firing rates in the cell caused by high stimulus concentration lead to the activation of calcium channels also in the somata. Low stimulation leads to lower firing rates which are not sufficient to evoke calcium influx into a soma.

I conclude from this example that with increasing odor concentration the number of KCs generating APs increases and that the firing rate increases with more intensive stimulation. Thus, scenarios 2 and 3 are both realized. Both principles match the mechanisms found in the AL where increasing odor concentration leads to an increasing number of active glomeruli and response strength in active glomeruli increases (Sachse and Galizia, 2003).

It was observed within this work that different odors evoke activity with rather similar time courses; the main difference between odors lies in the response strength. It was often found that hexanal evokes a stronger response than octanol. Why two odors are responded to with different activity strength can be explained by different vapor pressures leading to different quantities of odor molecules in the air which is therefore a concentration effect.

The vapor pressure of hexanal is two orders higher than that of 1-octanol (6al: 11.3 mm Hg (25°C), 8ol: 0.0794 mm Hg (25°C)), (Guerrieri et al., 2005). Higher vapor pressure leads to higher activity (Sachse et al., 1999). The dilution of different odorants could have been adjusted to equal effective vapor pressure but since other conditions like temperature could not be brought under full control, I refrained from adjusting odor dilutions and used equal dilutions in volume (v/v).

GABA impact on odor concentration sensitivity

I have shown that the odor intensity is mirrored in the strength of KC response. Still, the correlation is not linear; the response increases slightly while odor dose increases over several orders of magnitude.

It is generally presumed that odor-evoked spatiotemporal patterns are mediated in the AL by local inhibitory interneurons and responses are tuned by an adaptive gain control mechanism to expand the dynamic range of odor responses (Assisi et al., 2007;Stopfer, 2005). This gain control makes sure that over a 1000fold increase in odor intensity, the responses observed at the AL output and the KC input is increasing only moderately (cockroach: Distler et al., 1998;Husch et al., 2009; locust: MacLeod et al., 1998;Stopfer et al., 2003; moth: Berg et al., 2009; *Drosophila*: Wilson and Laurent, 2005;Kim and Wang, 2009;Root et al., 2008;Olsen and Wilson, 2008;Silbering and Galizia, 2007; honeybee: Sachse and Galizia, 2002). In addition to local inhibition in the AL, it was also shown that at the PN boutons in the calyx inhibitory events occur; their number increases with increasing odor intensity. This inhibition might be caused by GABAergic input (Yamagata, 2008) via third party MB extrinsic neurons.

In this work, I therefore tested the effect of GABAergic transmission at the level of KCs by usage of different GABA antagonists. I found that the dose response curves over the same range of odor intensities become much steeper in slope and the calcium response at high stimulus concentrations increases, even fourfold when a GABA antagonist was applied. Most effective is the $GABA_A$ receptor blocker picrotoxin (PTX). PTX has often been shown to be effective in insects (Perez-Orive et al., 2002;MacLeod et al., 1998;Stopfer et al., 1997;Sachse and Galizia, 2002). The increase evoked by PTX application compared with responses in the same animals before drug application was

significant for odor concentrations ranging from 1% to 100% odor dilution (+ further 1:10 dilution in permanent airstream).

Another $GABA_A$ blocker, BMI, which has a different molecular target (Rotte et al., 2009), had less strong impact but also led to an increased response, mainly at the 1% odor concentration, which is still a rather strong odor intensity. However, the effect is less prominent. This might be due to a lower effectiveness of this drug in the honeybee. Also it might be that it targets a different $GABA_A$ receptor subtype which is less involved in regulation response strength.
Nevertheless, also the $GABA_B$ receptor blocker CGP54626 causes a significant response increase at odor concentrations ranging from 1% to 100%.

The used drugs were bath applied to the whole brain. Therefore, it is unknown, where the receptors responsible for the described effect are located. GABAergic transmission mostly involved in the olfactory pathway occurs in the AL, where at least two inhibitory networks act and are involved in shaping the response of olfactory PNs. Previous investigations on honeybee lACT PNs after PTX ($GABA_A$ blocker) and CGP54626 ($GABA_B$ blocker) application resulted in increased response in some active glomeruli and, in addition, PTX increases the number of active glomeruli and enhances spontaneous activity. Some active glomeruli are more excited under PTX, whereas inhibited glomeruli are even more inhibited, but overall more glomeruli are active and the summed odor response is increased. PTX seems to mediate the global gain control in the honeybee AL (Sachse and Galizia, 2002). Recordings from PN presynaptic boutons show that lACTs generally show more inhibition (Yamagata, 2008). It is proposed that there is a global inhibitory network which is PTX sensitive (Sachse and Galizia, 2002) and a rather specific, local inhibitory network which uses transmission via $GABA_B$ receptors (Gühmann, 2007a) in the honeybee AL. Also in the *Drosophila* AL PTX usages revealed interglomerular inhibitions (Silbering and Galizia, 2007). In the zebrafish, GABA networks exist in the olfactory bulb. Blocking $GABA_A$ receptors enhances excitatory responses and abolishes fast oscillations in the local field potential indicating that this circuit balances excitation and inhibition, regulates total output, and synchronizes odor-dependent neuronal ensembles. Inhibiting $GABA_B$ changes the amplitude and the time course in a subset of

mitral cell responses indicating that this networks modulates OB output (Tabor et al., 2008).
Thus, inhibitory GABAergic networks could cause the effects seen in KCs via changes in the response properties of the PNs. BMI evoked effects are also likely to be caused in the AL since BMI was found not to be effective in honeybee cultured KCs (Grünewald and Wersing, 2008).
Neuronal activity transferred from the AL might be further mediated in the calyx. KCs are in direct association to GABA immunoreactive PCT neurons (Bicker et al., 1985). It was shown in electron microscopy studies that GABAergic neurons form synapses and reciprocal synapses with bigger profiles assumed to belong to PNs (or the VUMmx1 neuron) and to smaller profiles probably belonging to KCs. Thus, PCT neurons form a feedback onto PNs and onto KCs (Ganeshina and Menzel, 2001). With increasing sensory input they might increase GABA release as a feedback signal.
It was shown that honeybee and *Drosophila* KCs have ionotrophic GABA receptors (Grünewald and Wersing, 2008;Liu et al., 2009;Liu et al., 2007). In the fly the overexpression of this receptor in the MB calyx led to reduced calcium responses to olfactory stimuli and the knockdown enhances responses. These results suggest that $GABA_A$ receptors in KCs selectively gate the magnitude of neuronal response to odors. In the *Drosophila* MB calyces also $GABA_B$ receptors were found (Enell et al., 2007).

To answer the question whether GABA mediated inhibition occurs in the AL or in the MB calyx it would be necessary to apply the drugs locally. It is very likely that more than one mechanism is active and that information is mediated at more than one level of processing via GABA mediated inhibition.

However, it is noteworthy that after GABA inhibition the dose dependency of KCs still exists, not all responses become equally high. Thus, one can conclude that dose dependency per se is not mediated by GABA inhibition. Other intrinsic mechanisms must be regulating dose responsiveness. It occurs certainly already on the level of the receptor neurons and is thus dependent on the amount of odor molecules available: More receptor input evokes higher response in PN. These get down regulated for higher concentrations. None of the GABA antagonists caused an effect on low odor concentrations: The dose

response does not get shifted towards lower concentration; the lower sensitivity threshold remains unaltered.
In PNs it was shown that lACT neurons are less concentration sensitive at higher odor concentrations compared to mACTs (Yamagata, 2008). This might be due to stronger inhibition at high concentrations on lACT neurons which is in accordance with the finding that PTX causes strong effects in lACT glomeruli (Sachse and Galizia, 2002).

This result shows that GABA inhibition itself is also concentration dependent. With increasing odor intensity the inhibition increases. This means, also GABAergic neuron must follow a dose dependency. Within the AL there are GABAergic interneurons which are likely to get (direct) input from receptor neurons (Boeckh and Tolbert, 1993). This way they "measure" input strength and increase their transmitter release onto PN. The shorter latency of LNs found in the honeybee AL fits this model (Krofczik et al., 2009).
In fact, science in *Drosophila* has shown that local interneurons show concentration dependent activity. (Asahina et al., 2009;Silbering et al., 2008;Stopfer et al., 2003).

4.3 Concentration sensitivity and GABA dependency of off-responses

Olfactory responses appear not only at the onset of odor stimulation, but also at the termination of an olfactory stimulus. Such off-responses can be found in KCs in responses to some odors; they are odor specific and occur in response to most alcohols as has been shown in this work (Figure 3-4). It cannot be resolved whether off-responses are generated in the same KCs as on-response or in different cells. Other authors showed with an electrophysiological approach in M*anduca* that most neurons showing off-response get activated only at odor offset, but some respond at odor onset as well (Ito et al., 2008). An example from the honeybee where a single cell was imaged, shows that the response in the soma consists of on- and off-response (Szyszka et al., 2005). This means that at least some KCs show both.
Off-responses also occur in PNs (Abel et al., 2001;Homberg, 1984). For PN boutons it was shown by optical imaging that mACT boutons are more prone to respond at stimulus offset than lACT with either excitation or inhibition (Yamagata, 2008). Boutons from

mACT respond to octanol with a dominating on- but also an off-response. For hexanal lACT boutons show an off-response besides the dominating on-response.
It is unclear how off-responses in KCs are generated. They could be just transferred from PNs already showing off-responses, quasi be a read out, or they could be newly generated in KC, for instance as a rebound from inhibited PN.
Also for off-responses in PNs it is unclear how they are generated. There are different possibilities: 1) Some receptor neurons show inhibition when stimulated by certain odors (de Bruyne et al., 2001), a rebound from this inhibition could lead to an off-response in a PN. 2) Some PNs get inhibition during odor stimulation by LNs. A rebound from such inhibition might result in an off-response.
This latter hypothesis is in accordance with the finding that LNs show shorter latency than PN. In consequence, LNs might thus inhibit any olfactory response in the PNs during the stimulus (Fujiwara et al., 2009;Krofczik et al., 2009). But later inhibition could also start with longer latency after odor onset, for instance after a phasic response, which might even be even driven by some feedback neurons. Often two types of inhibition act together: an early phase mediated by ionotrophic receptors and a later phase mediated by metabotrophic receptors (Olsen and Wilson, 2008).
PN boutons in the calyx also show inhibition (Yamagata, 2008). This might lead to a rebound generating an off-response in KC.
All these possibilities include a GABAergic or otherwise inhibitory mechanism. It also might be that off-responses are evoked by an excitatory transmitter release at odor offset or via another pathway like the cAMP pathway as proposed for olfactory receptor cells. It is further suggested in the same publication that the generation mechanism of off-responses is different from that of on-responses (Kashiwayanagi et al., 1994).

Remarkably, I found in KCs that off-response occur only after an odor stimulus lasting at least 3 seconds. For stimuli shorter than 3 seconds, no off-response occurs. This finding is in accordance with findings in *Manduca* (Ito et al., 2008). This favors a rebound effect from a (long lasting) inhibition.

I found in honeybee KCs no correlation between stimulus duration and response magnitude. It is rather the stimulus duration which defines whether on off-response occurs at all. On the contrary, in rodents' whisker neurons the off-response magnitude was shown

to increase as the stimulus duration increases from 200 to 1,400 ms (Kyriazi et al., 1994). It is suggested that stimulus onset evokes central inhibition having two components, a strong one lasting only few tens of milliseconds and a weaker one lasting many hundreds of milliseconds.

Interestingly, the strength of off-responses also shows a positive correlation to the odor concentration. That means off-responses do not only code the end of any stimulus. More lateral inhibition at higher odor concentration can lead to increased rebound at odor offset. It was shown before that GABA mediated inhibition itself is concentration dependent. Therefore, increased lateral, long lasting inhibition could lead to an increased off-response.

If off-responses are a result of a rebound from GABA inhibition, as it is generally assumed, the blocking of GABA receptors should lead to the disappearance of off-responses. In fact, blocking GABA receptors does not totally abolish off-responses, rather the application of PTX results in the lateral calyx in a decreased off-response but in the median calyx it leads to an increased off-response as it does for the on-response, too. This implicates that there are different mechanisms besides GABAergic inhibitions evoking off-responses in KCs. In the lateral calyx, off-responses could be a rebound from inhibition and blocking inhibition also blocks off-responses. In the examples from the median calyx, were blocking inhibition causes increased off-responses, there must be another network or pathway that evokes off-responses.

Off-responses were only impaired by treatment with PTX; the other GABA antagonists did not influence them. In conclusion, a later phase of inhibition, as it might be mediated by metabotrophic receptors (Olsen and Wilson, 2008), is not causing off-responses.

4.4 Differences between the lateral and the median calyx

Another finding of this work was a difference between the two calyces of each mushroom body, the median and the lateral calyx. To our knowledge, this is the first time that differences between the two calyces could be shown. Dual calyces evolved to increase the sensory input area of the MB. Both calyces get input from the same neurons and their KCs project to the output lobes. The Kenyon cell organization and projection in the two calyces

was described as indistinguishable; each calyx of a pair would receive essentially identical input (Strausfeld et al., 1998). For two beetles of the scarabaeidae family structural differences between median and lateral calyces were described recently (Panov, 2009). On the level of morphology, Abel et al. (Abel et al., 2001) have detected that individual PNs show different innervation patterns in the two calyces of a MB. Especially for mACT PNs examples of neurons were shown which arborize differently in the median and in the lateral calyx. It is unknown which region in lateral calyx corresponds to which region in the median one, but Rybak proposes that calyces might be rotated by 180° (Rybak, 1994) based on KC projections in the α-lobe.

In the lateral calyx nearly 30,000 clawed KCs develop, whereas only about 20,000 are in the median one (Witthöft, 1967).

I demonstrated in this work that at least in the calyx area I have imaged, odors of higher intensity are responded to more strongly in the lateral calyx (Figure 3-12). Data were obtained by imaging the main part of the whole anterior side of the lip neuropil. It is striking that for hexanal the dose response curves in both calyces have an exponential shape whereas for octanol these curves are sigmoid in both calyces. In contrast, the magnitudes at higher odor concentrations differ between calyces. This leads to the assumption that the respective firing patterns causing the shape of the response curve are already evoked in PNs rather than in KCs. The differences in response strength might be caused by stronger GABA mediated local inhibition in the median calyx, an idea reconfirmed by experiments with GABA inhibitors: While absolute response strength was higher in the lateral calyx than in the median one, I could further show that the $GABA_A$ blocker PTX has higher impact in the median calyces (Figure 3-17) implying that GABA inhibition is indeed stronger in those median calyces. This inhibition could occur from GABAergic interneurons - the PCT neurons, although there is no evidence that these neurons have different innervation pattern in the two calyces (Grünewald, 1999a;Bartels, 2007).

Of course, it cannot be ruled out that differences in response strength between the two calyces are due to artifacts like different staining intensity or different foci in the microscope. However, I could not find any plausible explanation for any systematic error: that there is always more functional dye in the lateral calyx is unlikely, although there are more clawed KCs in the lateral calyx. The confocal scans performed after imaging have

not affirmed stronger staining in lateral calyces. A smaller distance between the tissue and the objective during the scanning process is also impossible, since the lateral calyx lies more posterior and distance is rather bigger than smaller.
Other indications against any methodological artifact are the physiological differences found as the different impact of GABA on response magnitudes at high odor concentration as well as on off-responses, as it was shown in a previous paragraph.

4.5 Temporal dynamics in Kenyon cells

In PNs, temporal coding is of great importance. Temporal dynamics can be distinguished into slow and fast dynamics (Galán et al., 2006;Galizia et al., 2000): 1) The sequence in which specific PNs fire is crucial for coding the odor identity. 2) Firing in PNs includes synchronization among populations of neurons, and 3) Firing is correlated to LFP oscillations of the brain (Lei et al., 2009;Tanaka et al., 2009;Christensen et al., 2003;MacLeod and Laurent, 1996;Laurent et al., 1996;Wehr and Laurent, 1996). Therefore, temporal features of MB intrinsic cells, the target cells of olfactory PNs, were investigated in this work.

Importance of stimulus length

In nature, the length of a stimulus has a meaning as well as its identity and intensity (Frasnelli et al., 2006). The persistence of a smell particularly provides information about the distance and the direction of the odor source, especially while a bee is flying through an odor plume.
In harnessed bees a 200 ms odor stimulus is sufficient for recognizing, learning, and discriminating odors. For low odor concentrations discrimination ability improves with stimulus time (Wright et al., 2009), a stimulus of more than 500 ms is recognized irrespective of its length (Fernandez et al., 2009).
On the neuronal level, the activity in clawed KCs is described as showing lifetime und spatial sparseness as well as temporal sparseness. The latter means that KCs respond only in a brief phasic way (Szyszka et al., 2005).

First, I questioned if this brief response profile changes with stimulus length. I applied stimuli of varying length to clawed KCs, as well as, for comparison, to lACT PNs and recorded the responses.

In PNs, stimuli with duration of 1, 2, or 3 seconds were used. I found that the phasic-tonic response clearly reflects stimulus length (Figure 3-27), and that the calcium level often abruptly decreases at odor offset. This is in accordance with other data from optical imaging of PNs in the AL as well as with electophysiological data (Sachse and Galizia, 2002;Müller et al., 2002). On the contrary, I found that in KCs the duration of the calcium response after odor onset is totally independent from stimulus length (Figure 3-28). KCs show a phasic response that decays equally fast, no matter how long the stimulus lasts. The same effect was recently shown in *Manduca sexta* (Ito et al., 2008). Besides this very homogeneous on-response, the stimulus length determines whether an off-response can be measured as it was already discussed above (see Figure 3-29).

GABA impact on stimulus length

Short responses were often interpreted as the result of inhibitory input by GABAergic feedback neurons (Szyszka et al., 2005;Perez-Orive et al., 2002). Findings by Yamagata (Yamagata, 2008) showing that inhibition in PN boutons occurs later than excitation does, supports this interpretation.

Thus, I investigated if the application of GABA antagonists changes the response length.

For all three drugs tested ($GABA_A$ blocker PTX and BMI, as well as the $GABA_B$ blocker CGP54626) no change in the temporal response profile could be observed although the response strength, and therefore the intracellular calcium level, was increased after drug application (Figure 3-30 et seq.). Taking into account that the signal reached higher amplitude after application of a GABA receptor blocker, whereas the normalized response curve looks the same, the decrease of the signal is even faster in absolute terms.

Thus, I conclude that the temporal sparsening of KCs is not mediated by any GABAergic inhibition; rather there must be a neuron-intrinsic mechanism responsible for appearance of only brief responses. The experimental results can be explained by a spike frequency adaptation (SFA) mechanism (Farkhooi et al., 2009) as it was also recently concluded from experiments in the cockroach (Demmer and Kloppenburg, 2009). Here, the cell facilitates very fast hyperpolarisation after spiking. This hyperpolarization could be caused

by calcium activated potassium channels as they are also described for honeybee KCs (Schäfer et al., 1994). Activation of those channels leads to a potassium influx that hyperpolarize the cell and thus dramatically slows down the action potential firing rate. SFA also explains why the calcium signal decays even faster after a high response magnitude: because more excitation at the beginning of stimulus onset leads to an increased hyperpolarization and thus a faster decay.
An underlying mechanism for this temporal fast and sparse response was recently found in the cockroach (Demmer and Kloppenburg, 2009): the authors show an enduring synaptic inhibitory input by GABA that permanently hyperpolarizes KCs. That means GABA keeps the cells silent, but when they get sufficiently depolarized, many calcium-channels open quickly and simultaneously, making 1 or 2 spikes enough to evoke a big calcium influx into the cell. The absence of spontaneous firing in KCs must thus be seen as a precondition for sparse responses during odor stimulation.

I conclude, that neither the length of a stimulus nor GABA transmission influences the length of the calcium response measured with optical imaging. Recent work in the honeybee described that an odor-sucrose pairing in an associative learning protocol can lead to prolonged odor responses in KCs (Szyszka et al., 2008). These prolonged responses might be due to modifications of postsynaptic channels, for instance at calcium dependent potassium channels which close and thus lead to a delayed repolarization. This results in an impaired decrease of the intracellular calcium concentration.

In my work I could only investigate slow temporal dynamics. On a finer time scale, GABA might mediate odor-evoked responses. Fast temporal characteristics like oscillation power and odor-evoked oscillatory synchronization of neurons phase-locked to LFP have been shown to depend on synaptic transmission via $GABA_A$ receptors in mice OB and in *Drosophila* AL (Tanaka et al., 2009;Nusser et al., 2001). How these temporal features are red out by downstream neurons is still unclear.

Discrimination of successive stimuli

Behavioral experiments with *Manduca sexta* have shown that the ability to follow odor pulses depends on the inter pulse interval, a 5 second interval leads to a better pulse-

following index than a 2 second interval but 2 Hz stimulation (ISI 0.5 s) can still be resolved. Pulse tracking is impaired when GABA is blocked (Lei et al., 2009).
The application of successive stimuli is used in massed learning protocols. Massed training is less effective in acquiring long-lasting memories (Menzel et al., 2001). In a recent work it was claimed (Liu et al., 2009) that $GABA_A$ receptors need to desensitize between learning trials and this is only done in spaced conditioning. Therefore, subsequent conditioning trials in spaced training are more effective.
These findings led me to the next question: I asked, how good KCs can resolve successive stimuli. I applied two stimuli with different ISI and compared the responses in PNs and in KCs.

A better ability to separate two stimuli, each lasting 1 second, was found in KCs (Figure 3-34, 3-35). Whereas in PNs an interval of 0.5 seconds between two stimuli can be resolved but leads to a clearly smaller second stimulus, the same protocol evokes in KCs two responses of the same magnitude. Even shorter inter-stimulus breaks can be resolved in KCs. A certain time window between two successive odor stimuli, namely 2 and 3 second inter-stimulus interval after a one second stimulus, even leads to an increased response to the second stimulus. This could be due to a synaptic facilitation: there are still free transmitter molecules available at the excitatory synapse; consequently a new stimulus evokes an even higher response.
Remarkably, this time window matches the time window when off-responses occur. It might be that 3 seconds is a critical or relevant time for free flying bees for distinguishing different stimuli effusing from different odor sources.

With respect to two successive stimuli I investigated the impact of GABA on the reduction of a stimulus following a first one with short delay.
When the odor stimuli are very short, 333 ms in my experiment, the application of two successive stimuli with an ISI of 0.5 seconds leads to a significantly reduced response during the second stimulus (Figure 3-36). In accordance to that, extracellular recordings performed at KCs in locusts revealed that a 500 ms inter pulse interval also evokes a response to the second and third stimulus but spiking is most frequent at the first one (Brown et al., 2005). This reduction is also not mediated by a prolonged $GABA_A$ receptor mediated inhibition: application of PTX evokes a significantly increased response to both

stimuli, but the ratio between the first and the second stimulus remains unaltered. I conclude that the reduced response occurring during the second stimulus, when the time difference between odor onsets of two successive stimuli is smaller than 1 second, is not mediated by GABA via PTX sensitive receptors. Instead, this reduced response is probably caused by some cell intrinsic properties like a reduced excitability during the relative refractory period which can in general last for several hundred milliseconds. During this period a second AP evokes smaller depolarization.

Further considerations on GABA function in the MB calyces

Using GABA antagonists I have shown that blocking GABA transmission in the honeybee brain increases calcium responses to intensive odor stimuli in MB intrinsic cells. As a result, sparseness in KCs is in part mediated by GABAergic interneurons. A gain control mechanism exists in the AL mediated by inhibitory LNs.
The temporal sparsening of KCs is not caused by GABA inhibition but by a SFA mechanism.

The role of GABAergic innervations in the MB is still unknown.
GABAergic interneurons which innervate the MB calyx and form a feedback loop from the MB output lobes (PCT neurons) could be involved in fine tuning odor responses (see also Yamagata, 2008) but mostly they might be involved in learning processes during associative learning (MacLeod et al., 1998). In *Drosophila* the $GABA_A$ receptor *Rdl* is highly expressed in the MBs and the AL. Behavioral tests with *Drosophila* having a *Rdl* mutation in MB KC suggest that this receptor is involved in olfactory learning: RDL suppresses olfactory learning via the olfactory (CS) pathway (Liu et al., 2007;Liu et al., 2009); a GABAergic anterior paired lateral neuron was found which innervates the mushroom body and is involved in olfactory learning. Learning suppresses the activity of this inhibitory neuron (Liu and Davis, 2009).
Interestingly, immuno-cytochemistry in the honeybee MB calyx revealed that the GABA immunoreactivity decreases strongly in adult bees within 4 weeks after emergence (Brill et al., 2008). This also favors that GABA plays a role in learning related neuronal plasticity. Since honeybees show division of labor, each individual bee has to undergo different tasks in her life which requires behavioral adjustment and learning.

KCs are often thought to function as coincidence detectors to acquire associations based on synchronous stimuli pairs or patterns (Grünewald et al., 2004). They are influences or reset by inhibitory feedback neurons which gives room for plasticity as demonstrated in KCs after associative learning (Szyszka et al., 2008). Learning and memory processes might be located in MB readout neurons (Smith et al., 2008;Hähnel, 2009;Okada et al., 2007;Grünewald, 1999b). These extrinsic neurons combine information about stimulus characteristics and assign them certain significance. GABA could also be released upon presynaptic activation by other neurons, like the VUMmx1, that project into the MB calyx and form putative excitatory synaptic contacts with KCs and GABAergic neurons. The VUMmx1 neuron branches in the same neuropils as KCs and PCT neurons (Hammer, 1993) and it also might be integrated in microcircuits within the calyx (Ganeshina and Menzel, 2001).

4.6 Perception of odor mixtures

In their natural environment bees are mostly surrounded by rich odor bouquets. Single component odors are rare. It is of high interest, how mixtures are perceived and whether they are presented as a novel odor quality or as a composition of single components. For this reason, mixtures are used and compared with their single components in investigations on the behavioral level (Smith, 1998) as well as on the cellular level.

To understand olfactory processing, mainly with respect to the function of inhibitory and excitatory interneurons in the olfactory pathway, the use of mixed odorants as defined stimuli is very helpful.

Odor mixture interaction can occur and therefore be studied on several levels of the olfactory pathway: in the peripheries with the odor receptors, in the first relay being the AL or OB, or in the higher order brain region: the mushroom body or the olfactory cortex. They were for instance studied in the honeybee while performing calcium imaging in the AL glomeruli and at the PN boutons in the MB calyx (Deisig et al., 2006;Guerrieri et al., 2005;Yamagata, 2008;Joerges et al., 1997), and also while recording intracellularly form PNs and AL interneurons (Krofczik et al., 2009).

To describe the mixture effects, three classes are defined (Deisig et al., 2006;Yamagata, 2008;Duchamp-Viret et al., 2003;Krofczik et al., 2009): 1) Responses to mixtures show

synergy which means that response to the mixture is higher than to the strongest component. 2) Responses to mixtures show hypoadditivity, which means the response is similar to the salient odor or slightly higher. 3) Response to mixtures show suppression, which means response is lower than to strongest component.

Usage of binary mixtures in the AL revealed that the responses to odor mixtures were complex and glomerulus-dependent (Joerges et al., 1997;Deisig et al., 2006;Galizia et al., 2000). Individual glomeruli show suppressed responses, but the number of active glomeruli increases in the mixture with increasing number of mixed odors (Deisig et al., 2006). For binary mixtures some glomeruli show suppression but most glomeruli respond with hypoadditivity. For tertiary mixtures the same proportion of glomeruli show hypoadditivity, but there is suppression in an increasing number of glomeruli (Deisig et al., 2006). In mitral cells of vertebrates mixtures produced a general suppression of evoked firing rates which is likely to be mediated by inhibitory interneurons (Davison and Katz, 2007).

Comparing the two ACT tracts, it could be shown that PNs of lACTs show most frequently a suppression effect when stimulated with a tertiary mixture although they show an excitatory response to all single components (Krofczik et al., 2009). No suppression was observed in mACT neurons.

In my work, I applied single odors and their tertiary mixtures while recording the calcium activity in clawed KCs and aimed to compare the results with previous findings in their upstream neurons.
I could show that clawed KCs respond to odor mixtures in a hypoadditive way. In only one bee out of seven a suppression effect was observed. I assume that a different subpopulation of KCs was stained in this bee for two reasons: no typical clawed KC somata could be seen in the confocal scan and this bee showed a high response to light stimulation.
The fact that clawed KCs show no suppression but rather hypoadditive responses corresponds to data from mACT PNs. This might lead to the assumption that clawed KCs are innervated by mACT PNs which is in accordance with the finding, that mainly mACT PNs innervate the outer part of the MB lip (Kirschner et al., 2006). It is known that the

dendrites of clawed KCs arborize in the outside margin of the calyx, the same region that is innervated by mACTs; but KCs span the whole lip. But it must be considered that mACT data result from individual neurons or boutons and KC data from big populations of neurons, therefore, comparisons can be only made with some limitations.
The fact that hypoadditive effects are measured in clawed KCs, implies that they also code for odor mixtures. It is supposable that other populations of KCs like KCs of class I respond with suppression effects. Further investigations are needed at this point.
Another explanation for an additive effect would be that some (lACT) PNs get newly recruited by the mixture which did not respond to single components (and were overseen in electrical recordings). This is in accordance with the finding that more glomeruli become activated with increasing number of components in the mixture (Deisig et al., 2006).
Also in locusts it was shown that some KCs respond specifically to an odor mixture, whereas some respond to the mixture and one single odor (Broome et al., 2006).

4.7 Methodological concerns

Calcium Imaging

Measuring intracellular calcium activity nicely reflects the activity that can be measured with electrophysiological methods (Moreaux and Laurent, 2007;Galizia and Kimmerle, 2004;Charpak et al., 2001). But wide field calcium imaging, as it was used in this work, has its constraints: light scatter hinders a high spatial resolution, the temporal resolution is limited by the CCD camera, and the penetration of the tissue by the excitation light is weak, thus only surfaces can be investigated. But since electrophysiological techniques in KCs in the honeybee are not established yet, calcium imaging is the preferred method.

Using a functional dye also might influence the intracellular processes, for instance the calcium sensitive dye itself is a buffer for calcium ions (Neher, 2008). The mass staining method used does not allow a very specific and reproducible staining but the staining can roughly be controlled by fixing the added rhodamine dye and inspecting the staining at the confocal microscope afterwards.
To improve data quality, two approaches for other techniques shall be discussed briefly.

Electroporation

The use of rather unselective dye injections could be avoided by local dye injections via intracellular staining (Galizia and Kimmerle, 2004), via local electroporation (Fujiwara et al., 2009), or by expressing genetic functional dyes in the neurons. Unfortunately, the variety of genetic tools, as it is available for *Drosophila melanogaster,* does not exist for other insect models like the honeybee. Therefore, exogenous proteins like fluorescent dyes cannot be inserted in the chromosomal genome and no genetic lines could be generated yet.

For inserting DNA into adult cells one can use viral infections, injections of naked DNA (gene gun), sonoporation, or DNA electrotransfer. By means of electroporation the cell membrane opens and extracellular DNA can enter the cell (for review see: Andre and Mir, 2004). Thus, exogenous genes can be brought into individual animals.

For the honeybee I tried an *in vivo* plasmid DNA electrotransfer which has become a common method in mammalian tissue for gene therapy, electrochemotherapy, and as a laboratory tool to study gene functions (Bigey et al., 2002). It is a physical method to overcome the barrier of the cell membrane by applying electric pulses. If the plasmid contains a suitable promoter, the gene might be expressed by the cell's transcription- and translation machinery.

This method has already been used for gene transfer into insect tissue (Golden et al., 2007;Thomas, 2003) and also in the adult honeybee brain (Kunieda and Kubo, 2004).

It is a suitable method for our laboratory to overcome the problem of unreliable staining by firstly using a plasmid carrying a GFP gene. I could show that the electroporation of living brains was successful and neurons expressed the respective gene. These achievements are a good basis to build on for expressing functional calcium sensitive dyes like chameleon dyes (Miyawaki et al., 1997) or G-Camp (Nakai et al., 2001) also in the honeybee brain and use these animals for *in vivo* imaging.

Genetically encoded proteins offer the possibility of long-term in vivo imaging without bleaching, they allow specific localization, and gene expression is a proof for the viability of the neurons. With specific promoters one could even aim to selectively stain subtypes of cells. Further progress needs to be undertaken to establish this method. In a next step, an effective plasmid carrying a gene for a calcium sensitive dye under a selective promoter is needed.

2-Photon Laser Scanning Microscopy

To better understand the olfactory coding in KCs it is necessary to be able to record data from individual cells, ideally from several individual cells simultaneously. This goal was not satisfyingly reached with the wide field calcium imaging.

An improvement for optophysiological measurements would be the use of a Multi- or 2-Photon Laser Scanning Microscope to achieve a better spatial resolution, improve the signal while performing calcium imaging by enhancing the contrast, and to achieve better penetration of the tissue when performing *in vivo* imaging (Denk et al., 1994; for review: Helmchen and Denk, 2005). It would allow addressing some questions which could not be answered during this work using a conventional fluorescence microscope. For instance one could better allocate calcium activity to a morphological structure, one could scan in deeper laying plains and this way also investigate KCs class I, and while reducing the spatial resolution one could increase temporal resolution and this way learn about the temporal tuning of MB neurons. Some preliminal approaches showing that the use of a 2-Photon Laser Scanning Microscope is applicable in honeybee were already undertaken (Szyszka, 2005).

Figure 4-1 shows a scan from a pretest I performed with a 2-Photon Microscope. There are somata of clawed KCs and their overlapping dendrites in the lip neuropil of a calyx in a honeybee MB visible. The cells were stained as in the other experiments described in this work, unfortunately, no odor-evoked calcium signals were obtained so far, but further efforts would be worth it working on to achieve better physiological data while performing calcium imaging.

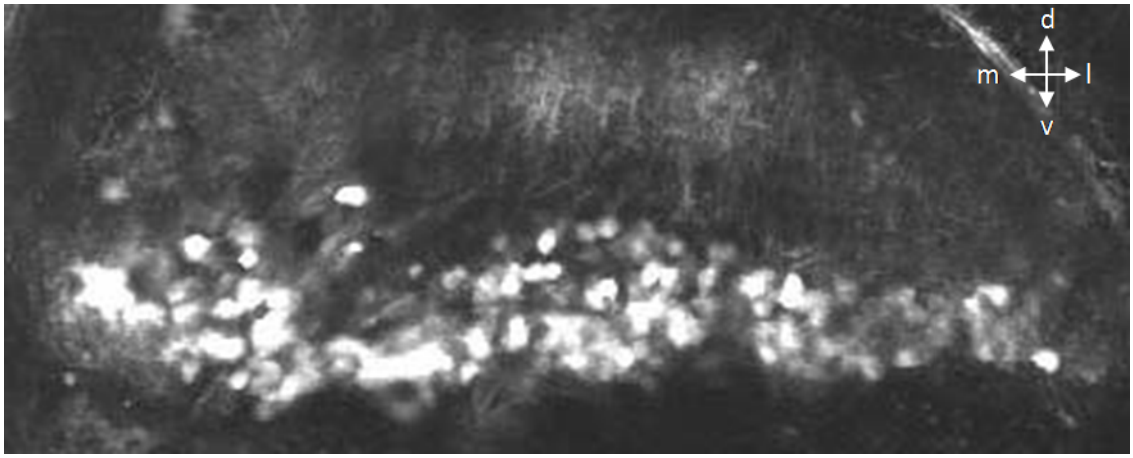

Figure 4-1: Clawed Kenyon cells at the outer brim of a median calyx, scanned with 2-Photon Laser Scanning Microscope
High resolutions scan of the calyx neuropil, area approx. 210x146 microns
At the top of the picture overlapping dendrites of clawed Kenyon cells in the MB lip can be seen, at the bottom of the picture outstandingly stained somata of clawed Kenyon cells at the outer brim of the calyx can be seen.

5. Outlook

This work gives some new insights in the functioning of Kenyon cells. However, their operation principles are still not deciphered completely and new questions arise.

The following directions for future work are of high interest:

1) In this work I could show that Kenyon cells responses are positively correlated with odor intensity. Yet, it is still not solved how this is done on the level of neuronal populations. It still needs to be unveiled whether increasing odor intensity is replied by an increasing number of cells or by an increased firing rate in a limited number of cells, i.e. whether for different concentrations the same cells are firing or different ones. There is evidence that both principles could be employed.
   To answer this, advanced techniques need to be applied in future work. This might be accomplished in electrophysiological approaches by recording several KC units simultaneously, or with improved optophysiological methods that need to be established. Such optophysiological methods should provide high spatial resolution and good signal-to-noise-contrast. This could be realized by laser scanning microscopy. This way, one could aim to resolve individual dendrites (after establishment of a fine staining method) or cell somata, presuming that somatic responses map cellular activity. Also imaging from somata of KC class I might be possible this way.

2) With respect to odor intensity I could show that the neurotransmitter GABA down regulates strong responses in a gain control mechanism. It is not known if the respective GABA transmission occurs in the MB calyx. To address this, GABA or GABA antagonists should be applied locally by local injections or by using caged compounds which get locally activated via photorelease.

   As to pharmacology and improved staining techniques (as discussed earlier in this work), laboratory tools from the field of molecular biology/biochemistry as well as from electro- or opthophysiological fields should be combined.

3) Another promising approach would be to look at temporal features of KC firing in much more detail, for instance with respect to odor intensity. Also here, techniques with higher temporal resolution are required. This way one could investigate if increasing stimulus concentration changes the response latency or the firing synchronicity of KC. Further, the influences of GABA on fine scale temporal characteristics could be addressed since it was shown, contrary to former expectations, that slow temporal dynamics of KCs are not impaired by GABA.

Reference List

1. Abel R, Rybak J, Menzel R (2001) Structure and response patterns of olfactory interneurons in the honeybee, *Apis mellifera*. Journal of Comparative Neurology 437: 363-383.

2. Ache BW, Young JM (2005) Olfaction: Diverse species, conserved principles. Neuron 48: 417-430.

3. Andre F, Mir LM (2004) DNA electrotransfer: its principles and an updated review of its therapeutic applications. Gene Ther 11 Suppl 1: S33-S42.

4. Asahina K, Louis M, Piccinotti S, Vosshall L (2009) A circuit supporting concentration-invariant odor perception in *Drosophila*. Journal of Biology 8: 9.

5. Aso Y, Grübel K, Busch S, Friedrich AB, Siwanowicz I, Tanimoto H (2009) The Mushroom Body of Adult *Drosophila* Characterized by GAL4 Drivers. Journal of Neurogenetics 23: 156-172.

6. Assisi C, Stopfer M, Laurent G, Bazhenov M (2007) Adaptive regulation of sparseness by feedforward inhibition. Nature Neuroscience 10: 1176-1184.

7. Bartels, R. (2007) Physiologie und Morphologie der GABA-immunoreaktiven Neurone (A3) der Pilzkörper von *Apis mellifera* L.
Diplom Thesis

8. Berg BG, Schachtner J, Homberg U (2009) gamma-Aminobutyric acid immunostaining in the antennal lobe of the moth Heliothis virescens and its colocalization with neuropeptides. Cell Tissue Res 335: 593-605.

9. Bicker G (1999) Histochemistry of Classical Neurotransmitters in Antennal Lobes and Mushroom Bodies of the Honeybee. Micros res tech 45: 174-183.

10. Bicker G, Kreissl S, Hofbauer A (1993) Monoclonal antibody labels olfactory and visual pathways in *Drosophila* and *Apis* brains. Journal of Comparative Neurology 335: 413-424.

11. Bicker G, Schäfer S, Kingan TG (1985) Mushroom body feedback interneurons in the honeybee show GABA-like immunoreactivity. Brain Res 360: 394-397.

12. Bigey P, Bureau MF, Scherman D (2002) In vivo plasmid DNA electrotransfer. Curr Opin Biotechnol 13: 443-447.

13. Boeckh J, Tolbert LP (1993) Synaptic Organization and Development of the Antennal Lobe in Insects. Micros res tech 24: 260-280.

14. Brill, M. F., Wegener, S., and Rössler, Wolfgang. (2008) Maturation of GABAergic innervation in the mushroom bodies of the adult honeybee brain. vol. 4., FENS Forum Abstracts, A143.4.

15. Brito Sanchez M, Chen C, Li J, Liu F, Gauthier M, Giurfa M (2008) Behavioral studies on tarsal gustation in honeybees: sucrose responsiveness and sucrose-mediated olfactory conditioning. Journal of Comparative Physiology A: Neuroethology, Sensory, Neural, and Behavioral Physiology 194: 861-869.

16. Brockmann A, Brückner D (1995) Projection pattern of poreplate sensory neurones in honeybee worker, *Apis mellifera L.* (Hymenoptera: Apidae). Int J Insect Morphol & Embryol 24: 405-411.

17. Broome BM, Jayaraman V, Laurent G (2006) Encoding and decoding of overlapping odor sequences. Neuron 51: 467-482.

18. Brown SL, Joseph J, Stopfer M (2005) Encoding a temporally structured stimulus with a temporally structured neural representation. Nature Neuroscience 8: 1568-1576.

19. Buck L, Axel R (1991) A Novel Multigene Family May Encode Odorant Receptors - A Molecular-Basis for Odor Recognition. Cell 65: 175-187.

20. Carlsson MA, Knusel P, Verschure PFMJ, Hansson BS (2005) Spatio-temporal Ca2+ dynamics of moth olfactory projection neurones. European Journal of Neuroscience 22: 647-657.

21. Charpak S, Mertz J, Beaurepaire E, Moreaux L, Delaney K (2001) Odor-evoked calcium signals in dendrites of rat mitral cells. Proceedings of the National Academy of Sciences of the United States of America 98: 1230-1234.

22. Christensen TA, Lei H, Hildebrand JG (2003) Coordination of central odor representations through transient non-oscillatory synchronization of glomerular output neurons, Proceedings of the National Academy of Sciences of the United States of America 100: 11076-11081.

23. Christensen TA, Pawlowski VM, Lei H, Hildebrand JG (2000) Multi-unit recordings reveal context-dependent modulation of synchrony in odor-specific neural ensembles. Nat Neurosci 3: 927-931.

24. Christensen TA, Waldrop BR, Hildebrand JG (1998) Multitasking in the olfactory system: Context-dependent responses to odors reveal dual GABA-regulated coding mechanisms in single olfactory projection neurons. J Neurosci 18: 5999-6008.

25. Daly KC, Chandra S, Durtschi ML, Smith BH (2001) The generalization of an olfactory-based conditioned response reveals unique but overlapping odour representations in the moth Manduca sexta. J Exp Biol 204: 3085-3095.

26. Davis RL (2004) Olfactory learning, Neuron 44: 31-48.

27. Davison IG, Katz LC (2007) Sparse and selective odor coding by mitral/tufted neurons in the main olfactory bulb, J Neurosci 27: 2091-2101.

28. de Bruyne M, Foster K, Carlson JR (2001) Odor Coding in the *Drosophila* Antenna. Neuron 30: 537-552.

29. Deisig N, Giurfa M, Lachnit H, Sandoz JC (2006) Neural representation of olfactory mixtures in the honeybee antennal lobe. Chemical Senses 31: E60.

30. Demmer H, Kloppenburg P (2009) Intrinsic Membrane Properties and Inhibitory Synaptic Input of Kenyon Cells as Mechanisms for Sparse Coding? J Neurophysiol 00183.

31. Denk W, Delaney KR, Gelperin A, Kleinfeld D, Strowbridge BW, Tank DW, Yuste R (1994) Anatomical and Functional Imaging of Neurons Using 2-Photon Laser-Scanning Microscopy. Journal of Neuroscience Methods 54: 151-162.

32. Distler PG, Gruber C, Boeckh J (1998) Synaptic connections between GABA-immunoreactive neurons and uniglomerular projection neurons within the antennal lobe of the cockroach, *Periplaneta americana*. Synapse 29: 1-13.

33. Ditzen, M. (2005) Odor concentration and identity coding in the antennal lobe of the honeybee *Apis mellifera*.
Dissertation

34. Duchamp-Viret P, Duchamp A, Chaput MA (2003) Single olfactory sensory neurons simultaneously integrate the components of an odour mixture. European Journal of Neuroscience 18: 2690-2696.

35. Dujardin F (1850) Mémoire sur le système nerveux des insectes. Ann Sci Nat Zool 14: 195-206.

36. Enell L, Hamasaka Y, Kolodziejczyk A, Nassel DR (2007) g-aminobutyric acid (GABA) signaling components in *Drosophila*: Immunocytochemical localization of GABA(B) receptors in relation to the GABA(A) receptor subunit RDL and a vesicular GABA transporter. Journal of Comparative Neurology 505: 18-31.

37. Faber T, Menzel R (2001) Visualizing mushroom body response to a conditioned odor in honeybees. Naturwissenschaften 88: 472-476.

38. Farkhooi F, Muller E, Nawrot M (2009) Sequential sparsing by successive adapting neural populations. BMC Neuroscience 10: O10.

39. Farris SM, Abrams AI, Strausfeld NJ (2004) Development and morphology of class II Kenyon cells in the mushroom bodies of the honey bee, *Apis mellifera*
Journal of Comparative Neurology 474: 325-339.

40. Farris SM, Robinson GE, Fahrbach SE (2001) Experience- and age-related outgrowth of intrinsic neurons in the mushroom bodies of the adult worker honeybee. J Neurosci 21: 6395-6404.

41. Fernandez P, Locatelli F, Person-Rennell N, Deleo G, Smith BH (2009) Associative conditioning tunes transient dynamics of early olfactory processing. J Neurosci 29: 10191-10202.

42. Fiala A, Spall T, Diegelmann S, Eisermann B, Sachse S, Devaud JM, Buchner E, Galizia CG (2002) Genetically expressed cameleon in *Drosophila melanogaster* is used to visualize olfactory information in projection neurons. Curr Biol 12: 1877-1884.

43. Frasnelli J, Wohlgemuth C, Hummel T (2006) The influence of stimulus duration on odor perception. International Journal of Psychophysiology 62: 24-29.

44. Friedrich RW, Korsching SI (1997) Combinatorial and chemotopic odorant coding in the zebrafish olfactory bulb visualized by optical imaging. Neuron 18: 737-752.

45. Fujiwara T, Kazawa T, Haupt SS, Kanzaki R (2009) Ca2+ imaging of identifiable neurons labeled by electroporation in insect brains. Neuroreport 20: 1061-1065.

46. Fukushima R, Kanzaki R (2009) Modular subdivision of mushroom bodies by kenyon cells in the silkmoth. The Journal of Comparative Neurology 513: 315-330.

47. Galán RF, Weidert M, Menzel R, Herz AVM, Galizia CG (2006) Sensory Memory for Odors Is Encoded in Spontaneous Correlated Activity Between Olfactory Glomeruli. Neural Computation 18: 10-25.

48. Galizia CG, Joerges J, Kuttner A, Faber T, Menzel R (1997) A semi-in-vivo preparation for optical recording of the insect brain, Journal of Neuroscience Methods 76: 61-69.

49. Galizia CG, Kimmerle B (2004) Physiological and morphological characterization of honeybee olfactory neurons combining electrophysiology, calcium imaging and confocal microscopy. Journal of Comparative Physiology A: Neuroethology, Sensory, Neural, and Behavioral Physiology 190: 21-38.

50. Galizia CG, Küttner A, Joerges J, Menzel R (2000) Odour representation in honeybee olfactory glomeruli shows slow temporal dynamics: an optical recording study using a voltage-sensitive dye. Journal of Insect Physiology 46: 877-886.

51. Galizia CG, McIlwrath SL, Menzel R (1999) A digital three-dimensional atlas of the honeybee antennal lobe based on optical sections acquired by confocal microscopy. Cell Tissue Res 295: 383-394.

52. Galizia CG, Nagler K, Holldobler B, Menzel R (1998) Odour coding is bilaterally symmetrical in the antennal lobes of honeybees (*Apis mellifera*). European Journal of Neuroscience 10: 2964-2974.

53. Galizia CG, Szyszka P (2008) Olfactory coding in the insect brain: molecular receptive ranges, spatial and temporal coding. Entomologia Experimentalis et Applicata 128: 81-92.

54. Ganeshina O, Menzel R (2001) GABA-Immunoreactive Neurons in the Mushroom Bodies of the Honeybee: An Electron Microscopic Study. J Comp Neurol 437: 335-349.

55. Ganeshina, O., Vorobyev, M., and Menzel, R. (2006) Synaptogenesis in the Mushroom Body Calyx During Metamorphosis in the Honeybee *Apis mellifera*: An Electron Microscopic Study. Journal of Comparative Neurology 497[6], 876-897.

56. Golden K, Sagi V, Markwarth N, Bin C, Monteiro A (2007) In vivo electroporation of DNA into the wing epidermis of the butterfly, Bicyclus anynana. Journal of Insect Science 7.

57. Gouwens NW, Wilson RI (2009) Signal Propagation in *Drosophila* Central Neurons, J Neurosci 29: 6239-6249.

58. Groh C, Rössler W (2008) Caste-specific postembryonic development of primary and secondary olfactory centers in the female honeybee brain. Arthropod Structure & Development 37: 459-468.

59. Gronenberg W, López-Riquelme GO (2004) Multisensory convergence in the mushroom bodies of ants and bees. Acta Biologica Hungarica 55: 31-37.

60. Grünewald B (1999a) Morphology of feedback neurons in the mushroom body of the honeybee, *Apis mellifera*. Journal of Comparative Neurology 404: 114-126.

61. Grünewald B (1999b) Physiological properties and response modulations of mushroom body feedback neurons during olfactory learning in the honeybee *Apis mellifera*. J Comp Physiol [A] 185: 565-576.

62. Grünewald B, Wersing A (2008) An ionotropic GABA receptor in cultured mushroom body Kenyon cells of the honeybee and its modulation by intracellular calcium. Journal of Comparative Physiology A: Neuroethology, Sensory, Neural, and Behavioral Physiology 194: 329-340.

63. Grünewald B, Wersing A, Wustenberg DG (2004) Learning channels. Cellular physiology of odor processing neurons within the honeybee brain. Acta Biologica Hungarica 55: 53-63.

64. Guerrieri F, Schubert M, Sandoz JC, Giurfa M (2005) Perceptual and neural olfactory similarity in honeybees. Plos Biology 3: 718-732.

65. Gühmann, M. (2007) Influence of $GABA_B$ Receptors on Olfactory Coding in the Honeybee Antennal Lobe, a Physiological and Anatomical Study. Diplom Thesis: Freie Universität Berlin, Studies of Bioinformatics .

66. Haehnel M, Froese A, Menzel R (2009) In vivo Ca2+ imaging of mushroom body neurons during olfactory learning in the honey bee. J Vis Exp 30.

67. Hähnel, M. (2009) Characterization of Mushroom Body Extrinsic Neurons in the Honeybee *Apis mellifera* and Their Role in Learning and Memory Formation: A Calcium Imaging Study.
Dissertation: Freie Universität Berlin, Institut für Biologie, Neurobiologie.

68. Hammer M (1993) An identified neuron mediates the unconditioned stimulus in associative olfactory learning in honeybees. n 366: 59-63.

69. Heisenberg M (1989) Genetic approach to learning and memory (mnemogenetics) in *Drosophila melanogaster*. Fortschritte der Zoology/Progress in Zoology 37: 3-45.

70. Heisenberg M (2003) Mushroom body memoir: From maps to models. Nature Reviews Neuroscience 4: 266-275.

71. Heisenberg M, Heusipp M, Wanke C (1995) Structural Plasticity in the *Drosophila* Brain. J Neurosci 15: 1951-1960.

72. Helmchen F, Denk W (2005) Deep tissue two-photon microscopy
Nature Methods 2: 932-940

73. Hildebrand JG, Shepherd GM (1997) Mechanisms of olfactory discrimination: converging evidence for common principles across phyla. Annu Rev Neurosci 20: 595-631.

74. Homberg U (1984) Processing of antennal information in extrinsic mushroom body neurons of the bee brain. J Comp Physiol [A] 154: 825-836.

75. Husch A, Paehler M, Fusca D, Paeger L, Kloppenburg P (2009) Calcium Current Diversity in Physiologically Different Local Interneuron Types of the Antennal Lobe. J Neurosci 29: 716-726.

76. Ito I, Ong RC, Raman B, Stopfer M (2008) Sparse odor representation and olfactory learning. Nat Neurosci.

77. Ito K, Suzuki K, Estes P, Ramaswami M, Yamamoto D, Strausfeld NJ (1998) The organization of extrinsic neurons and their implications in the functional roles of the mushroom bodies in *Drosophila melanogaster meigen*. Learning and Memory 5: 52-77.

78. Jefferis GSXE, Potter CJ, Chan AI, Marin EC, Rohlfing T, Maurer CR, Luo LQ (2007) Comprehensive maps of *Drosophila* higher offactory centers: Spatially segregated fruit and pheromone representation
10. Cell 128: 1187-1203.

79. Joerges J, Kuttner A, Galizia CG, Menzel R (1997) Representations of odours and odour mixtures visualized in the honeybee brain. 387: 285-288.

80. Johard HAD, Enell LE, Gustafsson E, Trifilieff P, Veenstra JA, Nassel DR (2008) Intrinsic neurons of *Drosophila* mushroom bodies express short neuropeptide F: Relations to extrinsic neurons expressing different neurotransmitters, Journal of Comparative Neurology 507: 1479-1496.

81. Kashiwayanagi M, Kawahara H, Kurihara K (1994) Forskolin enhanced off-response in the turtle olfactory system. Journal of Physiology-Paris 88: 309-314.

82. Kent LB, Robertson HM (2009) Evolution of the sugar receptors in insects

83. Kenyon FC (1896) The brain of the bee - A preliminary contribution to the morphology of the nervous system of the Arthropoda. Journal of Comparative Neurology 6: 134-210.

84. Kim S, Wang J (2009) Lateral inhibition and concentration-invariant odor perception. Journal of Biology 8: 4.

85. Kirschner S, Kleineidam CJ, Zube C, Rybak J, Grunewald B, Rossler W (2006) Dual olfactory pathway in the honeybee, *Apis mellifera* Journal of Comparative Neurology 499: 933-952

86. Komischke B, Sandoz JC, Malun D, Giurfa M (2005) Partial unilateral lesions of the mushroom bodies affect olfactory learning in honeybees *Apis mellifera* L. European Journal of Neuroscience 21: 477-485.

87. Krofczik S, Khojasteh U, de Ibarra NH, Menzel R (2008) Adaptation of microglomerular complexes in the honeybee mushroom body lip to manipulations of behavioral maturation and sensory experience Developmental Neurobiology 68: 1007-1017.

88. Krofczik S, Menzel R, Nawrot MP (2009) Rapid odor processing in the honeybee antennal lobe network. Front Comput Neurosci 2: 1-9.

89. Kunieda T, Kubo T (2004) In vivo gene transfer into the adult honeybee brain by using electroporation. Biochemical and Biophysical Research Communications 318: 25-31.

90. Kyriazi HT, Carvell GE, Simons DJ (1994) OFF response transformations in the whisker/barrel system. J Neurophysiol 72: 392-401.

91. Laurent G (2002) Olfactory network dynamics and the coding of multidimensional signals, Nature Reviews Neuroscience 3: 884-895.

92. Laurent G, MacLeod K, Stopfer M, Wehr M (1998) Spatiotemporal structure of olfactory inputs to the mushroom bodies, Learn Mem 5: 124-132.

93. Laurent G, Wehr M, Davidowitz H (1996) Temporal representations of odors in an olfactory network. J Neurosci 16: 3837-3847.

94. Lei H, Riffell JA, Gage SL, Hildebrand JG (2009) Contrast enhancement of stimulus intermittency in a primary olfactory network and its behavioral significance, J Biol 8: 21.

95. Liu X, Buchanan ME, Han KA, Davis RL (2009) The GABAA Receptor RDL Suppresses the Conditioned Stimulus Pathway for Olfactory Learning. J Neurosci 29: 1573-1579.

96. Liu X, Davis RL (2009) The GABAergic anterior paired lateral neuron suppresses and is suppressed by olfactory learning. Nat Neurosci 12: 53-59.

97. Liu X, Krause WC, Davis RL (2007) GABAA Receptor RDL Inhibits *Drosophila* Olfactory Associative Learning. Neuron 56: 1090-1102.

98. MacDermott AB, Role LW, Siegelbaum SA (1999) Presynaptic ionotropic receptors and the control of transmitter release. Annual Review of Neuroscience 22: 443-485.

99. MacLeod K, Backer A, Laurent G (1998) Who reads temporal information contained across synchronized and oscillatory spike trains? n 395: 693-698.

100. MacLeod K, Laurent G (1996) Distinct mechanisms for synchronization and temporal patterning of odor-encoding neural assemblies, Science 274: 976-979.

101. Masek P, Heisenberg M (2008) Distinct memories of odor intensity and quality in *Drosophila*. Proceedings of the National Academy of Sciences 105: 15985-15990.

102. Masuda-Nakagawa LM, Gendre N, O'Kane CJ, Stocker RF (2009) Localized olfactory representation in mushroom bodies of *Drosophila* larvae, Proc Natl Acad Sci U S A 106: 10314-10319.

103. Masuda-Nakagawa LM, Tanaka NK, O'Kane CJ (2005) Stereotypic and random patterns of connectivity in the larval mushroom body calyx of *Drosophila*. Proc Natl Acad Sci U S A 102: 19027-19032.

104. Mauelshagen J (1993) Neural Correlates of Olfactory Learning-Paradigms in An Identified Neuron in the Honeybee Brain, J Neurophysiol 69: 609-625.

105. Mazor O, Laurent G (2005) Transient dynamics versus fixed points in odor representations by locust antennal lobe projection neurons Neuron 48: 661-673.

106. Menzel R (1983) Neurobiology of learning and memory: the honey bee as a model system. Naturwiss 70: 504-511.

107. Menzel R, Manz G, Menzel R, Greggers U (2001) Massed and spaced learning in honeybees: the role of CS, US, the intertrial interval, and the test interval. Learn Mem 8: 198-208.

108. Menzel R, Manz G (2005) Neural plasticity of mushromm body-extrinsic neurons in the honeybee brain. The Journal of Experimental Biology 208: 4317-4332.

109. Mezler M, Muller T, Raming K (2001) Cloning and functional expression of GABA(B) receptors from *Drosophila*. European Journal of Neuroscience 13: 477-486.

110. Miyawaki A, Llopis J, Heim R, McCaffery JM, Adams JA, Ikura M, Tsien RY (1997) Fluorescent indicators for Ca2+based on green fluorescent proteins and calmodulin. n 388: 882-887.

111. Mobbs PG (1982) The Brain of the Honeybee *Apis Mellifera* I. The Connections and Spatial Organization of the Mushroom Bodies. Philosophical Transactions of the Royal Society of London Series B-Biological Sciences 298: 309-354.

112. Mombaerts P, Wang F, Dulac C, Chao SK, Nemes A, Mendelsohn M, Edmondson J, Axel R (1996) Visualizing an olfactory sensory map. Cell 87: 675-686.

113. Moreaux L, Laurent G (2007) Estimating firing rates from calcium signals in locust projection neurons *in vivo*. Frontiers in Neural Circuits 1.

114. Müller D, Abel R, Brandt R, Zockler M, Menzel R (2002) Differential parallel processing of olfactory information in the honeybee, *Apis mellifera* L. Journal of Comparative Physiology A: Neuroethology, Sensory, Neural, and Behavioral Physiology 188: 359-370.

115. Murthy M, Fiete I, Laurent G (2008) Testing odor response stereotypy in the *Drosophila* mushroom body. Neuron 59: 1009-1023.

116. Nakai J, Ohkura M, Imoto K (2001) A high signal-to-noise Ca2+ probe composed of a single green fluorescent protein. Nature Biotechnology 19: 137-141.

117. Neher E (2008) Details of Ca2+ dynamics matter. Journal of Physiology-London 586: 2031.

118. Nusser Z, Kay LM, Laurent G, Homanics GE, Mody I (2001) Disruption of GABA(A) receptors on GABAergic interneurons leads to increased oscillatory power in the olfactory bulb network. J Neurophysiol 86: 2823-2833.

119. Okada R, Menzel R (2006) Associative plasticity of mushroom body extrinsic neurons during olfactory learning in honeybees. Comparative Biochemistry and Physiology B-Biochemistry & Molecular Biology 145: 417.

120. Okada R, Rybak J, Manz G, Menzel R (2007) Learning-related plasticity in PE1 and other mushroom body-extrinsic neurons in the honeybee brain. J Neurosci 27: 11736-11747.

121. Olianas MC, Onali P (1999) GABA(B) receptor-mediated stimulation of adenylyl cyclase activity in membranes of rat olfactory bulb. British Journal of Pharmacology 126: 657-664.

122. Olsen SR, Bhandawat V, Wilson RI (2007) Excitatory interactions between olfactory processing channels in the *Drosophila* antennal lobe (vol 54, pg 89, 2007). Neuron 54: 667.

123. Olsen SR, Wilson RI (2008) Lateral presynaptic inhibition mediates gain control in an olfactory circuit. n 452: 956-9U3.

124. Panov A (2009) Some cetoniinae (Coleoptera, Scarabaeidae) have structurally different medial and lateral calyces of mushroom bodies. Entomological Review 89: 21-25.

125. Paulk AC, Phillips-Portillo J, Dacks AM, Fellous JM, Gronenberg W (2008) The Processing of Color, Motion, and Stimulus Timing Are Anatomically Segregated in the Bumblebee Brain. J Neurosci 28: 6319-6332.

126. Pelz C, Gerber B, Menzel R (1997) Odorant intensity as a determinant for olfactory conditioning in honeybees: Roles in discrimination, overshadowing and memory consolidation. J Exp Biol 200: 837-847.

127. Perez-Orive J, Mazor O, Turner GC, Cassenaer S, Wilson RI, Laurent G (2002) Oscillations and sparsening of odor representations in the mushroom body. Science 297: 359-365.

128. Reidl J, Starke J, Omer DB, Grinvald A, Spors H (2006) Independent component analysis of high-resolution imaging data identifies distinct functional domains. Neuroimage 34: 94-108.

129. Root CM, Masuyama K, Green DS, Enell LE, Nassel DR, Lee CH, Wang JW (2008) A presynaptic gain control mechanism fine-tunes olfactory behavior. Neuron 59: 311-321.

130. Rotte C, Witte J, Blenau W, Baumann O, Walz B (2009) Source, topography and excitatory effects of GABAergic innervation in cockroach salivary glands. J Exp Biol 212: 126-136.

131. Rubin BD, Katz LC (1999) Optical imaging of odorant representations in the mammalian olfactory bulb. Neuron 23: 499-511.

132. Rybak, J. (1994) Die strukturelle Organisation der Pilzkörper und synaptische Konnektivität protocerebraler Interneuronen im Gehirn der Honigbiene, *Apis mellifera*. Eine licht- und elektronenmikroskopische Studie. Dissertation: Freie Universität Berlin.

133. Rybak J, Menzel R (1993) Anatomy of the mushroom bodies in the honey bee brain: the neuronal connections of the alpha-lobe. J Comp Neurol 334: 444-465.

134. Sachse S, Galizia CG (2002) Role of inhibition for temporal and spatial odor representation in olfactory output neurons: A calcium imaging study. J Neurophysiol 87: 1106-1117.

135. Sachse S, Galizia CG (2003) The coding of odour-intensity in the honeybee antennal lobe: local computation optimizes odour representation. European Journal of Neuroscience 18: 2119-2132.

136. Sachse S, Rappert A, Galizia GC (1999) The spatial representation of chemical structures in the antennal lobe of honeybees: steps towards the olfactory code. European Journal of Neuroscience 11: 3970-3982.

137. Sachse S, Peele P, Silbering A, Guhmann M, Galizia CG (2006) Role of histamine as a putative inhibitory transmitter in the honeybee antennal lobe. Frontiers in Zoology 3: 22.

138. Schäfer S, Bicker G (1986) Distribution of GABA-like immunoreactivity in the brain of the honeybee. Journal of Comparative Neurology 246: 287-300.

139. Schäfer S, Rosenboom H, Menzel R (1994) Ionic currents of Kenyon cells from the mushroom body of the honeybee. J Neurosci 14: 4600-4612.

140. Schröter U, Menzel R (2003) A New Ascending sensory tract to the calyces of the honeybee mushroom body, the subesophageal-calycal tract. Journal of Comparative Neurology 465: 168-178.

141. Shang YH, Claridge-Chang A, Sjulson L, Pypaert M, Miesenbock G (2007) Excitatory local circuits and their implications for olfactory processing in the fly antennal lobe. Cell 128: 601-612.

142. Silbering AF, Galizia CG (2007) Processing of odor mixtures in the *Drosophila* antennal lobe reveals both global inhibition and glomerulus-specific interactions. J Neurosci 27: 11966-11977.

143. Silbering AF, Okada R, Ito K, Galizia CG (2008) Olfactory Information Processing in the *Drosophila* Antennal Lobe: Anything Goes? J Neurosci 28: 13075-13087.

144. Smith BH (1998) Analysis of interaction in binary odorant mixtures. Physiol Behav 65: 397-407.

145. Smith D, Wessnitzer J, Webb B (2008) A model of associative learning in the mushroom body. Biological Cybernetics 99: 89-103.

146. Spors H, Wachowiak M, Cohen LB, Friedrich RW (2006) Temporal dynamics and latency patterns of receptor neuron input to the olfactory bulb. J Neurosci 26: 1247-1259.

147. Spors H, Grinvald A (2002) Spatio-Temporal Dynamics of Odor Representations in the Mammalian Olfactory Bulb. Neuron 34: 301-315.

148. Stocker RF, Lienhard MC, Borst A, Fischbach KF (1990) Neuronal architecture of the antennal lobe in *Drosophila melanogaster*. Cell Tissue Res 262: 9-34.

149. Stopfer M (2005) Olfactory Coding: Inhibition Reshapes Odor Responses. Current Biology 15: R996-R998.

150. Stopfer M, Bhagavan S, Smith BH, Laurent G (1997) Impaired odour discrimination on desynchronization of odour-encoding neural assemblies. n 390: 70-74.

151. Stopfer M, Jayaraman V, Laurent G (2003) Intensity versus identity coding in an olfactory system. Neuron 39: 991-1004.

152. Strausfeld NJ (2002) Organization of the honey bee mushroom body: Representation of the calyx within the vertical and gamma lobes. Journal of Comparative Neurology 450: 4-33.

153. Strausfeld NJ, Hansen L, Yongsheng L, Gomez RS, Ito K (1998) Evolution, Discovery, and Interpretations of Arthropod Mushroom Bodies. Learning & Memory 5: 11-37.

154. Strausfeld NJ, Homberg U, Kloppenburg P (2000) Parallel organization in honey bee mushroom bodies by peptidergic Kenyon cells (vol 424, pg 179, 2000). Journal of Comparative Neurology 428: 760.

155. Strube-Bloss, M. F. (2008) Characterization of Mushroom Body Extrinsic Neurons of the Honeybee: Odor Specificity, Response Reliablity, and Learning Related Plasticity.
Dissertation: Freie Universität Berlin, Institut für Biologie - Neurobiologie.

156. Szyszka, P. (2005) Odor coding and neural plasticity in the mushroom body of the honeybee.
Dissertation: Freie Universität Berlin, Institut für Biologie - Neurobiologie.

157. Szyszka P, Ditzen M, Galkin A, Galizia CG, Menzel R (2005) Sparsening and temporal sharpening of olfactory representations in the honeybee mushroom bodies. J Neurophysiol 94: 3303-3313.

158. Szyszka P, Galkin A, Menzel R (2008) Associative and non-associative plasticity in Kenyon cells of the honeybee mushroom body. Frontiers in Systems Neuroscience 2-3.

159. Tabor R, Yaksi E, Friedrich RW (2008) Multiple functions of GABA(A) and GABA(B) receptors during pattern processing in the zebrafish olfactory bulb. European Journal of Neuroscience 28: 117-127.

160. Tanaka NK, Ito K, Stopfer M (2009) Odor-evoked neural oscillations in *Drosophila* are mediated by widely branching interneurons,
J Neurosci 29: 8595-8603.

161. Tanaka NK, Tanimoto H, Ito K (2008) Neuronal assemblies of the *Drosophila* mushroom body, Journal of Comparative Neurology 508: 711-755.

162. Thomas JL (2003) Electroporation, an alternative to biolistics for transfection of Bombyx mori embryos and larval tissues. J Insect Sci 3: 17.

163. Velarde RA, Robinson GE, Fahrbach SE (2009) Coordinated responses to developmental hormones in the Kenyon cells of the adult worker honey bee brain (*Apis mellifera* L.). Journal of Insect Physiology 55: 59-69.

164. Vosshall LB, Wong AM, Axel R (2000) An olfactory sensory map in the fly brain. Cell 102: 147-159.

165. Waldrop B, Christensen TA, Hildebrand JG (1987) GABA-mediated synaptic inhibition of projection neurons in the antennal lobes of the sphinx moth, *Manduca sexta*. J Comp Physiol [A] 161: 23-32.

166. Wang YL, Guo HF, Pologruto TA, Hannan F, Hakker I, Svoboda K, Zhong Y (2004) Stereotyped odor-evoked activity in the mushroom body of *Drosophila* revealed by green fluorescent protein-based Ca2+ imaging. J Neurosci 24: 6507-6514.

167. Wang YL, Wright NJD, Guo HF, Xie ZP, Svoboda K, Malinow R, Smith DP, Zhong Y (2001) Genetic manipulation of the odor-evoked distributed neural activity in the *Drosophila* mushroom body. Neuron 29: 267-276.

168. Wehr M, Laurent G (1996) Odour encoding by temporal sequences of firing in oscillating neural assemblies, 384: 162-166.

169. Weinstock GM and honeybee genome consortium (2006) Insights into social insects from the genome of the honeybee *Apis mellifera*. n 443: 931-949.

170. Wilson RI, Laurent G (2005) Role of GABAergic inhibition in shaping odor-evoked spatiotemporal patterns in the *Drosophila* antennal lobe. J Neurosci 25: 9069-9079.

171. Witthöft W (1967) Absolute Anzahl und Verteilung der Zellen im Hirn der Honigbiene. Z Morph Tiere 61: 160-184.

172. Wright GA, Carlton M, Smith BH (2009) A Honeybee's Ability to Learn, Recognize, and Discriminate Odors Depends Upon Odor Sampling Time and Concentration. Behavioral Neuroscience 123: 36-43.

173. Wright GA, Thomson MGA, Smith BH (2005) Odour concentration affects odour identity in honeybees. Proceedings of the Royal Society B-Biological Sciences 272: 2417-2422.

174. Wüstenberg DG, Boytcheva M, Grunewald B, Byrne JH, Menzel R, Baxter DA (2004) Current- and Voltage-Clamp Recordings and Computer Simulations of Kenyon Cells in the Honeybee. J Neurophysiol 92: 2589-2603.

175. Yaksi E, von Saint PF, Niessing J, Bundschuh ST, Friedrich RW (2009) Transformation of odor representations in target areas of the olfactory bulb. Nat Neurosci 12: 474-482.

176. Yamagata, N. (2008) Neural basis of olfactory processing in social insects. Dissertation: Graduate School of Life Sciences, Tohoku University, Department of Developmental Biology and Neurosciences.

177. Yarali A, Ehser S, Hapil FZ, Huang J, Gerber B (2009) Odour intensity learning in fruit flies. Proceedings of the Royal Society B: Biological Sciences.

178. Zube C, Kleineidam CJ, Kirschner S, Neef J, Rossler W (2008) Organization of the olfactory pathway and odor processing in the antennal lobe of the ant Camponotus floridanus. Journal of Comparative Neurology 506: 425-441.